

# **Oncology Treatment Discovery**

Editors-in-Chief

**Vincent J. Cogliano**

*U.S. Environmental Protection Agency, USA*

**Chong Li**

*Chinese Academy of Sciences, China*

BIO-BYWORD SCIENTIFIC PUBLISHING PTY LTD

(619 649 400)

Level 10

50 Clarence Street

SYDNEY NSW 2000

Copyright © 2024. Bio-Byword Scientific Publishing Pty Ltd.

Complimentary Copy



## Oncology Treatment Discovery

### Focus and Scope

*Oncology Treatment Discovery* is a peer-reviewed, open access journal. It accepts manuscripts relevant to experimental and clinical cancer research. The journal publishes the latest findings in cancer research, including preliminary results, repeated argumentation studies and negative results. The journal welcomes various types of submissions, e.g. research papers, clinical research reports, review articles. Content covers topics that advance clinical practice, challenge the status quo, advocate change in health policy, genomic instability, growth promoting signals, growth inhibitory signals, cell death, tumour microenvironment, carcinogenesis and cancer prevention and tackle issues related to global oncology.

### About Publisher

Bio-Byword Scientific Publishing is a fast-growing, peer-reviewed and open access journal publisher, which is located in Sydney, Australia. As a dependable and credible corporation, it promotes and serves a broad range of subject areas for the benefit of humanity. By informing and educating a global community of scholars, practitioners, researchers and students, it endeavors to be the world's leading independent academic and professional publisher. To realize it, it keeps creative and innovative to meet the range of the authors' needs and publish the best of their work.

By cooperating with University of Sydney, University of New South Wales and other world-famous universities, Bio-Byword Scientific Publishing has established a huge publishing system based on hundreds of academic programs, and with a variety of journals in the subjects of medicine, construction, education and electronics.

### Publisher Headquarter

BIO-BYWORD SCIENTIFIC PUBLISHING PTY LTD

Level 10

50 Clarence Street

Sydney NSW 2000

Website: [www.bbwpublisher.com](http://www.bbwpublisher.com)

Email: [info@bbwpublisher.com](mailto:info@bbwpublisher.com)



## Table of Contents

- 1 Clinical Effects of Laparoscopic Surgery in Radical Surgery for Colorectal Cancer**  
*Guodong Zhao, Zhe Shi, Liang Xue, Shugang Sun*
- 7 Construction of Lactobacillus casei-loaded Water-in-oil High Internal Phase Emulsion and its Study on Anti-breast Cancer Properties**  
*Miao Tong, Qiao Peng*
- 20 Tissue Engineering of Cornea via Type 1 Collagen Biomaterials – A perspective**  
*Kirubanandan Shanmugam*
- 38 Long Non-coding RNA and Progression of Breast Cancer**  
*Usama Ahmed, Muhammad Abubakar, Salma Saeed Khan, Baqa ur Rehman*
- 65 Clinical Effects of Laparoscopic Radical Colon Cancer Treatment with Complete Mesocolic Resection for Colon Cancer**  
*Liang Xue, Zhe Shi, Shugang Sun, Guodong Zhao*
- 72 Expression of Serum DCLK1 in Gastric Cancer Patients and Its Relationship with CEA, CA19-9, and CA72-4**  
*Baoming Guo, Zheng Jiao, Jianzhou Li, Jing Pan, Huiqi Liu*
- 79 Clinical Efficacy of Autologous Bone Marrow Mesenchymal Stem Cell Transplantation for the Treatment of Patients with Refractory Cirrhotic Ascites**  
*Lianqing Li, Haibo Chen, Hongfei Zhao, Jiping Zhu, Shaofeng Li*
- 85 Research Progress on Negative Emotions Influencing the Incidence of Breast Cancer**  
*Wei Liu, Ruibo Shi, Yurong Zhou, Rong Guo, Jianjun Wei, Xinming Fan, Zhizhong Ren, Rongtian Zhang*



# Clinical Effects of Laparoscopic Surgery in Radical Surgery for Colorectal Cancer

Guodong Zhao\*, Zhe Shi, Liang Xue, Shugang Sun

Affiliated Hospital of Hebei Engineering University, Handan 056000, Hebei Province, China

\*Corresponding author: Guodong Zhao, zgddl@163.com

**Copyright:** © 2024 Author(s). This is an open-access article distributed under the terms of the Creative Commons Attribution License (CC BY 4.0), permitting distribution and reproduction in any medium, provided the original work is cited.

**Abstract:** Objective: To investigate the clinical application effect of laparoscopic surgery in radical surgery for colorectal cancer. Methods: 78 patients who were treated with radical surgery for colorectal cancer in a tertiary hospital during the period from January 2021 to December 2023 were selected as the study subjects in this study. According to the different surgical methods, the patients were divided into the laparoscopic surgery group (40 cases in the experimental group) and the traditional open surgery group (38 cases in the control group). The operation time, intraoperative bleeding, postoperative recovery (including postoperative anal exhaustion time, time to get out of bed, and hospitalization time), complication rate, and therapeutic effect were observed in the two groups. Results: Patients in the experimental group were better than the control group in terms of intraoperative blood loss, operation time, postoperative anal exhaust time, time to get out of bed, and postoperative hospitalization time ( $P < 0.05$ ). Patients in the experimental group had significantly better treatment effects and complication rates than those in the control group ( $P < 0.05$ ). Conclusion: Compared with the open group, the overall prognosis of laparoscopic colorectal cancer patients is better, and laparoscopy has a protective effect on tumor recurrence or metastasis after radical surgery for colorectal cancer, and it can reduce the incidence of postoperative abdominal infection.

**Keywords:** Laparoscopic surgery; Colorectal cancer; Effect

**Online publication:** October 2, 2024

## 1. Introduction

Colorectal cancer is one of the diseases with the highest morbidity and mortality in the world. China is a large country with the incidence of colorectal cancer and its incidence rate is ranked number 3 among malignant tumors. With the continuous progress of medical technology, laparoscopic surgery has become an important development direction of surgical operation at present. Compared with open surgery, laparoscopic surgery is widely used because of its advantages of less trauma, faster postoperative recovery, less pain, fewer complications, etc. Among them, laparoscopic radical resection of colorectal cancer has higher clinical advantages, including shorter hospitalization time, fewer complications and lower morbidity and mortality, etc. In 2015, the American Cancer Society proposed the concept of “radical bowel resection,” which means that the

surgery is performed with the concept of “radical bowel resection.” The concept of “radical bowel resection” refers to surgery that preserves the patient’s colorectal structures as much as possible and achieves the effect of radical removal of diseased tissue. For most patients with early colorectal cancer whose tumor diameter is  $\leq 3$  cm, without lymph node metastasis or with  $\leq 3$  lymph node metastases, minimally invasive treatment, i.e., laparoscopic radical colorectal cancer surgery, is an option <sup>[1]</sup>. However, in recent years, some studies have also shown that although the complication rate of laparoscopic radical colorectal cancer surgery is low, it may lead to the occurrence of postoperative anastomotic fistula, so most scholars currently believe that minimally invasive surgery should still be based on traditional radical colorectal surgery. With the development of endoscopic technology, endoscopic polypectomy has gradually replaced traditional radical colorectal surgery as the standard program for the treatment of early colorectal cancer. As for patients with intermediate to advanced colorectal cancer, radical surgical treatment is still required due to the risk of lymph node metastasis and distant metastasis, especially for patients with extensive stage <sup>[2]</sup>. At present, laparoscopic anus-preserving surgery for low rectal cancer has been gradually carried out in China. However, there is a lack of sufficient clinical evidence to support whether anal preservation surgery for low rectal cancer can prolong patients’ survival. In addition, some scholars have conducted relevant studies on whether neoadjuvant chemotherapy combined with laparoscopic anal preservation surgery can further improve the prognosis of patients, but the conclusions are not the same, which may be due to the small sample size and different inclusion populations.

2. Information and Methods

2.1. General information

Seventy-eight patients who were treated with radical surgery for colorectal cancer in a tertiary hospital during the period from January 2021 to December 2023 were selected as the study subjects. All patients were diagnosed with colorectal cancer by pathologic diagnosis, and all met the criteria for laparoscopic surgery. According to the different surgical methods, the patients were divided into the laparoscopic surgery group (experimental group) and the traditional open surgery group (control group). Among them, there were 40 patients in the experimental group and 38 patients in the control group. There was no significant difference between the two groups of patients in terms of age, gender, tumor site, pathological type, etc., and they were comparable, as shown in Table 1.

Table 1. Comparison of general information

General information		Control group (n = 38)	Experimental group (n = 40)	t/ $\chi^2$ -value	P-value
Age (years)		55.37 $\pm$ 5.12	55.40 $\pm$ 5.10	0.026	0.979
Sex (cases)	Male	25 (65.79)	27 (67.50)	0.026	0.873
	Female	13 (34.21)	13 (32.50)	0.026	0.873
Tumor size (cm)		3.21 $\pm$ 0.80	3.22 $\pm$ 0.79	0.056	0.956
Tumor stage (case)	I stage	22 (57.89)	23 (57.50)	0.001	0.972
	II stage	16 (41.11)	17 (42.50)	0.001	0.972

2.2. Methods

Patients in the experimental group were treated by laparoscopic radical surgery for colorectal cancer. The surgical procedure is as follows: After general anesthesia, patients take the truncated position and routinely disinfect and spread the towel. Make 1 cm and 0.5 cm puncture holes at the lower edge of the umbilicus and

the left and right sides of the umbilicus respectively and establish pneumoperitoneum. Tumor location and size were explored through laparoscopy to determine the scope of surgery. Tumor resection and lymph node dissection were carried out using the ultrasonic knife and electric knife and attention was paid to protecting the surrounding organs and blood vessels during the operation. After surgery, the resection specimen was removed through a small incision and the incision was sutured.

Patients in the control group were treated with traditional open radical colorectal cancer surgery. The surgical process is similar to that of the experimental group, but the surgery is performed in a direct open abdominal way.

### 2.3. Observation indexes

- (1) Surgical time: Record the time required from the beginning of anesthesia to the end of surgery for both groups.
- (2) Intraoperative bleeding: Record the amount of bleeding during surgery in both groups.
- (3) Postoperative recovery: Including postoperative anal defecation time, time to get out of bed and hospitalization time.
- (4) Complication rate: Record the postoperative complications occurring in the two groups of patients, such as incision infection, intestinal obstruction, anastomotic fistula and so on.
- (5) Therapeutic effect: According to the patients' postoperative pathological results and follow-up, the therapeutic effect of the two groups was evaluated, and the number of patients with good prognoses was assessed.

### 2.4. Statistical methods

SPSS 19.0 was used for analysis. Measurement data were described by mean  $\pm$  standard deviation (SD), independent sample t-test was used for inter-group comparison, paired t-test was used for intra-group comparison, count data were expressed as %,  $\chi^2$  test was used for inter-group comparison, and  $P < 0.05$  was considered statistically significant.

## 3. Results

### 3.1. Observation and comparison of operation time, intraoperative blood loss, postoperative recovery and other indicators

Patients in the experimental group are better than the control group in terms of intraoperative blood loss, operation time, postoperative anal exhaustion time, time to get out of bed and postoperative hospitalization time ( $P < 0.05$ ), as shown in Table 2.

**Table 2.** Comparison of the indexes of operation time, intraoperative blood loss and postoperative recovery between the two groups of patients

Groups	Intraoperative blood loss (mL)	Surgical time (min)	Postoperative anal defecation time (h)	Time to get out of bed (d)	Postoperative hospitalization time (d)
Control group ( $n = 38$ )	264.60 $\pm$ 60.30	165.88 $\pm$ 30.72	4.96 $\pm$ 1.60	6.50 $\pm$ 1.06	12.36 $\pm$ 2.20
Experimental group ( $n = 40$ )	223.58 $\pm$ 60.24	124.90 $\pm$ 30.80	2.01 $\pm$ 1.56	5.32 $\pm$ 1.10	8.03 $\pm$ 2.01
<i>t</i> -value	3.005	5.881	8.244	4.820	9.082
<i>P</i> -value	0.004	0.000	0.000	0.000	0.001

### 3.2. Observation of the complication rate and treatment effect of patients in the two groups

The treatment effect and complication rate of patients in the experimental group are significantly better than those in the control group ( $P < 0.05$ ), as shown in Table 3.

**Table 3.** Comparison of the complication rate and treatment effect of patients in the two groups [ $n$  (%)]

Groups	Treatment effect	Complication rate
Control group ( $n = 38$ )	25 (65.79)	13 (34.21)
Experimental group ( $n = 40$ )	35 (87.50)	5 (12.50)
$t$ -value	5.174	5.174
$P$ -value	0.023	0.023

## 4. Discussion

The 5-year survival and local recurrence rates after laparoscopic radical colorectal cancer surgery are significantly higher than those of conventional open surgery. A prospective study comparing the prognosis of laparoscopic radical left hemicolectomy (LE-R0) with that of open radical left hemicolectomy for colorectal cancer (LR-R1) found that at a median follow-up of 14.3 months, there were no significant differences in death, recurrence, distant metastasis and time to disease-free survival between the two groups of patients; whereas, in subgroup analyses, the primary endpoint events in the LE-R0 group has a higher overall survival (OS) and local recurrence rate, 81.7% and 69.2%, respectively, whereas the disease-free survival (DFS) and local recurrence rate were lower in the LR-R1 group, 92.2% and 59.1%, respectively, suggesting that LE-R0 is a better treatment option <sup>[3]</sup>. Another meta-analysis included 11 randomized controlled trials (RCTs) comparing LE-R0 with LR-R1 for the treatment of limited radical rectal cancer, and the results showed an increase in median OS of 13.8 months (95% CI: 7.8–16.2) in the LE-R0 group compared with LR-R1, but no statistically significant differences were found with any other aspects between the two groups <sup>[4]</sup>. An RCT evaluating the clinical outcomes of laparoscopic-assisted radical resection in situ (ESD) compared with open conventional surgery (OR) showed that there was no difference between the two procedures at a higher risk of recurrence <sup>[5]</sup>. However, patients in both groups had a shorter mean number of days of hospitalization postoperatively, and the incidence of adverse events was lower in the LE-ESD group. Another multicenter RCT study compared the efficacy of LE-R0 versus LR-R1 for the treatment of early-stage rectal cancer and found that at baseline, there was no difference between the two procedures, but the LE-R0 group had a lower rate of complications, which included pneumothorax, intestinal obstruction, and incision infection <sup>[6]</sup>. Another meta-analysis included 23 prospective randomized controlled studies comparing the effects of LE-R0 and LR-R1 on the prognosis of patients with complicated colorectal cancer and the results showed that the OS and DFS of the LE-R0 group were significantly better than those of the LR-R1 group, whereas there was no difference in the rates of local recurrence and distant metastasis, suggesting that LE-R0 may improve clinical outcomes <sup>[7]</sup>. In addition, a meta-analysis included 12 RCT studies comparing LE-R0 with LR-R1 in the application of postoperative chemotherapy regimens for radical colorectal cancer, and the results showed that there was no significant difference between the two groups, but the number of retroperitoneal lymph node dissection in the LE-R0 group was less, which might affect the dose and length of postoperative radiotherapy, leading to lower adherence to chemotherapy, but there was also no significant difference in the risk of distant recurrence or death between the two groups <sup>[8]</sup>.

In this study, patients in the experimental group were better than the control group in terms of



intraoperative blood loss, surgical time, postoperative anal defecation time, time to get out of bed, and postoperative hospitalization time ( $P < 0.05$ ) and patients in the experimental group had a significantly better therapeutic effect and complication rate than those in the control group ( $P < 0.05$ ), which indicated that the effect of laparoscopic surgery was better than that of ordinary open surgery and a randomized controlled study showed that, compared with ordinary open group compared with the normal open group, intraoperative bleeding was significantly reduced in the laparoscopic group ( $P < 0.05$ ), but the difference in the incidence rate of postoperative adverse reactions was not statistically significant ( $P > 0.05$ ), which may be due to the differences in age, gender, smoking history, colorectal cancer stage and clinicopathologic features between the two groups <sup>[9]</sup>. However, due to the lack of randomized controlled trials, this study still needs to be further confirmed. Another retrospective study compared the incidence of postoperative complications between the conventional laparoscopic open group and the laparoscopic group, and the results showed that no serious complications occurred in either group. However, this study concluded that compared with the conventional laparoscopic open group, patients in the sub-laparoscopic group had a longer postoperative temperature recovery time, shorter hospitalization time and lower total costs, thus demonstrating that laparoscopy can significantly improve patients' postoperative quality of life and have a certain impact on patients' prognosis <sup>[10]</sup>.

There is no uniform consensus about the effect of intraoperative abdominal chemotherapy, such as the National Comprehensive Cancer Network (NCCN) guidelines recommend that laparoscopic total pelvic lymph node dissection or laparoscopic local lymph node biopsy can be considered for patients with early colorectal cancer that is not associated with lymph node metastasis or distant metastasis. However, patients with limited or minimally invasive colorectal cancer confirmed by postoperative pathology have a high rate of postoperative lymph node positivity, so the NCCN guideline suggests that pelvic lymph node dissection is not recommended, but it also points out that these patients still need to receive at least one systemic chemotherapy, and if metastatic disease occurs, they should undergo a second chemotherapy. Based on the above, this study believes that laparoscopic local lymph node biopsy + peritoneal instillation chemotherapy treatment can be considered for patients who meet the above criteria if the patient voluntarily requests pelvic and abdominal lymph node dissection and the operator believes that it meets the indications for surgery. Although there is a lack of double-blind controlled trials to clarify whether laparoscopic IPC improves patients' prognosis, some prospective studies have shown that laparoscopic IPC reduces the risk of postoperative adverse reactions.

## 5. Conclusion

In summary, laparoscopic colorectal cancer patients have a better overall prognosis compared with the open group, and laparoscopy is protective against tumor recurrence or metastasis after radical surgery for colorectal cancer, and it reduces the incidence of postoperative abdominal infections. However, there is still controversy about whether IPCs improve the long-term survival of patients with laparoscopic colorectal cancer, which may be due to small samples or short follow-up times. Meanwhile, some studies have also shown that prophylactic antibiotic use can reduce postoperative complications and mortality. Therefore, the authors believe that larger and longer prospective randomized controlled studies should be conducted to further confirm the above views. In addition, although the effects of laparoscopic surgery and IPC on patients' prognosis have been reported in the literature, there is still a lack of in-depth studies on the potential adverse effects it produces in treatment and the relationship between different doses and frequencies of IPC and patients' prognosis.

## Disclosure statement

The authors declare no conflict of interest.

## References

- [1] Li X, Li J, Wang W, et al., 2023, Comparison of Recent Efficacy of Laparoscopic Surgery with Specimen Retrieved via Natural Cavity and Laparoscopic-assisted Surgery in Radical Rectal Cancer. *Journal of Xi'an Jiaotong University (Medical Edition)*, 44(6): 990–995.
- [2] Sun L, Wan B, Guan B, et al., 2023, Observations on the Effect of Laparoscopic Surgery in the Treatment of Early and Middle Stage Colorectal Cancer. *Chinese Community Physician*, 39(29): 47–49.
- [3] Kong D, Li Z, Zhang S, 2023, Clinical Efficacy of Laparoscopic Radical Colorectal Cancer Treatment for Colorectal Cancer and its Effect on Gastrointestinal Function. *Systemic Medicine*, 8(20): 116–119+127.
- [4] Gao Y, Han X, Mao W, 2023, Study on Factors Affecting the Quality of Resuscitation After Anesthesia for Laparoscopic Surgery in Elderly Patients with Colorectal Cancer. *Life Science Instrumentation*, 21(5): 42–45.
- [5] Dong Y, 2023, Effect of Laparoscopy in Radical Surgery for Colorectal Cancer. *Chinese Community Physician*, 39(28): 50–52.
- [6] Liu Q, Enrietu, Wang T, 2023, Research Progress of Laparoscopic Surgery in the Diagnosis and Treatment Mode of Progressive Colorectal Cancer. *Journal of Practical Clinical Medicine*, 27(19): 143–148.
- [7] Wei C, Wei Y, Meng S, et al., 2023, Efficacy of Reduced-aperture Laparoscopic Surgery for Colorectal Cancer and its Effect on Perioperative Indicators and Immunoinflammatory Response in Patients. *Electronic Journal of Modern Medicine and Health Research*, 7(19): 10–12.
- [8] Xia T, Wang Y, Sun X, et al., 2023, Comparative Analysis of Recent Efficacy of da Vinci Robot and Laparoscopic Surgery in Low and Intermediate Rectal Cancer. *Journal of Xuzhou Medical University*, 43(9): 662–668.
- [9] Si H, Yan Q, Li G, et al., 2023, Evaluation of Clinical Effects of Laparoscopic Surgery and Open Surgery for Colorectal Cancer. *Progress of Modern General Surgery in China*, 26(9): 725–726 + 744.
- [10] Kong D, Zuo G, 2023, Comparative Observation on Postoperative Rehabilitation of Colorectal Cancer Patients by Conventional Laparoscopic Surgery and NOSES. *Contemporary Clinical Journal of Medicine*, 36(4): 31–32.

### Publisher's note

Bio-Byword Scientific Publishing remains neutral with regard to jurisdictional claims in published maps and institutional affiliations.



# Construction of *Lactobacillus casei*-loaded Water-in-oil High Internal Phase Emulsion and its Study on Anti-breast Cancer Properties

Miao Tong\*, Qiao Peng

School of Chemistry, Chemical Engineering and Life Sciences, Wuhan University of Technology, Wuhan 430070, Hubei Province, China

\*Corresponding author: Miao Tong, tongmiao0801@163.com

**Copyright:** © 2024 Author(s). This is an open-access article distributed under the terms of the Creative Commons Attribution License (CC BY 4.0), permitting distribution and reproduction in any medium, provided the original work is cited.

**Abstract:** *Objective:* To prepare an oil-in-water high internal phase emulsion containing *Lactobacillus casei*, and to optimize and characterize the preparation process. To explore the therapeutic effect of the probiotic-carrying emulsion on in situ breast cancer in mice. *Methods:* Using corn oil, sodium alginate, polyglycerin ricinoleate and *L. casei* as raw materials, the high internal phase emulsion containing probiotic oil-in-water was prepared by high-speed homogenization method. The optimal preparation process was obtained through single factor investigation, microstructure characterization, stability investigation and in vitro simulation digestion experiment. Ten female BALB/c mice (SPF grade, 18–20 g) were selected. After the *in situ* breast cancer model was successfully established, the mice were randomly divided into experimental group and control group, with 5 mice in each group. The mice were administrated with probiotic-loaded emulsion and normal saline respectively, and were administrated with the stomach every other day for 10 days. The change of tumor volume during treatment and tumor mass at the end of treatment were recorded. *Results:* The optimum process of emulsion was: With the concentration of 5% Polyglycerin ricinolate, 75% aqueous volume, 3000r/min homogenizing speed, 30 s homogenizing time and 2% aqueous sodium alginate concentration, a high internal phase emulsion with a particle size of  $9.33 \pm 1.74 \mu\text{m}$  and an appearance of milky paste was prepared. The inclusion rate of probiotics reached  $90.97 \pm 27.09\%$ . Breast cancer anti-tumor experiment showed that the tumor inhibition rate of the experimental group reached 33.78% compared with the control group. *Conclusion:* Water-in-oil high internal phase emulsion can effectively protect *L. casei* and reduce the loss of live probiotic when probiotics pass through the digestive fluid environment. Oral intragastric high internal phase emulsion containing *L. casei* oil-in-water has a certain therapeutic effect on breast cancer.

**Keywords:** *Lactobacillus casei*; High interior phase emulsion; Process optimization; Probiotic embedding; Anti-breast cancer

**Online publication:** October 2, 2024

## 1. Introduction

*Lactobacillus casei* belongs to the genus *Lactobacillus*, Gram-positive, facultative anaerobes. Together with *L. acidophilus* and *Bifidobacterium*, it is known as the three major probiotics. After entering the intestinal,

*L. casei* can colonize the intestinal tract and live in great quantities, regulate the intestinal flora balance, and improve human gastrointestinal function<sup>[1]</sup>. At the same time, the study showed that *L. casei* can lower blood pressure, lower cholesterol, improve lactose intolerance, regulate the body's immune, cancer inhibition<sup>[2]</sup>. Usually, probiotics for oral drug delivery way, while probiotics to temperature, environmental factors including oxygen, humidity, pH value of highly sensitive, oral delivery process will in turn through the stomach and small intestine, colon, of which the low pH of the gastric fluid can seriously affect the survival of probiotic. This process will lead to serious loss of probiotic activity at the same time, research has shown that only a sufficient number of viable probiotics ( $\geq 10^7$  CFU/g) released into the human gut can exert its probiotic effect<sup>[3]</sup>. Therefore, due to the characteristics of high safety of biomaterials and good adaptability *in vivo*, it will be an effective method to solve this problem to equip intestinal probiotics with appropriate biomaterials to give them a protective effect and enable probiotics to target the colon<sup>[4]</sup>.

High internal phase emulsion preparation process because of its moderate and more applicable probiotic protection effect<sup>[5]</sup>. The concept of high internal phase emulsion (HIPEs) was put forward by Lissant in the 1960s and refers to the dispersed phase volume fraction of 74.05% or more of the emulsion<sup>[6]</sup>. HIPEs discussed in recent years as a pharmaceutical, food, cosmetics and hot research topic in the field of oil industry. Most sub-embedding methods have greater damage to probiotics, such as the microgel process. Due to dehydration and high temperature, the activity of probiotics was greatly damaged by spray drying. In contrast, high internal phase emulsion is more suitable for probiotic protection due to its mild preparation process. Sodium alginate can bind with bivalent cation ( $\text{Ca}^{2+}$ ,  $\text{Ba}^{2+}$ ) according to the characteristics of the formation of three dimensional network gel due to its high biocompatibility and is often used for the package of probiotic microgel preparation<sup>[7]</sup>. Besides, sodium alginate gel and thickening properties, biodegradable, cheap accessible features, which makes sodium alginate have extensive application value. Sodium alginate is also associated with lowering serum cholesterol, triglycerides, and blood glucose, thus preventing diseases such as hypertension, diabetes, and obesity.

Based on the above content, Michelle CL *et al.* (2019) chose a model by *L. casei*, polyglycerol castor alkyl resin (PGPR) and sodium alginate (SA) as the emulsifier and thickener respectively<sup>[8]</sup>. The preparation of a load of probiotics water-in-oil high internal phase emulsion (w/o HIPEs), at the same time on the storage stability, microbial load capacity, investigation and get the best preparation technology of *in vitro* digestion conditions. At the same time, the anti-tumor effect of the probiotic emulsion was further investigated in the breast cancer model mice implanted with 4T1 cells.

## 2. Materials and methods

### 2.1. Animal feeding

BALB/c mice (female, 18–20 g, SPF grade, License No.: SCXK (E) 2021-0027) were purchased from Hubei Beient Bio-Technology Co., Ltd. They were housed at the SPF Animal Experimental Center of Hubei Provincial Institute for Food and Drug Control (Optics Valley Campus). All animal experimental procedures followed the guidance principles of the Animal Care and Use Committee of the Hubei Provincial Institute for Food and Drug Control and were conducted under aseptic conditions in an SPF environment.

### 2.2. Materials and equipment

*L. casei* (Chinese Typical Culture Preservation Center, strain preservation number AB 2011138); Reagent grade Corn oil (Lot No. C805618), Shanghai Maclin Biochemical Technology Co., Ltd. Sodium alginate (Lot No. C13554334), Shanghai Maclin Biochemical Technology Co., Ltd.; Polyglycerin ricinoleate (PGPR, Lot No. C14639818), Shanghai Maclin Biochemical Technology Co., Ltd. MRS Broth (Lot No. HB0384-

1), Haibo Biotechnology Co., Ltd. Pepsin (pig source), Shanghai Maclin Biochemical Technology Co., Ltd. Trypsin (Biotechnology level), Shanghai Maclin Biochemical Technology Co., Ltd. Pharmaceutical grade TWEEN 80, Shanghai Aladdin Biochemical Technology Co., Ltd. Aseptic PBS (pH 7.4, 500 mL), Gibco, USA; Purified water, laboratory made. High-speed Homogenizer (FSH-2A), Xicheng Xinrui Instrument Factory, Jintan District; Inverted fluorescence microscope (DP72), OLYMPUS Corporation, Japan; pH meter (PHS-3E), Shanghai Leimi Instrument Co., Ltd. Petri dish (90 mm × 15 mm), Beijing Lanjieke Technology Co., Ltd. 50 mL centrifugal tube, 15 mL centrifugal tube, Corning Life Science (Wujiang) Co., Ltd. Disposable sterile syringe (1 mL), Shanghai Jinta Medical Equipment Co., Ltd.

### **2.3. The preparation of probiotic HIPEs**

The preparation method of HIPEs in the experiment was improved by previous studies. The specific process was as follows:

- (1) A one-step emulsification method was used to prepare probiotic emulsion and an appropriate amount of sodium alginate was added into deionized water to prepare 2% sodium alginate solution for use;
- (2) Take 4 mL of probiotic solution (incubated in a 37°C constant temperature incubator and MRS Broth for 2–3 days) and centrifuge it three times;
- (3) After centrifugation, rinse with an equal volume of PBS buffer solution with the probiotic solution;
- (4) Centrifuge again to discard the supernatant, mix 15 mL of 2% sodium alginate with probiotics to prepare a water phase, and then set aside for use;
- (4) Take 5 mL corn oil and an appropriate amount of 1 mL PGRP and mix well to form the oil phase, set aside;
- (5) The water phase is slowly poured into the oil phase at one time and then the high-speed homogenizer is used to stir and homogenize at 3,000 r/min for 30 s to obtain the probiotic-carrying w/o high internal phase emulsion.

### **2.4. HIPEs preparation technology of the single-factor investigation**

According to the results of the preliminary experiment, the blank emulsion was taken as the experimental object, and the appearance of the emulsion after its preparation and standing at room temperature for 24 h was taken as the investigation index. A single-factor experiment was designed to investigate the effects of water phase ratio, PGRP concentration, homogenizing machine speed, homogenizing time and sodium alginate concentration on the preparation of the emulsion, and screen out the factors that have a greater impact on the preparation of the emulsion.

### **2.5. Morphological characterization of HIPEs**

#### **2.5.1. The microstructure of emulsion**

Using an optical microscope microscopic morphology of the latex was characterized, and the blank emulsion a few points on the slide, pressing with the cover glass to remove bubbles, let stand slides to the emulsion to fill the space between the glass and cover glass, through appropriate magnification to observe the microscopic structure of the emulsion.

#### **2.5.2. Particle size measurement**

In order to measure the average particle size of droplets in HIPEs samples, the study used ImageJ software (ImageJ 1.53 K, Nation Institutes of Health, USA) for image analysis. The software calculated the droplet diameter by analyzing the particle size of the emulsion droplet under the optical microscope through image

pixels. At least 100 particles per sample were analyzed.

## **2.6. Stability test**

### **2.6.1. Placement stability test**

Studying the stability of the emulsion in a certain storage period is necessary because the emulsion is unstable in thermodynamics, there is a tendency of coalescence. Puts emulsion samples 3 mL screw in the samples of glass bottles, in 25°C at room temperature, outdoor place, taking picture as record every 7 days.

### **2.6.2. pH stability testing**

Before preparation of the emulsion, methyl orange was in the water phase as a pH indicator, then placed good emulsion preparation in different pH (1, 2, 3, 4, 5) aqueous solution of hydrochloric acid, solution during the filming of a soak 6 h color and emulsion, record emulsion layer state.

## **2.7. *Lactobacillus casei* was counted**

By plate count method to calculate the sample in the number of living bacterium, the specific method for the preparation of microbial load good w/o HIPEs five times diluted with sterile corn oil, will be diluted emulsion with a sterile saline solution containing the 0.5% of polysorbate 80 further dilution to the appropriate concentration, then, take the diluent 0.1 mL evenly coated in MRS agar plate. Then, the agar plates were placed upside down in a constant temperature incubator at  $36 \pm 1^\circ\text{C}$  and incubated for 48 h. The number of viable probiotic colonies in the loaded emulsion was calculated by counting the colonies grown on the agar plates. All the above operations were performed in an ultra-clean workbench.

## **2.8. Storage stability test**

Placed microbial load emulsions in 4°C refrigerator save, at the same time will not join the aseptic package of *Lactobacillus casei* PBS buffer (pH = 7.4), also put in 4°C refrigerator save, take out the sample regularly, with live probiotic counting in ultra-clean workbench.

## **2.9. In vitro digestion simulation of water-in-oil high internal phase emulsion**

### **2.9.1. The preparation of simulated gastric intestinal fluid**

According to 2020 edition pharmacopoeia of the People's Republic of China <sup>[9]</sup>, simulated gastric fluid (SGF) was prepared as follows: 16.4 mL dilute hydrochloric acid, adding water about 800 mL and pepsin 10 g, shake well, add water dilute to 1,000 mL, 0.22 µm membrane filter in addition to probiotic and quick simulated gastric fluid. Simulated intestinal fluid was prepared by taking potassium dihydrogen phosphate 6.8 g, water 500 mL solution, with a 0.1 mol/L sodium hydroxide solution to adjust pH value to 6.8, mixing two solutions, diluted to 1,000 mL with water, and then filtered through 0.22 µm filter membrane to remove probiotic.

### **2.9.2. The experimental process**

To evaluate the gastroprotective capabilities of HIPEs for probiotics, an in vitro digestion experiment mimicking gastrointestinal conditions was conducted based on previous research methodologies <sup>[10]</sup>. Probiotic-loaded HIPEs (1 mL) were incubated in preheated sterile simulated gastric fluid (SGF) at 37°C for 2 hours under agitation at 120 rpm/min to simulate gastric digestion. Subsequently, the emulsion was transferred to simulated intestinal fluid (SIF) and incubated under the same conditions to simulate intestinal digestion for an additional 2 hours. Plate counts were performed at three stages: Before digestion, after simulated gastric digestion, and after simulated intestinal digestion, to assess the protective efficacy of HIPEs against probiotics. All materials and

procedures were conducted under sterile conditions in a laminar flow hood.

## 2.10. Anti-tumor experiments in vivo

After one week of adaptive feeding, 4T1 cells in the logarithmic phase of growth were taken, digested, centrifuged and resuspended in PBS buffer for three times, followed by dilution to  $2 \times 10^6$  cells/mL in PBS. The cell suspension was inoculated subcutaneously into the right mammary gland of mice in 200  $\mu$ L per mouse. When the tumor volume reached 90–110 mm<sup>3</sup>, 10 mice were randomly divided into two groups, the control group and the bacterial emulsion group, with 5 mice in each group. In order to ensure the effect of emulsion dosage volume by 200  $\mu$ L to fill the stomach with medicine (such as control group by gastric volume normal saline). The mice were administrated every other day for a total of 5 times. The body weight of the mice was recorded every day, and the length and short diameter of the transplanted tumor of the mice were measured. The tumor volume and tumor inhibition rate were calculated according to equations (1) and (2), respectively.

$$V = \frac{1}{2} \times \text{short diameter}^2 \times \text{long diameter} \quad (1)$$

$$TGI = \frac{\text{Tumor quality in control group} - \text{Tumor quality in the treatment group}}{\text{Tumor quality in control group}} \times 100\% \quad (2)$$

## 2.11. Data analysis

All experiments are conducted at least three times, and according to these values to compute the mean and standard deviation. Statistical analysis software (SSPS) was used for data analysis. Analysis of variance and t-test were used to test for significant differences between trials ( $P < 0.05$  indicated as \*).

# 3. Results and discussion

## 3.1. Preparation and process screening of W/O HIPEs

By putting a polyglycerol castor alkyd resin (PGPR) and sodium alginate as emulsifier and stabilizer, thickener respectively, under the condition of high speed homogeneous, preparation of corn oil as continuous phase, sodium alginate solution as the dispersed phase of w/o HIPEs, in the process of preparing HIPEs, PGPR concentration, water phase ratio, homogenization speed, homogenization time and sodium alginate concentration can affect the stability and preparation effect of emulsion. A single factor experiment was designed to investigate the above factors and screen out the most influential factors on the stability and preparation effect of the emulsion.

### 3.1.1. Effect of PGPR concentration on the stability and preparation of the emulsion

Fixed at 1.5% of the concentration of alginate, water accounted for 75%, homogeneous speed 4000 r/min, the homogeneous time 45 s. The effects of PGPR concentration (0%, 2.5%, 5%) on the stability and preparation efficiency of the emulsion were investigated. The results are shown in **Figure 1** (The left shows the newly prepared finished appearance, and the right shows the appearance placed for 24 hours) and **Table 1**. Therefore, PGPR concentration of 5% was chosen.

**Table 1.** Results of PGPR dosage investigation

PGPR	0%	2.5%	5%
Appearance	Translucent emulsion	White cream	White cream
Separation	Yes	No	No





**Figure 1.** Appearance analysis of different concentrations of PGPR emulsions

### 3.1.2. Effect of water phase ratio on emulsion stability and preparation effect

The concentration of alginate was fixed at 1.5%, PGPR at 5%, homogenization speed at 4,000 r/min, and homogenization time at 45 s. Inspection water accounted for 60%, 65%, 75%, 85%, the stability of emulsion and preparation of effects. The results are shown in **Figure 2**, **Table 2**, choice of water phase accounted 75%.

**Table 2.** Results of water phase proportion investigation

Water phase	55%	65%	75%	85%
Appearance	White cream	White cream	White cream	White cream
Separation	No	No	No	Yes



**Figure 2.** Appearance analysis diagram of emulsions with different aqueous phase proportions

### 3.1.3. Effect of homogenization speed on the stability and preparation effect of emulsion

Fixed at 1.5% of the concentration of alginate, PGPR concentration 5%, water accounted for 75%, homogeneous, and time is 45 s. Examine homogeneous speed 3,000, 4,000, 5,000 r/min effects on stability of emulsion and preparation. The results are shown in **Figure 3** and **Table 3**, and the homogenization speed was selected as 3,000 r/min.

**Table 3.** Results of homogeneous rotational speed investigation

Homogeneous speed	3,000 r/min	4,500 r/min	6,000 r/min
Appearance	White cream	White cream	White cream
Separation	No	No	No



**Figure 3.** Appearance analysis diagram of emulsions with different homogeneous speed

### 3.1.4. Homogeneous time effects on the stability of emulsion and preparation

Fixed at 1.5% of the concentration of alginate, PGPR concentration of 5%, water accounted for 75%, homogeneous, and the speed of 4,000 r/min. Homogeneous time 45 s, 30 s, 60 s effects on stability of emulsion and preparation. The results are shown in **Figure 4** and **Table 4**. The duration of homogenization was selected as 30s.

**Table 4.** The results of homogeneous time investigation

Homogeneous time	30 s	45 s	60 s
Appearance	White cream	White cream	White cream
Separation	No	No	No



**Figure 4.** Appearance analysis diagram of emulsions with different homogenization time

### 3.1.5. Effect of sodium alginate concentration on the stability and preparation of emulsion

The concentration of PGPR was fixed at 5%, the proportion of the water phase was 75%, the homogenization speed was 4,000 r/min, and the homogenization time was 45 s. The effects of 0%, 1%, 1.5% and 2% sodium alginate on emulsion stability and preparation efficiency were investigated. The results are shown in **Figure 5** and **Table 5**. According to the results of single factor experiment, the proportion of water phase, PGPR and sodium alginate concentration were the main factors affecting the stability and preparation effect of the emulsion. Preparation technology, therefore, choose water accounted for 75%, 5% concentration of PGPR, homogeneous speed 3,000 r/min, the homogeneous time 30 s. The optimal concentration of sodium alginate needs to be further determined by subsequent experiments.

**Table 5.** Results of SA concentration investigation

SA	0%	1.0%	1.5%	2%
Appearance	Partial emulsification	White cream	White cream	White cream
Separation	Yes	No	No	No



**Figure 5.** Appearance analysis of emulsions with different SA concentrations

### 3.2. HIPEs microstructure characterization

The preparation of sodium alginate concentration was 1%, 1.5%, and 2%, three different formulations of HIPEs, the HIPEs were characterized by the confocal microscope, three different formulations of emulsions can observe water droplets, and fit closely, showed the characteristics of the high internal phase emulsion, microstructure and particle size distribution as shown in **Figure 6**. Results showed that 1%, 1.5%, and 2% in three different formulations of HIPEs diameter were  $21.01 \pm 5.90 \mu\text{m}$ ,  $20.91 \pm 7.85 \mu\text{m}$  and  $9.33 \pm 1.74 \mu\text{m}$ . When sodium alginate concentration increases, the emulsion droplet size decreases, and the droplet size is more uniform. The result may be due to the concentration of sodium alginate in droplets increasing, the viscosity increase of the emulsion system, system of dispersed phase is not easy to gather and condense to form larger droplets. At the same time, sodium alginate forms a three-dimensional network structure in the droplet, which can stabilize the droplet structure<sup>[11]</sup>. However, the higher the concentration, the denser the network structure inside the droplet, and the weaker the tendency of droplet aggregation, making the particle size decrease with the increase of sodium alginate concentration.

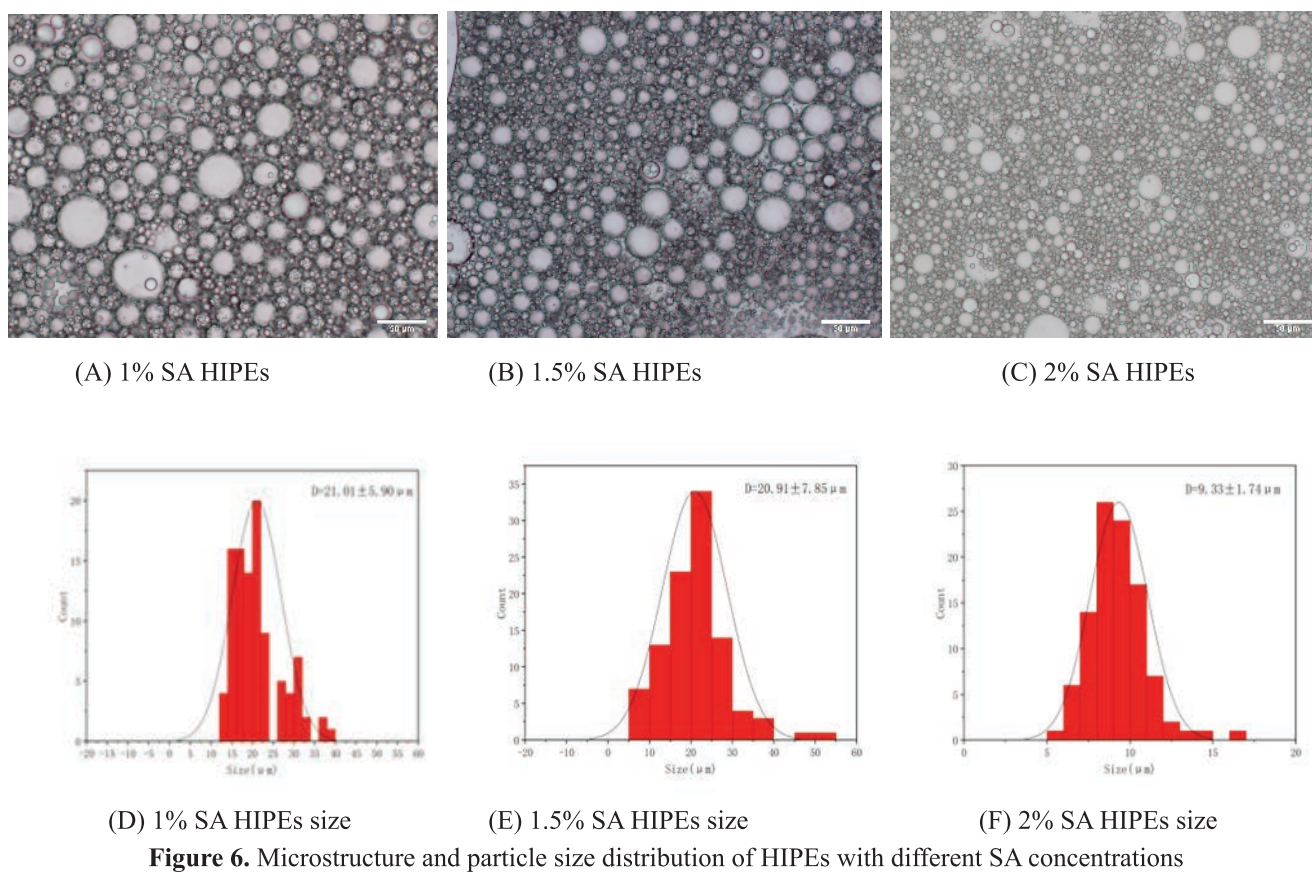


**Figure 6.** Microstructure and particle size distribution of HIPEs with different SA concentrations

### 3.3. Evaluation of stability

#### 3.3.1. Stability of placement

To investigate the stability of HIPEs, 3 mL of three emulsions with SA concentrations of 1%, 1.5%, and 2% were placed in glass bottles with threaded mouths at room temperature, respectively, and observed every 7 days, and images were taken, as shown in **Figure 7**, according to the results from the 14th day, 1% and 1.5% concentration of SA HIPEs appear stratified, the former layer is more obvious than the latter, 2% concentration of SA HIPEs layered began from 21 days, with the increase of mixing time, emulsion layering is more obvious. The stability difference might be due to the following two reasons:

- (1) Three HIPEs droplet sizes with the concentration of rising and falling, generally, larger droplet size



suggests HIPEs will with the passage of time is not stable, because of their small particle size has a larger surface area, which has a higher bulk density and stability <sup>[12]</sup>.

- (2) With the higher concentration of sodium alginate, the higher the concentration of sodium alginate in droplet formation of the gel network structure is more stable close <sup>[13]</sup>, at the same time, the higher the layered system makes the dispersed phase viscosity is not easy to gather.

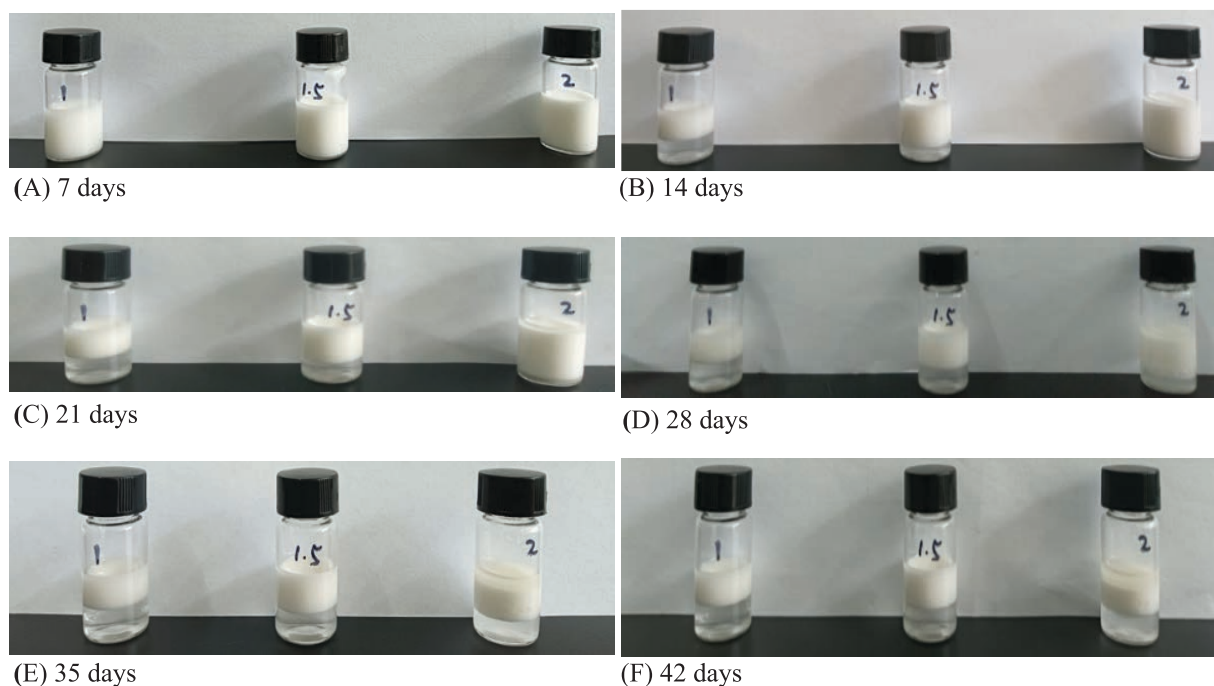


**Figure 7.** Results of HIPEs placement stability at different SA concentrations

### 3.3.2. Stability of pH

Probiotics are easy to be inactivated in acidic conditions because there is a high concentration of hydrogen ions leading to damage to the cell membrane. Therefore, the stability of HIPEs in hydrochloric acid under different pH conditions (1, 2, 3, 4, 5) was evaluated according to the reference scheme <sup>[14]</sup>. An acid-base indicator (methyl orange) was added to the aqueous phase. The stability of HIPEs to acid was evaluated and the results are shown in **Figure 8**. The results showed that the structure of HIPEs at 1% SA concentration in water was extremely unstable and could not maintain its morphology, and the aqueous phase containing methyl orange was largely transferred into hydrochloric acid. 1.5% and 2% concentrations of SA HIPEs in hydrochloric acid can maintain the stability of the basic form, color itself did not change. Compared with 2%, and 1.5% HIPEs there is still a small amount of water in the hydrochloric acid. The above results can be attributed to the difference in emulsion viscosity, the lower the viscosity, the more unstable the emulsion forms in hydrochloric acid, and the viscosity difference between the emulsions may be due to the positive correlation between the viscosity of the emulsion and the viscosity of the dispersed phase (aqueous phase). With the increase of the concentration of sodium alginate, the thickening effect becomes stronger and the viscosity of the emulsion increases.

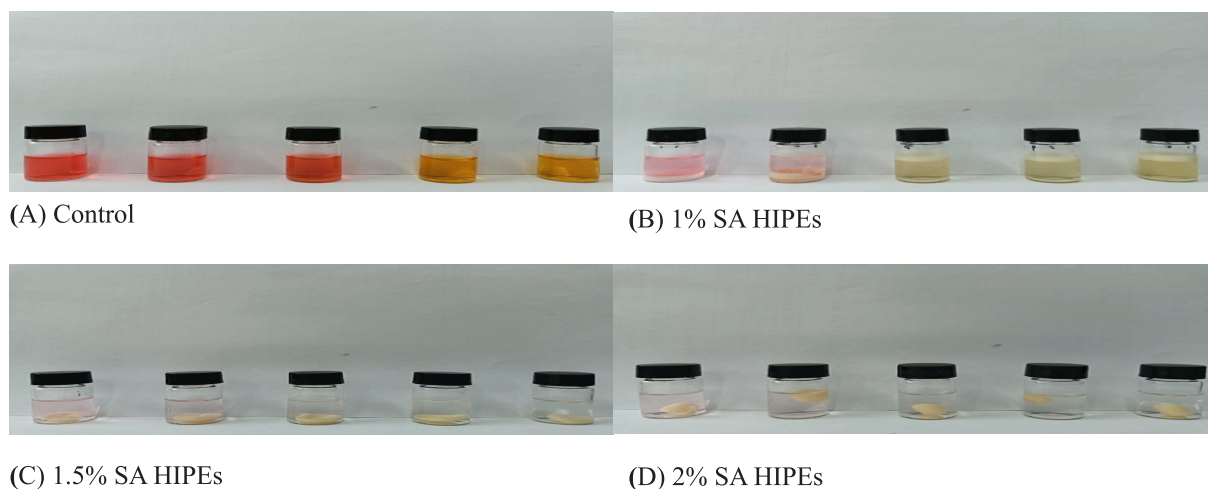


**Figure 8.** Stability of emulsions under different pH conditions

### 3.3.3. Storage stability evaluation

The survival situation during the embedding process is necessary. If a large number of probiotics die during the preparation process, the subsequent protection is meaningless, and the quality of the embedding process is measured by the embedding rate. In addition, the survival of probiotics during storage with loaded HIPEs was of concern, so the number of viable probiotics was measured after 5 days of storage at 4°C for both encapsulated and unencapsulated probiotics (**Figure 9**). As shown in **Figure 10**, the microbial load of the 2% concentration of SA HIPEs embedding rate was  $90.97 \pm 27.09\%$  is significantly higher than 1.5% concentration of SA the embedding rate was  $56.12 \pm 11.03\%$ , which may be due to the higher concentration of SA to form the more populated gel mesh structure, reduced the probiotics in the process of high-speed homogeneous mechanical damage. After 5 days storage at 4°C, the number of viable probiotics in 1.5% SA group increased from  $8.06 \pm 0.09 \log \text{CFU/mL}$  to  $7.60 \pm 0.19 \log \text{CFU/mL}$ . 2% of the number of living bacterium SA group from  $8.30 \pm 0.08 \log \text{CFU/mL}$  –  $7.79 \pm 0.17 \log \text{CFU/mL}$ . The number of viable probiotics in the unembedded group increased from  $8.30 \pm 0.12 \log \text{CFU/mL}$  to  $7.34 \pm 0.07 \log \text{CFU/mL}$ . The storage stability of embedded probiotics was better than that of unembedded probiotics, indicating that loading probiotics into HIPEs could increase the viability of probiotics, which may be due to the oil layer of W/O emulsion isolating the erosion of external water, oxygen, inorganic salts and other substances, thereby protecting the probiotics dispersed in the aqueous phase and improving the survival of probiotics.

$$\text{Embedding rate} = \frac{\text{The actual number of viable bacterial colonies after embedding}}{\text{After the embedding theory of living bacterium colony number}} \times 100\% \quad (3)$$

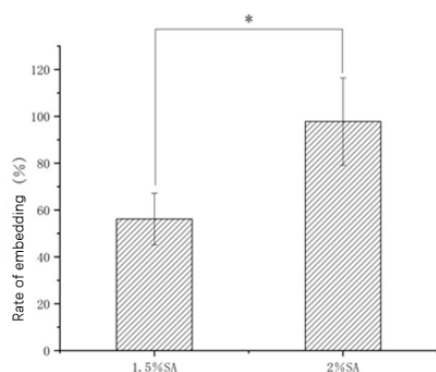


**Figure 9.** The embedding rate ( $n = 3$ )

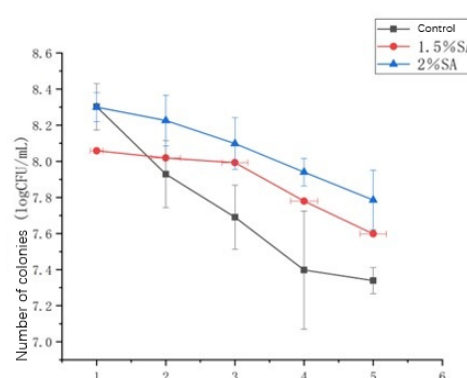


**Figure 10.** Count of viable probiotics stored at 4°C ( $n = 3$ )

### 3.4. HIPEs in vitro simulated digestion experiments

Simulated digestion in vitro can directly reflect the protective effect of HIPEs on probiotics, which has a guiding significance for the digestion of HIPEs in vivo. The simulated digestion results in vitro are shown in **Figure 11**. After digestion with gastric fluid, the viable number of probiotics without emulsion protection increased from  $8.32 \pm 0.16$  log CFU/mL to 0 CFU/mL. 1.5% and 2% after simulated gastric fluid to digest HIPEs SA concentration of  $8.06 \pm 0.09$  log CFU/mL and  $7.91 \pm 0.25$  log CFU/mL and  $8.30 \pm 0.08$  log CFU/mL and  $8.05 \pm 0.16$  log CFU/mL. After simulated intestinal fluid digestion, they were  $7.43 \pm 0.57$  log CFU/mL and  $7.76 \pm 0.15$  log CFU/mL. The results showed that *L. casei* was difficult to survive in the strong acid environment of gastric fluid, and the protective effect of HIPEs of 2% SA was slightly better than that of 1.5% SA. According to the previous stability analysis, the HIPEs of 2% SA were more stable, so it could better isolate the damage of *L. casei* contained in it by strong acid, enzyme and inorganic salt.

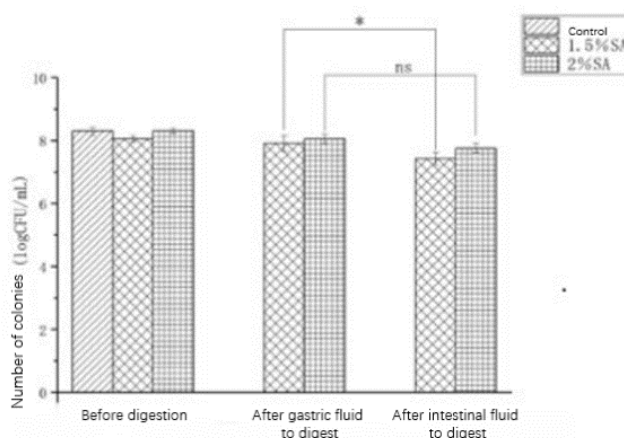


**Figure 11.** Probiotic count at different stages of simulated digestion in vitro ( $n = 3$ )

### 3.5. Probiotics HIPEs antitumor evaluation

Results as shown in **Figure 12** and shown in **Table 6**, compared with gastric normal saline control group, to fill the stomach take *Lactobacillus casei* HIPEs treatment group tumor volume growth, be suppressed, the 14th day control tumor size  $1,565.85 \text{ mm}^3$ , this could be due to *L. casei* engraftment in colon in mice, improve the intestinal flora environment<sup>[15,16]</sup>, at the same time, *L. casei* showed an inhibitory effect on tumor growth. The tumor inhibition rate reached 33.78%, and the figure shows the volume change trend of the mice. There was no abnormal change in the body weight of the mice in the treatment group, which was attributed to the fact that there was no significant negative effect on the appetite and metabolism of the mice during the treatment with probiotic-loaded HIPEs.

**Table 6.** Tumor quality and inhibition rate in each group

Group	Tumor quality (g)	Tumor growth inhibition rate (TGI)
Control	$0.57 \pm 0.12$	/
Probiotic	$0.38 \pm 0.20$	33.78%

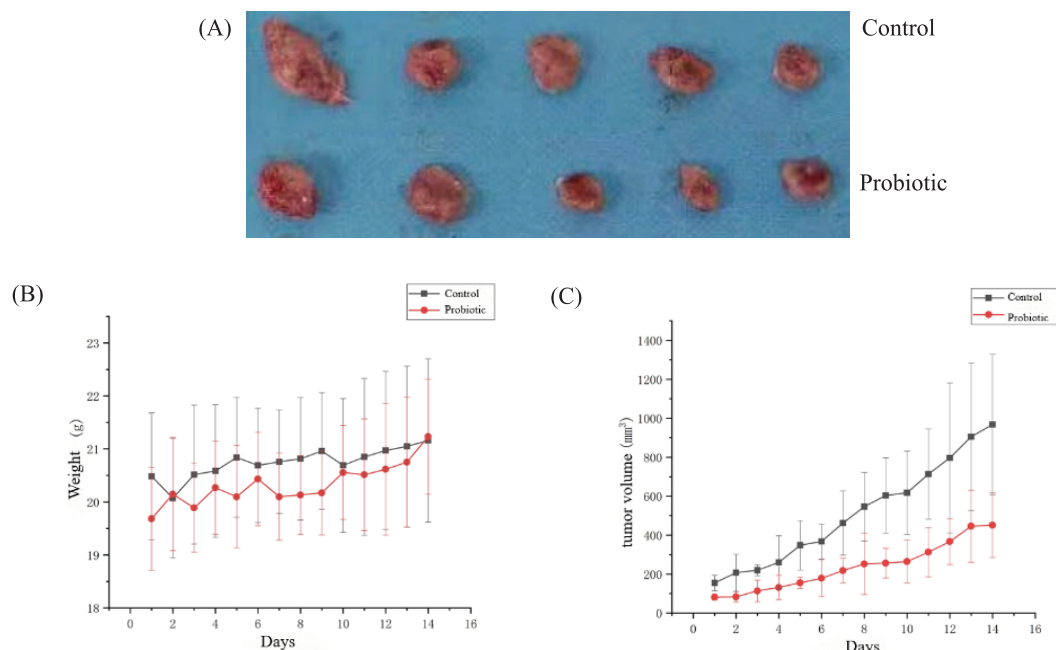


**Figure 12.** (A) Physical tumor images of control group and treatment group; (B) Weight change curve of mice in control group and treatment group; (C) Tumor volume change curve between treatment group and control group ( $n = 5$ )

## 4. Conclusion

In this study, a w/o HIPE was developed to encapsulate *L. casei*, focusing on preparation, stability, appearance, microstructure, and *in vitro* digestion. The optimized formulation included 5% polyglycerol polyricinoleate, 75% aqueous phase volume, homogenization at 3,000 rpm for 30 seconds, and 2% sodium alginate in the aqueous phase. Post *in vitro* digestion, the w/o HIPE maintained *L. casei* viability above  $10^7$  CFU/mL, demonstrating effective probiotic encapsulation and gastrointestinal protection. The emulsion's outer oil phase shielded probiotics from gastric acid and intestinal enzymes, highlighting its potential in food and medical applications. Additionally, the study explored w/o HIPE's potential in breast cancer therapy, showing a 33.78% tumor inhibition rate versus controls. Future research should investigate its antitumor mechanisms and synergies with chemotherapy to enhance *L. casei*'s therapeutic benefits.

## Disclosure statement

The authors declare no conflict of interest.

## References

- [1] Chen C, Zhang XC, Yuan HB, et al., 2019, Research Progress and Advanced Technology of Probiotics Embedding. Chinese Journal of Food Science, 23(1): 384–396.
- [2] Le J, Li RY, Li X, et al., 2022, Research Progress of Intestinal Flora and Cancer Occurrence and Treatment. Journal of Kunming University of Science and Technology (Natural Science Edition), 47(1): 70–75.
- [3] Tian WJ, Zhu YD, Yue LF, et al., 2016, Research Status of Probiotics Microencapsulation. Chinese Journal of Food Science, 16(8): 186–194.
- [4] Zhang RY, Yi YR, Zhao JC, et al., 2023, Dietary Fiber Microcapsule Research Progress in the Application of

Probiotics Embedding. *Journal of Food and Fermentation Industry*, 49(23): 324–331.

- [5] Zhang Y, Xie YF, Liu H, et al., 2022, Probiotic Encapsulation in Water-in-Oil High Internal Phase Emulsions: Enhancement of Viability Under Food and Gastrointestinal Conditions. *Lwt*, 163: 113499.
- [6] Wei J, Chen YL, Gao YX, et al., 2022, Preparation of High Internal Phase Lotion and Its Application in Food. *Chinese Journal of Food*, 22(4): 418–429.
- [7] Guo X, Wang Y, Qin Y, et al., 2020, Structures, Properties, and Application of Alginic Acid: A Review. *International Journal of Biological Macromolecules*, 162: 618–628.
- [8] Michelle CL, Chen T, Raheleh R, et al., 2019, Ultrastable Water-in-Oil High Internal Phase Emulsions Featuring Interfacial and Biphasic Network Stabilization. *ACS Applied Materials Interfaces*, 11(29): 26433–26441.
- [9] Wang LF, Wang CY, Li JW, et al., 2023, *Chinese Journal of Microecology*, 35(11): 1280–1285/1291.
- [10] Liu YL, 2021, Anti-Tumor Effect of Bifidobacterium Encapsulated in Chitosan/Alginate Microgel Combined with Small Molecule PD-L1 Inhibitor on Rectal Cancer in situ, thesis, Jilin University.
- [11] Saehun M, Yongdoo C, Shin-Joung R, et al., 2010, Preparation and Characterization of Water/Oil/Water Emulsions Stabilized by Polyglycerol Polyricinoleate and Whey Protein Isolate. *Journal of Food Science*, 75(2): E116–25.
- [12] Chen T, Michelle CL, Seyedramin P, et al., 2018, Sonochemically Synthesized Ultrastable High Internal Phase Emulsions via a Permanent Interfacial Layer. *ACS Sustainable Chemistry Engineering*, 6(11): 14374–14382.
- [13] Patel RA, Rodriguez Y, Lesaffer A, et al., 2014, High Internal Phase Emulsion Gels (HIPE-gels) Prepared Using Food-Grade Components. *RSC Advances*, 35: 18136–18140.
- [14] Zhang Y, 2022, Construction of Probiotics Loaded Water-in-Oil Emulsion and Development of Related Products, thesis, Nanchang University.
- [15] Liang ZY, Liu Y, Xue ML, et al., 2017, Inhibitory Effect of Lactobacillus casei on Dimethylbenzanthracene-Induced Breast Tumor in Rats and Its Immunological Mechanism. *Cancer, Aberration, Mutation*, 29(1): 7–12.
- [16] Félix A, Silvia C, Gabriela P, et al., 2015, Inhibition of Growth and Metastasis of Breast Cancer in Mice by Milk Fermented with Lactobacillus casei CRL 431. *Journal of Immunotherapy (Hagerstown, Md: 1997)*, 38(5): 185–96.

**Publisher's note**

Bio-Byword Scientific Publishing remains neutral with regard to jurisdictional claims in published maps and institutional affiliations.



# Tissue Engineering of Cornea via Type 1 Collagen Biomaterials – A perspective

**Kirubanandan Shanmugam\***

Independent Research Professional, Chennai, Tamilnadu, India

*\*Corresponding author:* Kirubanandan Shanmugam, [ksh1005@yahoo.com](mailto:ksh1005@yahoo.com)

**Copyright:** © 2024 Author(s). This is an open-access article distributed under the terms of the Creative Commons Attribution License (CC BY 4.0), permitting distribution and reproduction in any medium, provided the original work is cited.

**Abstract:** Engineering corneal tissue has advanced significantly in recent years. Engineering a biocompatible, mechanically stable and optically clear tissue presents significant engineering hurdles. Two fundamental strategies have been explored by researchers to address these issues: (1) cell-based methods for controlling cells extracellular matrix and (2) scaffold-based methods for supplying dense, transparent matrices for cell growth. Both approaches have had considerable level of success. Additionally, new developments in innervating a tissue-engineered construct have been developed. Future research must concentrate on enhancing the mechanical stability of engineered constructions and the host reaction to implantation. Type 1 collagen biomaterial has been used for the construction of scaffolds or implantation for cornea repair. Various methods for the fabrication of the scaffolds have been described and mentioned tissue engineering applications for cornea repair and regeneration. Given this correspondence, type 1 collagen was a potential base biomaterial for tissue engineering scaffold fabrication for effective repair/restoration/regeneration of cornea.

**Keywords:** Cornea repair; Tissue engineering; Type 1 collagen; Biomaterial; Fabrication methods; Clinical practice

**Online publication:** October 2, 2024

## 1. Introduction

Tissue engineering offers a promising approach to cornea repair by utilizing a combination of cells, scaffolds and growth factors to regenerate damaged corneal tissue. In the context of corneal repair, researchers are exploring various strategies to develop bioengineered corneal substitutes that can mimic the structure and function of the native cornea. One common approach involves seeding corneal cells onto biocompatible scaffolds that provide structural support and guidance for tissue regeneration. These scaffolds can be made from natural or synthetic materials and are designed to degrade over time as the new tissue forms. In addition to scaffolds, growth factors play a crucial role in promoting cell proliferation, differentiation, and tissue remodeling during corneal repair. By incorporating growth factors into the engineered constructs, researchers can enhance the regenerative capacity of the cells and accelerate the healing process. Overall, tissue engineering holds great promise for cornea repair by offering customized solutions that can address the specific needs of individual patients. As research in this field progresses, it can be expected to see more advanced and effective

strategies for treating corneal injuries and diseases.

Tissue engineering of the cornea is a rapidly advancing field aimed at addressing the significant global need for corneal replacements due to disease, injury or congenital defects. The cornea is a critical component of the eye, contributing to vision by focusing light onto the retina. Damage to the cornea can lead to impaired vision or blindness. Tissue engineering offers promising solutions by developing biocompatible, functional corneal substitutes. Here's an overview of the current state, challenges, and future perspectives in corneal tissue engineering:

## **2. Current approaches in corneal tissue engineering: Scaffold-based techniques**

- (1) **Biodegradable polymers:** Polymers such as collagen, gelatin, and synthetic materials like polylactic-glycolic acid (PLGA) are used to create scaffolds that mimic the extracellular matrix of the cornea.
- (2) **Nanofibrous scaffolds:** Electrospinning techniques produce nanofibrous scaffolds that closely resemble the natural structure of the corneal stroma, promoting cell attachment and growth.
- (3) **Hydrogels:** Hydrogels, such as those based on hyaluronic acid or polyethylene glycol, provide a hydrated environment conducive to cell survival and proliferation.
- (4) **Cell-based approaches:** Stem cells such as mesenchymal stem cells (MSCs), limbal stem cells, and induced pluripotent stem cells (iPSCs) are explored for their ability to differentiate into corneal cells (keratocytes, epithelial cells, and endothelial cells).
- (5) **Cell sheets:** Culturing corneal cells into cell sheets without the use of scaffolds for transplantation to repair damaged corneal tissue.
- (6) **Decellularized corneal matrices:** Natural corneal scaffolds involve the decellularization of donor corneas to remove cellular components while preserving the extracellular matrix. This scaffold can then be recellularized with patient-specific cells.
- (7) **3D Bioprinting:** Layer-by-layer printing can be carried out using bio-inks composed of cells and biomaterials to print corneal constructs layer-by-layer, replicating the complex architecture of the cornea.

## **3. Challenges in corneal tissue engineering**

In corneal tissue engineering, several challenges need to be addressed for successful clinical translation. One major challenge is achieving proper cellular organization and alignment within the engineered tissue to mimic the native corneal structure accurately. Ensuring appropriate mechanical strength and transparency while promoting integration with the surrounding tissues is crucial for functional outcomes. Another challenge is developing biomaterials that are biocompatible, biodegradable and capable of supporting cell growth and differentiation. Achieving proper innervation and vascularization within the engineered corneal tissue is another hurdle as these are essential for maintaining tissue health and functionality. Controlling the immune response to prevent rejection of the implanted tissue is also a significant challenge in corneal tissue engineering. Additionally, scaling up production methods to meet the demand for corneal transplants worldwide is a logistical challenge that needs to be addressed. Overall, addressing these challenges through interdisciplinary collaborations, innovative biomaterials, advanced fabrication techniques and thorough preclinical testing will be essential for the successful development and clinical application of engineered corneal tissue.

- (1) **Biocompatibility and immunogenicity:** Ensuring that engineered corneal tissues are biocompatible and do not elicit an immune response upon implantation is critical for their success.

- (2) Mechanical properties: Replicating the unique mechanical properties of the native cornea, such as transparency, strength, and elasticity, remains a significant challenge.
- (3) Cell source and viability: Finding reliable and ethically acceptable sources of corneal cells and ensuring their long-term viability and functionality in engineered tissues.
- (4) Vascularization and innervation: Engineering corneal tissues that integrate well with the host's vasculature and nerve supply to maintain transparency and function.
- (5) Scaffold degradation: Controlling the degradation rate of scaffolds to match tissue regeneration without compromising the structural integrity of the corneal construct.

#### 4. Future perspectives

- (1) Advanced biomaterials and smart materials: Development of smart biomaterials that respond to environmental cues to promote cell growth and tissue regeneration.
- (2) Bioactive molecules: Incorporation of growth factors, peptides and other bioactive molecules to enhance cell proliferation and differentiation.
- (3) Gene editing and regenerative medicine (CRISPR/Cas9): Utilizing gene-editing technologies to correct genetic defects in corneal cells or enhance their regenerative capabilities.
- (4) Regenerative approaches: Combining tissue engineering with regenerative medicine techniques to improve outcomes.
- (5) Personalized medicine (Patient-specific scaffolds): Using patient-specific cells and 3D printing technologies to create customized corneal implants tailored to individual patient needs.
- (6) Clinical translation and trials (Regulatory approvals): Navigating regulatory pathways to bring engineered corneal tissues from the lab to clinical practice.
- (7) Long-term studies: Conducting long-term clinical trials to assess the safety, efficacy, and durability of engineered corneal tissues.
- (8) Interdisciplinary collaboration research: Encouraging collaboration between material scientists, biologists, clinicians and engineers to accelerate advancements in corneal tissue engineering.
- (9) Funding and support: Securing funding and support from governmental and non-governmental organizations to drive research and development efforts.

Tissue engineering of the cornea holds great promise for addressing the global shortage of donor corneas and providing new treatments for corneal diseases and injuries. Advances in biomaterials, cell biology and engineering technologies are driving progress in this field. Overcoming the existing challenges through innovative research and interdisciplinary collaboration will be key to realizing the full potential of engineered corneal tissues and improving patient outcomes.

Corneal repair is a critical area in ophthalmology due to the importance of the cornea in vision. Several approaches have been developed to repair or replace damaged corneal tissue, ranging from traditional methods to advanced tissue engineering techniques. Here's an overview of various approaches for cornea repair.

- (1) Traditional approaches: Corneal transplantation (Keratoplasty)
  - (a) Penetrating keratoplasty (PK): Full-thickness corneal transplant where the entire damaged cornea is replaced with a donor cornea.
  - (b) Lamellar keratoplasty: Partial-thickness transplant where only the affected layers of the cornea are replaced.
  - (c) Anterior lamellar keratoplasty (ALK): Replaces the front layers of the cornea.



- (d) Deep anterior lamellar keratoplasty (DALK): Replaces all layers down to Descemet's membrane.
- (e) Descemet's stripping endothelial keratoplasty (DSEK/DMEK): Replaces only the damaged endothelial layer.
- (f) Corneal cross-linking (CXL): A procedure used to treat keratoconus and other corneal ectasias by strengthening the collagen fibers in the cornea using riboflavin (vitamin B2) and ultraviolet light.
- (g) Amniotic membrane transplantation: Use of amniotic membrane, which has anti-inflammatory and anti-scarring properties, to promote healing of the corneal surface.
- (2) Advanced approaches: Tissue engineering and biomaterials
  - (a) Scaffold-based techniques: Use of biodegradable polymers, hydrogels, and nanofibrous scaffolds to create structures that mimic the corneal extracellular matrix.
  - (b) Decellularized corneal matrices: Removing cells from donor corneas to create a scaffold that can be recellularized with patient-specific cells.
- (3) Cell-based therapies
  - (a) Stem cell therapy: Use of stem cells (e.g., limbal stem cells, mesenchymal stem cells, and induced pluripotent stem cells) to regenerate damaged corneal tissue.
  - (b) Cell sheets: Culturing corneal cells into sheets that can be transplanted to repair the cornea.
  - (c) Gene therapy (Gene editing): Using techniques like CRISPR/Cas9 to correct genetic defects in corneal cells or to enhance their regenerative capabilities.
- (4) 3D bioprinting (Layer-by-layer printing): Utilizing 3D bioprinting technology to create corneal structures with precise architecture and cell placement, closely replicating natural corneal tissue.
- (5) Artificial corneas (Keratoprotheses)
  - (a) Synthetic implants: Development of biocompatible synthetic corneas, such as the Boston Keratoprosthesis and the AlphaCor, to replace damaged corneal tissue.
  - (b) Hydrogel-based implants: Newer approaches use hydrogels that are similar to natural corneal tissue, promoting integration and reducing the risk of rejection.
- (6) Nanotechnology
  - (a) Nanomaterials: Incorporation of nanomaterials to improve the mechanical properties and biocompatibility of corneal implants.
  - (b) Nanomedicine: Use of nanoparticles for targeted drug delivery to the cornea to promote healing and reduce inflammation.
- (7) Bioactive molecules
  - (a) Growth factors: Incorporation of growth factors and cytokines in scaffolds or hydrogels to promote cell proliferation and differentiation.
  - (b) Anti-inflammatory agents: Use of bioactive molecules to reduce inflammation and enhance healing.
- (8) Regenerative medicine
  - (a) Combination therapies: Combining cell therapy, gene therapy, and tissue engineering to create more effective treatments for corneal repair.
  - (b) Patient-specific treatments: Development of personalized medicine approaches, using patient-specific cells and materials to create customized corneal implants.
- (9) Interdisciplinary collaboration
  - (a) Cross-field innovations: Collaboration between material scientists, biologists, engineers, and clinicians to develop novel materials and techniques for corneal repair.
  - (b) Clinical translation: Bridging the gap between laboratory research and clinical application through

robust clinical trials and regulatory approvals.

Various approaches for corneal repair offer a range of solutions from traditional methods like keratoplasty to cutting-edge techniques involving tissue engineering, stem cell therapy, and 3D bioprinting. The field is evolving rapidly, with promising advancements that aim to improve the outcomes for patients with corneal damage. Future developments will likely focus on enhancing the biocompatibility, functionality, and accessibility of these treatments, ultimately contributing to better vision health worldwide.

Corneal vision loss affects 10 million people worldwide, with approximately 40,000 corneal transplants performed annually in the United States. The growing need for corneal transplants is limited to allogenic and synthetic materials. Recently, autologous limbal stem cell transplantation has been an effective therapeutic option for corneal regeneration <sup>[1]</sup>. However, allogenic materials from human donors are the preferred choice, but they have limitations such as the limited availability of quality donor graft material with their consent and tissue rejection in the host person <sup>[2]</sup>. Traditional penetrating keratoplasty has been replaced by partial lamellar keratoplasty, which has increased implant success rates. The need for transplantable cadaveric corneas in developing countries is also increasing due to limited cadaveric donation <sup>[3]</sup>. Keratoprotheses, synthetic homologs, are used for full-thickness corneal replacement in severe ocular surface pathologies and eyes with limbal stem cell deficiency. The Boston type-1 keratoprosthesis is the most common, but its short-term visual recovery is limited by complications like glaucoma and endophthalmitis <sup>[4]</sup>. Osteo-odonto-keratoprosthesis has shown good long-term anatomical survival rates and is currently the most common treatment for end-stage inflammatory corneal diseases <sup>[5]</sup>.

The human cornea is a transparent, avascular connective tissue that provides the optical interface, protection from infections, and transparency. It consists of three distinct cellular layers: (1) corneal epithelium, (2) stroma, and (3) endothelium, separated by Bowman's layer and Descemet's membranes. Figure 1 reveals the structure of cornea in the eye. The corneal epithelium is a stratified, non-keratinized squamous tissue with nociceptive nerve endings and a biological barrier function. It regulates water and soluble components transfer into or out of the stroma, allowing coherent light refraction. The tear film serves as a reservoir for antibacterial and growth factors, maintaining epithelial homeostasis, proliferation, and repair. Bowman's membrane, a 15 µm thick acellular layer, may act as a molecular barrier or contribute to corneal shape. The corneal stroma, comprising approximately 90% of the overall cornea thickness, consists of aligned collagen fibrils called lamellae. The keratocytes maintain the matrix components of the lamellar connective tissue. Descemet's membrane anchors the corneal endothelial layer, while the endothelium removes water from the stroma and maintains stromal hydration. The cornea's functions require a corneal substitute or tissue model to provide protection, transparency, and substantial refractive power. The stroma, a dense connective tissue, provides lateral tensile strength, while the epithelium protects the stroma and endothelium from chemical injuries. The cornea's transparency is determined by collagen interfibrillar spacing and tissue state of hydration <sup>[6]</sup>.

Two primary strategies are being investigated to meet the increasing demand for corneal transplants: (1) allogenic and (2) synthetic materials. Currently, allogeneic tissue from human donors is the recommended option. However, donated corneal tissue is in short supply globally. Furthermore, tissue rejection frequently restricts this approach's long-term efficacy. On the other hand, because they have a high rate of graft failure, synthetic homologs to donor corneal grafts are generally regarded as temporary substitutes until appropriate donor tissue becomes available. To eliminate the necessity for animal testing of commercial items, tissue-created cornea analogues would offer efficient alternatives and substitutes for corneal tissue. This overview covers recent developments towards meeting these needs as well as outlooks for the future <sup>[7]</sup>.

In addition to that, type 1 collagen from bovine tendons has been used in research and clinical trials for

cornea repair. Collagen is a key structural protein in the cornea, providing support and strength to the tissue. By using type 1 collagen derived from bovine tendons, researchers and medical professionals aim to provide a biomimetic scaffold that can support corneal tissue regeneration and repair. The use of type 1 collagen from bovine tendons for cornea repair involves creating a scaffold that mimics the natural extracellular matrix of the cornea. This scaffold can be used to support the growth and organization of corneal cells, promoting tissue regeneration and repair. In some cases, this scaffold may be combined with corneal cells or other growth factors to further enhance the repair process. Clinical trials and research studies have shown promising results for the use of type 1 collagen from bovine tendons in cornea repair. This approach has the potential to offer a biocompatible and effective treatment for corneal injuries, diseases and abnormalities. It is important to note that the use of bovine-derived collagen raises ethical and safety considerations, and alternative sources of collagen, such as recombinant or human-derived collagen, are also being explored for cornea repair applications. Additionally, regulatory approval and further clinical validation are necessary before this approach becomes widely available for cornea repair in clinical settings<sup>[8]</sup>.

This paper deals with the tissue engineering of cornea via type 1 collagen biomaterial and various methods for scaffold fabrication which is used to reconstruct the damaged cornea. In addition to that, this paper reviews the tissue engineering strategies for damaged cornea into a regenerated cornea.

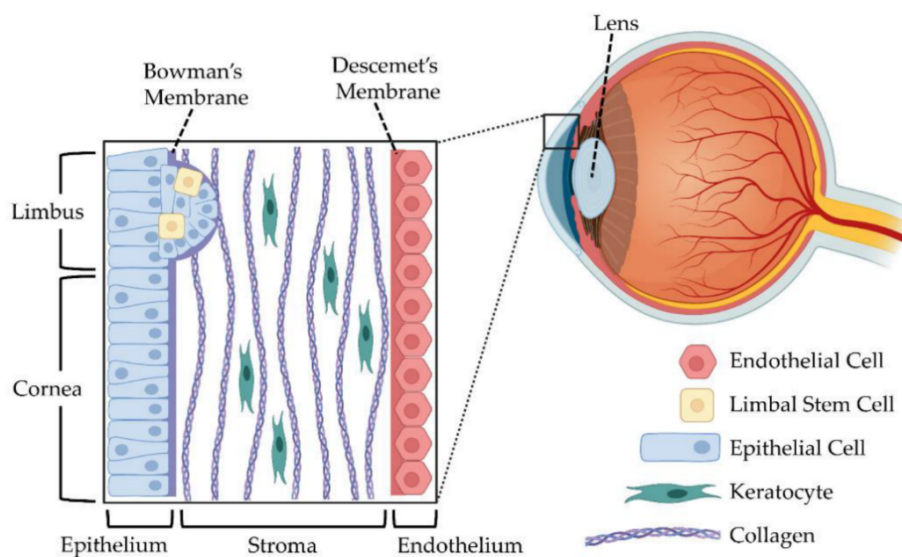


**Figure 1.** The outermost layer of the human eye is called the cornea. The stroma, endothelium, and epithelium are some of the layers that make up this translucent, avascular tissue. The limbus, Bowman's membrane, and Descemet's membrane are other elements<sup>[9]</sup>. Produced with Biorender.com.

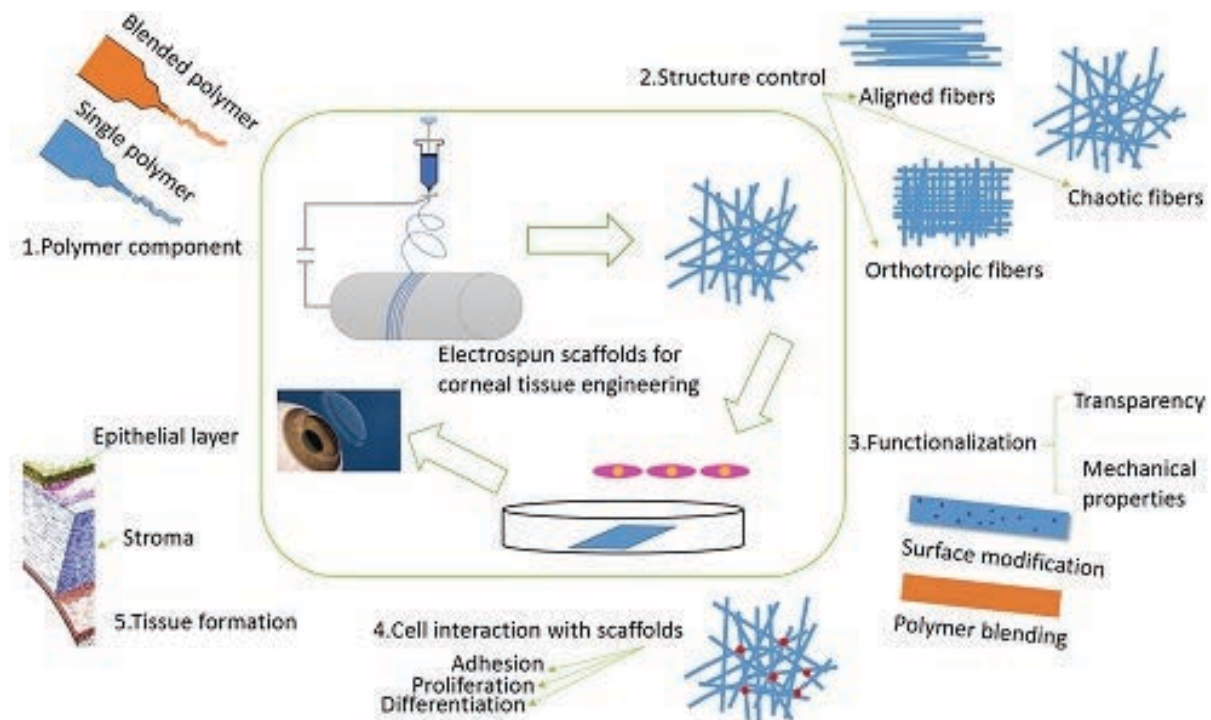


**Figure 2.** Corneal tissue engineering.

## 5. Treatment of cornea repair via tissue engineering

Corneal repair through tissue engineering involves creating bioengineered corneal tissue to replace damaged or diseased corneas. This process typically begins by obtaining cells, such as corneal epithelial cells, stromal cells and endothelial cells, from the patient or a donor. These cells are then grown and expanded in culture to develop into functional corneal tissue. Various approaches can be used in corneal tissue engineering, including scaffold-based techniques where cells are seeded onto a scaffold that mimics the structure of the cornea, or scaffold-free techniques where cells are grown into sheets or layers without a scaffold. These bioengineered tissues can then be transplanted onto the damaged cornea to promote healing and restore vision. Advantages of corneal repair through tissue engineering include a reduced risk of rejection compared to traditional corneal transplants, as well as the potential for customized treatments tailored to the individual patient. Ongoing research in this field aims to improve the effectiveness and availability of tissue-engineered corneal replacements for patients in need of corneal repair. Figure 2 demonstrates the process of corneal tissue engineering for the repair/regenerate/restoration of the cornea.

The cornea is the transparent, dome-shaped surface that covers the front of the eye. It plays a crucial role in focusing light into the eye and protecting the eye from dust, debris, and other harmful particles. The cornea also helps to shield the eye from harmful UV rays. It is made up of highly specialized cells and proteins that help maintain its clarity and shape. When the cornea becomes damaged or diseased, it can lead to vision problems and require medical treatment or surgery <sup>[10]</sup>.

The repair of the cornea involves various treatments and procedures, depending on the extent and nature of the damage. Some common methods for repairing the cornea include (1) Medications: For minor injuries or infections, topical medications such as antibiotics, antiviral drugs, or corticosteroids may be prescribed to help the cornea heal and reduce inflammation. (2) Corneal transplantation: In cases of severe damage or disease, a corneal transplant may be necessary. This involves replacing the damaged corneal tissue with healthy donor



tissue from a deceased individual. (3) Phototherapeutic keratectomy (PTK): This laser procedure is used to remove damaged or diseased corneal tissue and promote the growth of healthy tissue. (4) Corneal collagen cross-linking: This procedure uses ultraviolet light and riboflavin eye drops to strengthen the cornea and prevent further deterioration in cases of conditions such as keratoconus. (5) Amniotic membrane transplantation: This involves placing a piece of amniotic membrane over the damaged area of the cornea to promote healing and reduce scarring. (6) Intacs: These are small plastic rings that are surgically inserted into the cornea to reshape it and improve vision in cases of conditions such as keratoconus. It's important to consult with an ophthalmologist or corneal specialist to determine the most appropriate treatment for your specific condition <sup>[11]</sup>.

At various levels of complexity, tissue engineering principles have been used to build functional corneal tissue equivalents. These range from techniques to replicate the natural innervation to engineering of the epithelium, stroma, and endothelium layers. By utilizing a wide range of biomaterial systems and cell types various techniques have resulted in full-thickness cornea tissue equivalents that are used in clinical settings. Specifically, the primary methods can be separated into four categories: (1) structures based only on cells, (2) decellularized, (3) synthetic, and (4) natural polymers combined with various cell types <sup>[12]</sup>.

### **5.1. Tissue engineering of corneal epithelium**

Tissue engineering of corneal epithelium involves creating functional corneal tissue in the lab for potential transplantation or research purposes. This process typically involves seeding corneal epithelial cells onto a scaffold that mimics the natural environment of the cornea, providing structural support and cues for cell growth and differentiation. Various techniques like bioprinting, cell sheet engineering, and scaffold-based approaches are utilized to create the engineered corneal tissue. The goal is to develop a tissue that closely resembles the native corneal epithelium in terms of structure and function. One key challenge in corneal tissue engineering is achieving proper cell organization and alignment to promote healthy tissue formation. Researchers also need to ensure that the engineered tissue is transparent, biocompatible, and promotes proper wound healing when transplanted. By advancing tissue engineering techniques and optimizing cell culture conditions, scientists aim to develop more effective treatments for corneal diseases and injuries, ultimately improving patient outcomes and reducing the reliance on traditional donor tissue for transplantation.

Epithelial and endothelial layers are crucial for maintaining corneal deturgescence (dehydrated cornea) and transparency. Cell sheet engineering, an advanced concept of tissue engineering has successfully generated the corneal epithelial layer in vitro, promoting functional stratified epithelium growth. However, high variability and extended culture time are major drawbacks. Human amniotic membranes have been used for corneal epithelial-derived expansion and reconstruction, but their high variability limits their use in clinical settings. Human donor corneal stromal tissues are proposed for human corneal epithelium growth, but the lack of corneal tissue donor availability affects their clinical potential. Reconstituted type I collagen hydrogels can encapsulate human corneal limbal epithelial cells, resulting in functional stratified epithelial layers. Chemically cross-linked collagen hydrogels are explored as corneal epithelium scaffolds due to their enhanced mechanical and optical properties. In addition to that, there are some biopolymers also in tissue engineering practice for cornea repair. For example, Silk has been exploited as a substrate for human epithelial cell growth and functional organization due to its optical properties, mechanical robustness, and versatile processability. Keratin-based substrates have been used for ocular surface reconstruction due to their good optical properties and ability to support epithelial cell growth in vitro <sup>[13]</sup>.

## 5.2. Regeneration of corneal stroma

The reconstruction of the corneal stroma is still challenging due to its complex structure, mechanical strength, and transparency. To address this, researchers have been exploring the development of functional corneal stroma substrates using synthetic polymers, natural-derived materials, and silk films. Synthetic polymers have been used for stromal corneal substrates due to their tuneable mechanical properties and the ability to direct stromal cell organization and differentiation in vitro. However, these materials lack adequate optical properties. Hydrogel films prepared from chitosan blended with poly(ethylene glycol) and poly(l, D-lactic acid) nanofibers have shown improved mechanical, optical, and biological performances. Silk films have also been developed to combine mechanical, biological, and optical properties, supporting corneal stromal cell differentiation in 2D and 3D film architectures <sup>[14]</sup>.

## 5.3. Corneal endothelium

Natural polymer substrates, including type I collagen, gelatin, decellularized tissues, chitosan, and chondroitin sulfate, have been the primary focus of contemporary research on endothelial layer engineering. These substrates have demonstrated signs of endothelium development. In a lamellar keratoplasty model, in which the endothelium and a portion of Descemet's membrane were removed, the clinical evaluation of decellularized amniotic membrane in conjunction with human corneal endothelial cells was conducted. This membrane was found to be capable of serving as an equivalent to corneal endothelium <sup>[14]</sup>.

## 5.4. Corneal innervation

With nociceptive nerve protrusions that terminate in the epithelium layer, the cornea is one of the most innervated tissues in the human body. To preserve the general health of the cornea, the corneal nerves serve as mechanical and temperature sensors. The pathological diseases known as dry eye are caused by a progressive absence of innervation, which eventually leads to diffuse corneal ulcers and a decrease in corneal sensitivity. Few attempts have been made to stimulate peripheral nerve proliferation within corneal tissue-engineered constructions, despite the crucial role that innervation plays in ocular functioning. According to in vitro research, the application of peptides generated from laminin to a substrate stimulated the proliferation of neurons and epithelial stratification. Additionally, employing cross-linked collagen replacements, functional nerve regeneration was demonstrated in a pig model undergoing deep lamellar keratoplasty, regaining prior nerve density one year after surgery <sup>[14]</sup>.

## 5.5. Replacement of full-thickness cornea via tissue engineering

Tissue engineering offers a promising approach for the replacement of full-thickness cornea by creating functional corneal equivalents. Using a combination of biomaterials, cells, and growth factors, researchers aim to develop corneal constructs that mimic the structure and function of native corneas. Various techniques such as decellularization of donor corneas, bio-printing, and cell seeding onto scaffolds are being explored to generate these corneal substitutes. One common strategy involves seeding corneal cells such as keratocytes, epithelial cells, and endothelial cells onto a biocompatible scaffold that mimics the native corneal architecture. By providing the necessary cues for cell growth, differentiation, and extracellular matrix production, these constructs can potentially integrate with the host tissue and restore vision. While significant progress has been made in the field of corneal tissue engineering, challenges such as achieving optimal transparency, biomechanical strength, and long-term integration remain to be addressed. Further research is needed to improve the functionality and clinical outcomes of engineered corneal replacements. Overall, tissue engineering holds great promise for the development of innovative solutions for corneal regeneration and transplantation.

In vivo implantation of corneal equivalent biomaterials without cells has been studied to study the integration of implanted biomaterials with native corneal tissue. Efforts have been made to mimic the three-layer structure of the cornea, using decellularized biological material. However, the use of acellular porcine cornea in rabbit lamellar keratoplasty led to the degradation of the tissue-engineered cornea. Further efforts have been made to develop in vitro corneal stroma equivalents, promoting nerve ingrowth, and engineered full-thickness cornea for tissue replacement. Biosynthetic corneas from cross-linked recombinant human collagen type III were implanted in human patients to enhance endogenous tissue regeneration. The implants were stably integrated, innervated, and vascularized for up to 2 years. Epithelial and stromal cell lines are extensively investigated for in vitro 3D cornea tissue models and surgical replacements. Primary human epithelial and stromal cells are mainly used in in vitro 3D tissue models and preclinical approaches. Human stromal stem cells have been used to repopulate mouse corneas and restore stromal thickness, fibril deficits, and transparency in cloudy corneas. These cells were found to be stably integrated into the mouse cornea for over 10 weeks without eliciting an immune response. This suggests that a bioengineered cornea populated with immune-privileged cells could supplement corneal replacements and in vitro models <sup>[14,15]</sup>.

## 6. Pros and cons for existing treatment for repair of cornea

There are pros and cons for existing treatment available for the treatment for the repair of cornea. The following pros and cons have been reported.

Pros: (1) Effective at treating corneal damage and diseases such as on as keratoconus, corneal ulcers, and corneal dystrophies. (2) Can improve vision and overall quality of life for patients. (3) Treatments such as corneal transplants have a high success rate. (4) Many treatment options are available, including medications, contact lenses, and surgical procedures.

Cons: (1) Some treatments may have risks and potential complications, such as infection or rejection of transplanted tissue. (2) Surgical procedures can be expensive and may require a long recovery time. (3) Availability of treatment options may be limited in certain areas. (4) Some treatments may only provide temporary relief and require ongoing maintenance.

Tissue engineering for the repair of the cornea involves the use of bioengineered materials and techniques to restore the structure and function of the cornea. The cornea is the transparent outer layer of the eye that plays a crucial role in vision, and damage or disease to the cornea can lead to vision impairment or loss. One approach to tissue engineering for corneal repair involves the use of synthetic or natural biomaterials to create a scaffold that mimics the structure of the cornea. This scaffold can be seeded with corneal cells, such as corneal epithelial cells or corneal stromal cells, and then implanted into the damaged area of the cornea. The cells can then grow and proliferate on the scaffold, eventually integrating with the surrounding tissue and restoring the function of the cornea. Another approach involves the use of stem cells to regenerate corneal tissue. Stem cells can be isolated from the patient's body, such as from the bone marrow or the limbus of the eye, and then expanded and differentiated into corneal cells. These cells can then be transplanted into the damaged cornea to promote tissue regeneration and repair. In addition to these approaches, tissue engineering for corneal repair may also involve the use of growth factors, gene therapy, and other advanced techniques to enhance the regenerative potential of the cornea. Overall, tissue engineering holds great promise for the repair of the cornea and the restoration of vision in individuals with corneal damage or disease. Ongoing research and development in this field continue to advance the potential for tissue-engineered corneal repair to become a standard treatment in the future.

The transplantation of full-thickness human corneas through penetrating keratoplasty is one current

strategy for addressing the scarcity of corneal donors. However, this operation requires access to eye banks, which delays the rapid recovery of corneas in emergency cases. Advances in corneal regenerative medicine are required to offer patients undergoing such high-risk grafts with alternatives.

Keratoprotheses (KPros), which consist of an optical core that softly communicates with the host's eye, are used as substitutes for donor corneas in high-risk corneal grafts. The Boston KPro and osteo-odonto-keratoprosthesis are two popular KPros that are not the best options for replacing the cornea because of problems with their irreversible insertion and related complications like infection that can require continuous use of antibiotics and immunosuppressants. The developments in KPros aim to maintain native corneal functions to facilitate epithelial growth. In addition to preventing infection and implant extrusion, this is required to maintain tear film. These kinds of developments have recently become possible because of enhanced lithographic and surface chemistry changing methods <sup>[16]</sup>.

## **7. Collagen biomaterials for tissue engineering of the cornea**

Collagen biomaterials have shown great potential for tissue engineering of the cornea. The cornea is a transparent, avascular tissue that plays a crucial role in vision. When damaged or diseased, the cornea can result in vision impairment or blindness. Tissue engineering aims to develop biomimetic materials that can replace or regenerate damaged corneal tissue. Collagen is the main structural protein in the cornea and provides it with its unique properties of transparency and strength. Therefore, collagen-based biomaterials are an attractive choice for corneal tissue engineering. These biomaterials can be derived from natural sources, such as animal tissues, or produced synthetically using recombinant technology. One common approach to using collagen biomaterials for corneal tissue engineering is to create a scaffold that mimics the structure and properties of the native cornea. This scaffold can then be seeded with corneal cells, such as corneal epithelial cells, keratocytes, or endothelial cells, to promote tissue regeneration. Collagen-based scaffolds can provide a suitable microenvironment for cell attachment, proliferation, and differentiation, ultimately leading to the formation of new corneal tissue. In addition to serving as a scaffold for cell growth, collagen biomaterials can also be used to deliver bioactive molecules, such as growth factors or drugs, to promote tissue regeneration and modulate the inflammatory response. Furthermore, collagen-based hydrogels have been investigated for their potential to serve as a carrier for corneal endothelial cell transplantation, which is a promising therapy for corneal endothelial dysfunction. Overall, collagen biomaterials hold great promise for tissue engineering of the cornea. Their biocompatibility, bioactivity, and ability to mimic the native corneal tissue make them an attractive choice for developing new therapies to treat corneal diseases and injuries. Continued research and development in this field are likely to lead to further advancements in corneal tissue engineering using collagen biomaterials.

Because collagen resembles native tissue and is the most abundant component of the cornea, using it in corneal implants improves implant grafting potential and promotes implant success. The tripeptide arginine-glycine-aspartic acid (RGD) sequence that makes up the collagen microstructure is recognized by neighbouring integrin receptors and is crucial for controlling cell activity. To produce a unique optical transparency, small leucine-rich proteoglycans (SLRPs) control the thickness of the corneal collagen fibrils during development. It is essential to comprehend how these developmental processes add to intricate corneal micro-anatomy to maintain corneal functionality as much as possible when creating corneal implants.

Collagen's capacity to functionalize robust chemical linkages with neighbouring fibrils is known as cross-linking. Collagen cross-linking in the cornea happens spontaneously as a result of an oxidative deamination event that happens inside the collagen's end chains. It has been suggested that keratectasia, or corneal ectasia,



frequently advances most quickly in youth or early adulthood but tends to stabilize in patients beyond middle age due to this natural cross-linking of collagen. Although crosslinking usually happens spontaneously over time, there are alternative mechanisms that can cause crosslinking to happen sooner than expected. Glycation is a process that occurs more frequently in diabetics and can result in the formation of new collagen connections. It has been demonstrated that oxidation can cause corneal cross-linkage by releasing oxygen free radicals in the pathway that is most pertinent to our subject. Researchers at the University of Dresden in Europe created the foundations for the corneal collagen cross-linking methods that were currently in use in the late 1990s. Via the oxidation process, collagen cross-linking was induced in the riboflavin-soaked corneas of rabbits and pigs using UV radiation. It was demonstrated that the resulting corneas were more rigid and resistant to enzymatic breakdown. The study also demonstrated that, as a result of fibril crosslinking, treated corneas had greater molecular weight collagen polymers.

According to safety studies, if the corneal thickness was greater than 400 microns and appropriate UV irradiation was maintained, the treatment did not harm the endothelium. Early findings from Dresden's human trials on UV-induced corneal cross-linking were encouraging in 2003. 16 patients with fast-developing keratoconus have participated in the original pilot research, and following therapy, all of the patients' progression stopped. Furthermore, 65% of patients showed an improvement in visual acuity, and 70% of patients experienced flattening of their steep anterior corneal curvatures (decreases in average and maximum keratometric values). No issues were reported. The FDA granted Avedro orphan drug status for its riboflavin ophthalmic solution formulation in late 2011, to be used in conjunction with the company's specific UVA irradiation equipment. On April 18, 2016, the FDA approved riboflavin and UV-induced corneal collagen cross-linking. The dearth of adequately conducted Randomized Controlled Trials has reduced the data supporting the use of CXL in the therapy of keratoconus, according to a 2015 Cochrane systemic review that examined the drug's efficacy in treating the condition <sup>[17]</sup>.

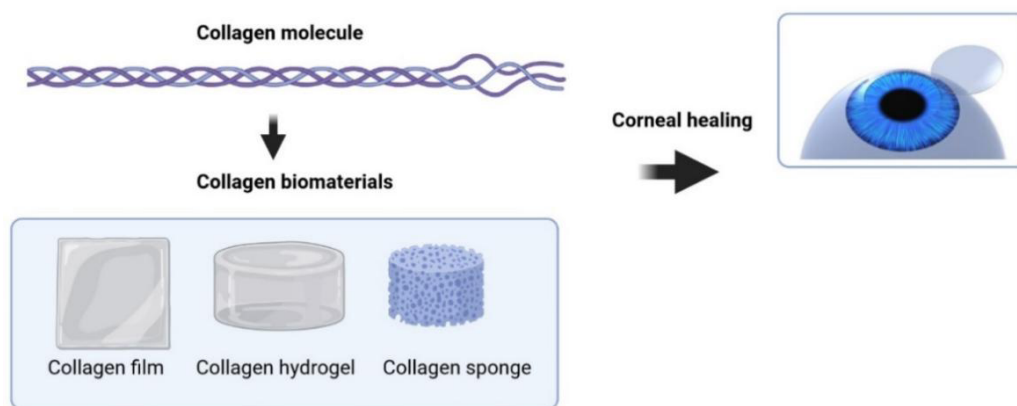


**Figure 3.** Application of collagen biomaterial in tissue engineering of cornea <sup>[18]</sup>.

## 8. Type 1 Collagen for tissue engineering scaffolds

Collagens are a significant class of structural proteins that are expressed in various tissues and have unique characteristics. Collagen gives transparency to the cornea and crystalline lens of the eye, although it is opaque in the skin. There are 28 different forms of collagen, and while they all have a triple helix structure, their  $\alpha$ -chain compositions vary, giving each type of collagen unique features. The diverse arrangement of collagen fibers also plays a role in the alteration of tissue shape. The discovery and use of collagen as a biomaterial

is a result of its significant capacity to create various tissues. The two main types of collagen present in the tissues of the cornea and lens are collagen type I (Col-I) and collagen type IV (Col-IV). For a clear vision, both collages offer structure and transparency. The utilization of these two forms of collagen as novel biomaterials in bioengineering distinct tissue to cure a range of ocular conditions that could result in blindness is examined in this article. Figure 3 shows the application of Type 1 collagen in corneal tissue engineering.

## 9. Fabrication Methods

Biofabrication methods for tissue engineering of the cornea involve utilizing advanced technologies to create functional corneal tissue for transplantation. Some key methods include:

- (1) 3D bioprinting: This technique involves layer-by-layer deposition of bio-inks containing corneal cells and biomaterials to create a 3D corneal structure with precise control over cell placement and architecture.
- (2) Electrospinning: Electrospinning is used to fabricate nanofibrous scaffolds that mimic the natural extracellular matrix of the cornea, providing a suitable environment for cell growth and tissue regeneration.
- (3) Decellularization and recellularization: This method involves removing cells from a donor cornea to create a scaffold that retains the structural integrity of the tissue. The scaffold can then be repopulated with patient-specific corneal cells to generate a functional cornea.
- (4) Self-assembly techniques: By providing the necessary cues and environment, corneal cells can self-organize and form a corneal tissue structure without the need for external scaffolds.

Overall, these biofabrication methods offer promising avenues for creating corneal tissue constructs that closely resemble the native cornea, with the potential to revolutionize corneal transplantation and improve outcomes for patients with corneal diseases or injuries. There are many fabrication methods for tissue engineering scaffolds for cornea repair and regeneration. The following methods have been reported and these methods also utilized Type 1 collagen as biomaterials <sup>[19]</sup>.

## 10. Bioprinting

Additive manufacturing includes bioprinting, which is a subset of 3D printing. Here, the basic method used is layer-by-layer material stacking to fabricate a scaffold or framework using computer images. With its advantages over traditional molding techniques, including the capacity to produce customized structures from recorded images and the repeatability of cell printing, bioprinting has gained attention recently. Recent research on in situ printing, which uses handheld printers to print biomaterials or cells directly onto wounded regions to repair wounds and speed healing, has provided us with an idea of what future surgeries might entail. Materials used in bioprinting relate to biomaterials, which are often organic materials like collagen, gelatine, and alginate, or bio-ink with a cell-laden ability, as opposed to materials utilized in regular 3D printing, such as plastics. Extrusion-based bioprinting, laser-assisted bioprinting, and inkjet bioprinting are the three techniques most commonly utilized in 3D bioprinting. In bioprinting, other technologies such as vat photopolymerization might also be employed.

Inkjet bioprinting is a fast and cost-effective method for fabricating various tissues, including bone, cartilage, blood vessels, and retinal layers. It involves depositing micro-drops of bio-inks onto a substrate, with techniques such as continuous inkjet printing (SIJ) and drop on demand inkjet printing (DOD). DOD has been used to fabricate corneal-like structures with corneal stromal cells, achieving good cell viability. Laser-assisted bioprinting involves a pulse laser applied to a laser absorption layer, allowing thermal expansion to

eject micro-droplets onto the substrate. This technique can precisely control the type and density of cells during printing, making it suitable for scaffold-free cell structures. However, it has high cell death rates, which may impact tissue long-term survival. Stereolithography (SLA) is a 3D bioprinting technique that uses a laser beam to initiate photo-polymerisation or photo-crosslinking in a selected area of bioink. This technique has been successfully used to print human corneal-like stroma and artificial cartilage and liver. Extrusion bioprinting is the most common bioprinting method, with shear-thinning bioink extruded from a syringe using pressure from air, pistons, or screws. Extrusion 3D printers, including single, multi-syringe, and joint syringes, are used in tissue engineering and surgery. They can print human skin with different layers, such as dermis and epidermis. Coaxial extrusion bioprinting has been used to crosslink alginate with calcium ions. Handheld devices like bio-pen and double syringe extrusion printers have been developed for treating cartilage injuries. For low viscous bioinks, a method called “freeform reversible embedding of suspended hydrogels (FRESH)” has been developed, printing low-viscosity bioinks in a supporting material for higher resolution and structural support. This technique has been used to print various human tissues <sup>[20]</sup>.

### **10.1. Type 1 collagen as bio-ink**

Col-I, a key component of the human corneal stroma, is often combined with other materials for corneal applications. Recent bio-inks have shown improved printability and transparency with increased collagen concentration and sodium alginate. However, the alginate structure could potentially inhibit cell proliferation. Overall, these bioinks offer potential for corneal applications. Collagen-based bio-ink has been explored using temperature-sensitive biomaterials and natural cross-linkers to facilitate the liquid-to-gel transition. A bio-ink primarily incorporating decellularised cornea was used to print a corneal model, with over 75% light transmittance and compatibility with human turbinate-derived mesenchymal stem cells. The study focuses on 3-D printing of corneal tissue using various printing methods, including FRESH, extrusion printing, DoD, and laser-assisted printing. Crosslinking methods used in these studies include natural biomaterials like alginate-calcium, gelatin, thrombin, and low-temperature agarose. Most studies use lower concentrations of Col-I to maintain transparency but require additional gentle crosslinkers. The only bioink with a higher Col-I concentration is 20 mg/mL of decellularised cornea with 86% collagen. The collagen sources are either animal-based or human tissue. Current studies are primarily proof-of-concept and focus on corneal stromal layers and cells. None of the projects use photo-crosslinking, which could be cytotoxic. However, studies have shown that cell viability can be enhanced by lowering the strength of the curing light. This could lead to the development of cell-encapsulating collagen-based bio-inks for cornea bioengineering <sup>[21]</sup>.

## **11. Electrospinning**

Globally, corneal disorders impact over 10 million individuals and are the second most common cause of visual loss. Since there is a significant scarcity of newly donated corneas and there is an uncertain danger of immunological rejection with conventional heterografts, it is imperative to replace pathologic corneal tissue with a corneal counterpart. The construction of a scaffold with mechanical characteristics and transparency akin to the natural cornea is critical for the regeneration of corneal tissues. Corneal tissue engineering has become a viable approach to the development of corneal tissue substitutes. High surface area-to-volume ratios and porosity in electrospun nanofibrous scaffolds mimic the structure of native extracellular matrix (ECM) protein fibres. Electrospinning polymer components, fibre architectures, and functionalization are versatile processes that have made it possible to fabricate nanofibrous scaffolds with the right mechanical strength, transparency, and biological characteristics for corneal tissue engineering. The current state of electrospun scaffold

development for corneal tissue engineering is reviewed in this paper. The main topics covered are electrospun materials (single and blended polymers), fibre structures (isotropic or anisotropic), functionalization (better mechanical properties and transparency), applications (corneal cell survival, phenotype maintenance, and corneal tissue formation), and future development prospects.

A high voltage is applied between a syringe and a deposition target (or collector) in the versatile fabrication process known as electrospinning, which draws nano- or micro-scale fibers from the material the syringe dispenses. The basic components of electrospinning equipment are a grounded collector, a spinneret (usually a hypodermic syringe needle) linked to a high-voltage power supply, and a high-voltage direct current power supply (5 to 50 kV). According to the theory underlying this technology, a droplet suspended on top of the pipe will form a charged jet when the repulsive force between charged particles in polymer solutions overcomes the surface tension of the solution. The droplet will then repeatedly split in the electrostatic field and the solvent will eventually evaporate, forming fibres on the collector. Three-dimensional (3D) fibrous scaffolds can be created by depositing these fibres in a designated collector. More than 200 polymers, both synthetic and natural (e.g., polycaprolactone (PCL), poly-L-lactic acid (PLLA), poly(lactide-co-glycolide) (PLGA), polyethylene oxide (PEO), collagen, gelatin, hyaluronate (HA), chitosan, silk fibroin (SF), etc.), have been successfully electrospun to nano- or micro-scale fibres to date. The chemical makeup of the polymer solution (molecular weight, concentration, and solvent), the applied voltage, the distance between the spinneret tip and the collector, the feeding rate, the capillary diameter, the humidity, and the temperature are some of the processing variables that can impact the fibre morphology. The morphology can be changed to create fibres with spindles on a string, uniform fibres, or beaded fibres, depending on the applied parameters.

Due to its close structural resemblance to native extracellular matrix (ECM), high surface area-to-volume ratio, and good porosity. All of which support cell adhesion and movement, proliferation, and differentiation, as well as its excellent mechanical properties, great material handling, suitability for implantation, and scalable production. Electrospinning has recently attracted increased interest for fabricating biomimetic engineering functional corneal tissue <sup>[22]</sup>.

## 12. Corneal implants

Corneal implants are medical devices used to treat various eye conditions affecting the cornea, the transparent front part of the eye that covers the iris and pupil. These implants are designed to improve vision by reshaping or replacing damaged corneal tissue. There are different types of corneal implants available, each serving a specific purpose. One common type of corneal implant is the intrastromal corneal ring segments, which are small, clear, arc-shaped devices inserted into the cornea to correct conditions like keratoconus or irregular astigmatism. Another type is the artificial cornea or keratoprosthesis, which is used when traditional corneal transplant surgery is not an option. Corneal implants can help improve vision, reduce dependence on glasses or contact lenses, and enhance the overall quality of life for individuals with corneal disorders. However, like any surgical procedure, there are risks and potential complications associated with corneal implants, so it is important to consult with an ophthalmologist or eye surgeon to determine the best treatment option for each case.

The basic collagen cross-linked cornea substitute was fabricated. N-hydroxysuccinimide (NHS) and 1-ethyl-3-(3-dimethylaminopropyl)carbodiimide (EDC) were combined with 10% porcine type I collagen at pH 5. Lamellar keratoplasty was used to implant the final homogenous solution into rabbits and minipigs after it had been molded to the dimensions of the cornea and allowed to cure. Following surgery, the implants were monitored for up to six months. Detailed slit lamp biomicroscopy, in vivo confocal microscopy, topography,



and esthesiometry for nerve function were all used in the clinical assessment of the cornea. Additionally, histopathologic analyses were carried out on rabbit corneas that were removed after six months. The optical clarity of cross-linked collagen was higher than that of human corneas (refractive index: 1.35). Just one out of every twenty-four surgical corneas implanted into rabbit and porcine corneas displayed a minor haze six months following surgery. Every other implant stayed optically clear and did not respond negatively. The topography revealed a smooth surface and a profile resembling the nonsurgical contralateral eye. The matrices that were implanted encouraged the regeneration of neurons, tear film, and corneal cells. There was a return of touch sensitivity, suggesting partial function. The implanted corneas displayed steady host-graft integration and did not exhibit any appreciable decrease in thickness. Water-soluble carbodiimides can be used as protein cross-linking reagents to stabilize collagen enough for use in the creation of implantable corneal matrix substitutes. The straightforward cross-linking technique would make it simple to create transplant matrices in locations where corneas are in scarce supply or where emergency perforation repairs require temporary patches.

Nowadays, the second most common cause of blindness worldwide is corneal illness. Currently, corneal transplantation is thought to be one of the most popular therapies for visual loss. In the development process, this work proposes a novel strategy that uses dual-crosslinked membranes made of N-hydroxysuccinimide (NHS), 1-ethyl-3-(3-dimethylaminopropyl) carbodiimide (EDC), and polyrotaxane multiple aldehydes (PRAs). EDC/NHS and PRAs crosslinked collagen, respectively, to create imine groups and stable amide linkages. When compared to membranes crosslinked with a single crosslinker, dual-crosslinked (Col-EDC-PRA) membranes demonstrated improved resistance to collagenase degradation and higher mechanical qualities due to the creation of a double interpenetrating network. Col-EDC-PRA membranes also have good water content and light transmittance properties. Col-EDC-PRA membranes were demonstrated in cell studies to be noncytotoxic and to differ very slightly from other membranes. The presence of stromal cells and neo-stroma, as shown in hematoxylin–eosin-stained histologic sections and optical coherence tomography images of the anterior segment, indicates that corneal stromal repair occurred in a rabbit keratoplasty model at 5 months. In addition, the surgical site showed no signs of inflammation, corneal neovascularization, or corneal rejection reaction. Overall, the findings showed that corneal tissue regeneration following a corneal defect was successfully facilitated by the dual-crosslinked membranes <sup>[23,24]</sup>.

### 13. Clinical challenges and limitations

Clinical challenges and limitations in cornea repair include the following. Addressing these challenges requires ongoing research into novel treatment modalities, improving surgical techniques, increasing donor awareness, and expanding access to specialized care for patients with corneal disorders.

- (1) Inadequate donor availability: There is a shortage of corneal donors, leading to delays in corneal transplant surgeries.
- (2) Graft rejection: The risk of immune-mediated rejection of the transplanted cornea remains a major challenge, requiring lifelong monitoring and management.
- (3) Complications post-surgery: Complications such as infection, inflammation, and graft failure can occur following corneal transplant surgery.
- (4) Corneal scarring: Severe corneal scarring due to trauma or infection can limit the success of corneal repair procedures.
- (5) Limited treatment options: Current treatment options for corneal diseases such as keratoconus or corneal ulcers are limited, with some cases requiring more advanced interventions like keratoprosthesis.



(6) Surgical expertise: Performing corneal transplant surgeries requires specialized training and expertise, limiting access in certain regions or healthcare settings.

(7) Cost of treatment: Corneal repair procedures can be costly, posing a barrier to access for some patients.

Several obstacles need to be cleared before bioengineered corneas are accepted as implant forms. The mechanical toughness and elasticity necessary for a longitudinally functional optical system are inherent to bioengineered collagen. Even though collagen cross-linking techniques have improved these inferior qualities, it is still a difficult task to determine the ideal blend ratios of biomaterials to build a corneal implant that is identical to the natural cornea. While both type I and type III collagen hydrogels are flexible and have tensile strength that is suitable for handling, type III collagen hydrogels alone provide a more accurate mechanical and optical replica of the original cornea in implants. Similarly, employing natural biomaterials increases the light transparency of corneal implants. Nevertheless, these materials are more challenging to electrospin, a regularly utilized fibre manufacturing technique used to improve the mechanical strength of biomaterials. As a result, corneal implants lose mechanical strength when they are designed without the electrospinning process. Therefore, it is necessary to produce implants that have as many properties as human corneal tissue if corneal implants are to be as useful in a clinical context as possible. Eventually, it will also be necessary to overcome the high costs linked to these intricate production processes. Ultimately, the best way to recreate native corneal tissue will depend on our ability to comprehend the molecular intricacy of corneal development, which is mostly represented by the stromal architecture.

## 14. Conclusion

Recent years have seen tremendous advancements in ocular tissue engineering. There are several engineering challenges in creating a biocompatible, mechanically stable, and optically transparent tissue. To tackle these problems, researchers have looked at two basic approaches: using cells to manage their extracellular matrix and using scaffolds to provide thick, transparent matrices for cell development. Each strategy has had some degree of success. Furthermore, novel advancements in tissue-engineered construct innervation have been created. Enhancing the mechanical stability of engineered constructs and the host response to implantation must be the focus of future studies. Biomaterial made of type 1 collagen has been utilized to implant or build scaffolds to restore corneas. A variety of scaffold-building techniques have been discussed, along with tissue engineering applications for corneal regeneration and repair. In light of this correlation, type 1 collagen was a viable biomaterial for the creation of tissue engineering scaffolds for corneal regeneration that works.

## Disclosure statement

The author declares no conflict of interest.

## Reference

- [1] Ting DS, Deshmukh R, Ting DS, et al., 2022, Corneal Disorders. *Ophthalmic Epidemiology: Current Concepts to Digital Strategies*, 113.
- [2] Fishman JA, Greenwald MA, Grossi PA, 2012, Transmission of Infection With Human Allografts: Essential Considerations in Donor Screening. *Clinical Infectious Diseases*, 55(5): 720–727.
- [3] Griffith M, Poudel BK, Malhotra K, et al., 2020, Biosynthetic Alternatives for Corneal Transplant Surgery. *Expert Review of Ophthalmology*, 15(3): 129–143.

- [4] Armitage WJ, Goodchild C, Griffin MD, et al., 2019, High-Risk Corneal Transplantation: Recent Developments and Future Possibilities. *Transplantation*, 103(12): 2468.
- [5] Tan A, Tan DT, Tan XW, et al., 2012, Osteo-Odonto Keratoprosthesis: Systematic Review of Surgical Outcomes and Complication Rates. *The Ocular Surface*, 10(1): 15–25.
- [6] Beuerman RW, Pedroza L, 1996, Ultrastructure of the Human Cornea. *Microscopy Research and Technique*, 33(4): 320–335.
- [7] Tan DT, Dart JK, Holland EJ, et al., 2012, Corneal Transplantation. *The Lancet*, 379(9827): 1749–1761.
- [8] Liu W, Merrett K, Griffith M, et al., 2008, Recombinant Human Collagen for Tissue Engineered Corneal Substitutes. *Biomaterials*, 29(9): 1147–1158.
- [9] Palchesko RN, Carrasquilla SD, Feinberg AW, 2018, Natural Biomaterials for Corneal Tissue Engineering, Repair, and Regeneration. *Advanced Healthcare Materials*, 7(16): 1701434.
- [10] Jameson JF, Pacheco MO, Nguyen HH, et al., 2021, Recent Advances in Natural Materials for Corneal Tissue Engineering. *Bioengineering*, 8: 161.
- [11] Mobaraki M, Abbasi R, Omidian Vandchali S, et al., 2019, Corneal Repair and Regeneration: Current Concepts and Future Directions. *Frontiers in Bioengineering and Biotechnology*, 7: 135.
- [12] Palchesko RN, Carrasquilla SD, Feinberg AW, 2018, Natural Biomaterials for Corneal Tissue Engineering, Repair, and Regeneration. *Advanced Healthcare Materials*, 7(16), 1701434.
- [13] Nishida K, 2003, Tissue Engineering of the Cornea. *Cornea*, 22(7): S28–S34.
- [14] Nosrati H, Abpeikar Z, Mahmoudian ZG, et al., 2020, Corneal Epithelium Tissue Engineering: Recent Advances in Regeneration and Replacement of Corneal Surface. *Regenerative Medicine*, 15(8): 2029–2044.
- [15] Ghezzi CE, Rnjak-Kovacina J, Kaplan DL, 2015, Corneal Tissue Engineering: Recent Advances and Future Perspectives. *Tissue Engineering Part B: Reviews*, 21(3): 278–287.
- [16] Mobaraki M, Abbasi R, Omidian Vandchali S et al., 2019, Corneal Repair and Regeneration: Current Concepts and Future Directions. *Frontiers in Bioengineering and Biotechnology*, 7: 135.
- [17] Liu W, Merrett K, Griffith M, et al., 2008, Recombinant Human Collagen for Tissue Engineered Corneal Substitutes. *Biomaterials*, 29(9): 1147–1158.
- [18] Sklenářová R, Akla N, Latorre MJ, et al., 2022, Collagen as a Biomaterial for Skin and Corneal Wound Healing. *Journal of Functional Biomaterials*. 13(4): 249.
- [19] Cen L, Liu W, Cui L, et al., 2008, Collagen Tissue Engineering: Development of Novel Biomaterials and Applications. *Pediatric Research*, 63(5): 492–496.
- [20] Duarte Campos DF, Rohde M, Ross M, et al., 2019, Corneal Bioprinting Utilizing Collagen-Based Bioinks and Primary Human Keratocytes. *Journal of Biomedical Materials Research Part A*, 107(9): 1945–1953.
- [21] Song Y, Hua S, Sayyar S, et al., 2022, Corneal Bioprinting Using a High Concentration Pure Collagen I Transparent Bioink. *Bioprinting*, 28: e00235.
- [22] Kong B, Mi S, 2016, Electrospun Scaffolds for Corneal Tissue Engineering: A Review. *Materials*, 9(8): 614.
- [23] Tidu A, Schanne-Klein MC, Borderie VM, 2020, Development, Structure, and Bioengineering of the Human Corneal Stroma: A Review of Collagen-Based Implants. *Experimental Eye Research*, 200: 108256.
- [24] Liu Y, Gan L, Carlsson DJ, et al., 2006, A Simple, Cross-Linked Collagen Tissue Substitute for Corneal Implantation. *Investigative Ophthalmology & Visual Science*, 47(5): 1869–1875.

#### **Publisher's note**

Bio-Byword Scientific Publishing remains neutral with regard to jurisdictional claims in published maps and institutional affiliations.

# Long Non-coding RNA and Progression of Breast Cancer

Usama Ahmed<sup>1\*</sup>, Muhammad Abubakar<sup>2</sup>, Salma Saeed Khan<sup>3</sup>, Baqa ur Rehman<sup>2</sup>

<sup>1</sup>Department of Medicine, School of Biomedical Engineering, Shenzhen University Medical School, Shenzhen 518060, China

<sup>2</sup>Department of Biosciences, COMSATS University Islamabad, Park Rd, Islamabad Capital Territory 45550, Pakistan

<sup>3</sup>Biomedical and Life Sciences, Kohsar University Murree, Murree 47150, Punjab, Pakistan

*\*Corresponding author:* Usama Ahmed, usama.med.19@gmail.com

**Copyright:** © 2024 Author(s). This is an open-access article distributed under the terms of the Creative Commons Attribution License (CC BY 4.0), permitting distribution and reproduction in any medium, provided the original work is cited.

**Abstract:** Breast cancer is a major problem in the health sector worldwide. The prevalence of breast cancer incidence is on the rise in many countries despite efforts to eradicate it. The substantial efforts for the treatment of breast cancer are quite successful but the main hindrance is early detection which in turn is dependent on various factors i.e. genetic history, environmental exposures, hormonal causes, and sedentary lifestyle. In previous studies, lncRNAs were known to modulate the progression of many cancers like gastric, lung, ovarian, and colorectal cancers. This study was designed to find these lncRNAs role in breast cancer development. Bioinformatics tools were used for in silico analysis of these lncRNAs LINC01356, LINC01357, ARF4-AS1, and FAM83B. These lncRNAs were evaluated in GEPIA2 for subtype analysis and survival probability, Phylo CSF UCSC genome browser for conserved sequences and protein-coding potential, BcGenExMiner for correlation analysis and UALCAN for protein-coding gene expression. These above-mentioned lncRNAs showed high expression in the basal subtype of TNBC as compared with other subtypes and they showed poor survival rates in the basal subtype. LINC01356 and LINC01357 showed positive correlation with TAF3 and SLC16A1. ARF4-AS1 positively correlated with ASB14 and FAM83B positively correlated with HCTR2. These lncRNAs showing positive correlation with different genes have a role in breast cancer development and progression.

**Keywords:**

**Online publication:** October 2, 2024

## 1. Introduction

Breast cancer is a complex and heterogeneous type of cancer and is a highly prevalent cancer among females exhibiting a high mortality rate whereas its frequency is low in males approximately 1%. It depends on multiple factors including genetic history, radiation exposure, environmental carcinogens, poor diet etc.<sup>[1]</sup>. Cancer is globally prevalent but differs in the incidence rate and mortality rate due to differences in genetic makeup, ethnicity and living standards<sup>[2,3]</sup>. Breast cancer involves multiple risk factors, such as some of which are modifiable risk factors that can be altered to reduce the incidence of breast cancer like dietary uptake, environmental exposure,

and sedentary lifestyle and some are non-modifiable risk factors which are unavoidable like genetic history and demographic variables which all lead towards progression of breast cancer <sup>[4,5]</sup>.

Long non-coding RNAs (lncRNAs) are non-coding RNA molecules of length greater than 200 nucleotides. About 98% human genome is transcribed into noncoding RNAs and only 2% is transcribed into protein coding transcript <sup>[6]</sup>. These RNAs are involved in the regulation of genetic expression through different post-transcriptional and epigenetic mechanisms. Their functionality involves housekeeping, genomic imprinting, translation, RNA degradation and protein kinetics <sup>[7,8]</sup>. lncRNA is categorized into five categories depending upon its origin in the genome including sense lncRNA, antisense lncRNA, bidirectional lncRNA, intronic lncRNA and intergenic lncRNA. lncRNAs are comparatively high in concentration in the nucleus as compared to mRNA whereas in cytoplasm, they are in lesser concentration associated with ribosomes <sup>[9]</sup>. lncRNAs biogenesis involves DNA elements i.e., promoters, enhancers, and intergenic regions through which they are transcribed <sup>[10]</sup>. Many mechanisms are undergoing their synthesis such as the breakage of ribonuclease P (RNaseP) to form mature ends, synthesis of circular structures and formation of small nucleolar RNA (snoRNA) <sup>[11]</sup>.

Initially, it was considered as nonfunctional component of RNA polymerase but later on, it has shown diversified functionality such as metabolic pathways, cellular developmental processes, imprinting, cell cycle regulation, transcription, translation, splicing, and mRNA decay. There are three levels of mRNA regulation. Epigenetic regulation, transcriptional and post-transcriptional regulation <sup>[12]</sup>. The genetic expression is usually regulated by various epigenetic factors like DNA methyl transferases and chromatin-modifying complexes and during tumor progression epigenetic silencing inactivates tumor suppressive genes <sup>[13]</sup>. So, lncRNA mainly targets this silencing to regulate processes like ANRIL, H19, and HOTAIR, achieve repress their transcriptional activity by chromatin-remodeling or histone-modifying proteins. lncRNAs can perform their function by interacting with RNA, DNA, protein and metal ions and forming tertiary structures <sup>[14]</sup>. This lncRNA action is categorized into five subtypes based on interacting molecules and effects i.e., lncRNA interacts with protein, DNA, and RNA and it can also act as a catalyst which results in its various biological roles <sup>[15]</sup>.

lncRNAs are involved in various human diseases and their progressions and breast cancer is one of them. lncRNAs such as XIST, H19 and MALAT1 were most comprehensively studied for their role in breast cancer progression <sup>[16]</sup>. XIST is downregulated lncRNA found in many cancer cell lines including breast tumors by suppressing AKT signaling so it is a tumor suppressor. H19 is expressed in luminal A and luminal B subtypes of breast cancer. It works by promoting proliferation and hindering apoptosis in cancerous cells so acts as a tumor progressor. MALAT1 is upregulated in luminal A, luminal B and HER2 subtypes, where it promotes cancer cell invasion and migration and targeting it slows tumor growth and metastasis so it also promotes cancer progression <sup>[17]</sup>. In the present study, differentially expressed lncRNAs were selected including LINC01356, LINC01357, ARF4-AS1, and FAM83B. The study is focused on the expression of lncRNAs and their role in triple negative breast cancer. This study explored their effect on breast cancer progression through correlation with protein-coding genes to elucidate their role in breast cancer.

## 2. Experimental plan

This study was designed to investigate the genetic expression of long non-coding RNA expression in breast cancer. It was divided into two parts of wet lab and dry lab. For this purpose, post-surgical breast cancer samples were collected for RNA isolation. Then due to COVID-19, the study moved toward in silico work. For in silico work, different bioinformatics tools were used to explore different features of lncRNA to predict their role in the progression of breast cancer.



## 2.1. Wet lab

The present study was first approved by the Ethical Review Committee of COMSATS University Islamabad. The samples that were collected for this study from various tertiary care hospitals involved blood samples of breast cancer patient and post-surgical normal tissue and tumor tissue. Before sample collection, the consent form was signed. After surgery, fresh tumor sample of size almost 5–6 mm was excised and a control sample of about 2 cm was removed from the surrounding region of the same patient. Tissue and blood was taken from the patient ignoring age, gender, and stage. Post-surgery samples were immediately shifted to RNA later® and were stored in a refrigerator at 2–8 °C. The sample was transferred from the hospital in an ice box along with ice packs and maintained at a temperature of 2–8 °C. Samples were still in RNA later® before RNA extraction so to preserve RNA integrity. Samples were removed from RNA later® and transferred to a petri dish having 1 mL chilled PBS DEPC. Trizol reagent method was used to extract RNA from samples. Surgical blades separate fats from tissue by cutting tissue into small pieces. These pieces were transferred to a glass homogenizer with 1mL PBS. After some time as crushing proceeds, 10 µL of Betamercptaethanol was added until the tissue softened. Then, 100 µL of the mixture was taken into Eppendorf tubes for extraction of DNA. After this, 1 mL triazole reagent was added to the remaining sample and further crushed for RNA extraction. When the sample was homogenized and it gave a pinkish milky appearance it was transferred in the Eppendorf tube then 200 µL chloroform was added for protein degradation and incubated at room temperature for 5 minutes after inversion so to separate nuclear protein. After incubation centrifugation of labeled Eppendorf containing crushed tissue was done at 12,000 rpm for 15 minutes at 4 °C. After centrifugation, three layers were formed. After which, the upper aqueous layer was transferred into newly labeled Eppendorf tubes for further RNA treatment.

After this step, 2 µL of glycogen and then an equal volume of isopropanol to separate the aqueous layer was added in a labeled Eppendorf tube. Then, sodium acetate which is equal to the volume of 1/10<sup>th</sup> aqueous layer was added so that the pellet became visible and tubes were stored at -20 °C overnight. Next day, the study thawed the mixture and then centrifugation was done at 12,000 rpm at 4 °C for 10–15 minutes. Now in the Eppendorf tube, the RNA pellet was carefully observed at the bottom of tube and the supernatant was removed by placing tip opposite to the pipette. 200 µL of 70% ethanol was added in each Eppendorf tube for washing the pellet. Again, the tubes were spined at 4 °C for 5 minutes at 12,000 rpm. After spinning, the supernatant was carefully removed with a pipette without touching the pellet and the leftover pellet was dried at a dry heater (thermoblock) at 70 °C for 1 minute along with DEPC water. The dried pellet was dissolved in nuclease-free water (DEPC). After that, 35–60 µL DEPC was used for pellet resuspension according to the size of the pellet, then vortex Eppendorf tubes by moving them on a rack. A short spin was done for 15 seconds, then again dry heat for 45 seconds at 70 °C. Then, they were shortly spun for 15 seconds and were stored at 20 °C for cold shock.

RNA integrity was confirmed by the technique of denaturing gel electrophoresis. 1.2% agarose was weighed and dissolved in 100 mL 1X TBE buffer by heating in a microwave until it was completely dissolved. Then, it was allowed to cool down and 172 µL bleach for denaturing was added. In the next step, 7 µL ethidium bromide was added and moved slowly to mix and poured into a gel tray to solidify. It was prepared by mixing 2 µL of loading dye with 6 µL of formamide and 5 µL RNA sample was mixed with 8 µL master mix. Then, it was short spun and heat shock at 70 °C for 1 minute was given followed by a short spin and then placed in a freezer for 1 minute. Samples were then loaded into gel wells and horizontal gel was run first at 300 mA for 10 minutes at 90 V and then run for 35 minutes at 100 V.

Another method utilized for RNA quantification was through a spectrophotometer where optical density was measured and results were given by OD value. Firstly, dilutions of 1:100 were prepared by using 198 µL DEPC water and 2 µL RNA. Then, the machine was turned on for 10 minutes before measuring. The blank



was set to zero after baseline correction. Then, the samples were filled in a cuvette and test sample was run and finally OD values were taken as 260/280 ratio.

## 2.2. Dry lab / in silico

To find a highly differentially expressed lncRNA, the study utilized multiple online software, such as Ensemble genome browser, Tanric and Lncar, as they are common databases giving phenotype-specific lncRNA. Expression of lncRNAs was screened out and further validated using data from The Cancer Genome Atlas (TCGA) database. Data was taken from the Atlas of lncRNA in cancer (TANRIC) database which was quantified based on  $\log_2$ RPKM value. Out of multiple candidates, 5 highly expressed candidates were selected, that is, DDIT4-AS1, ASH1L-AS1, LINC01356, LINC01357 and ARF4-AS1. Tissue-specific gene expression and regulation of selected lncRNAs were determined using the Genotype-Tissue Expression database (GTEx). This database was utilized to find out what changes occur at the genomic level that led to the conversion of healthy cells into faulty cells that cause various diseases. So, the database was targeted to find out the root cause of the disease and to develop treatment accordingly for improvement in diagnostic and therapeutic hallmarks. By applying filters of the chosen organ, the study checked tissue-specific expression analysis of targeted 5 lncRNAs in breast tissue and whole blood. Overall survival analysis of breast cancer patients was calculated by comparing them with healthy individuals using GEPIA 2 (Gene expression profiling interactive index). GEPIA was previously used but later it was upgraded to GEPIA2 to provide insights with more functioning. It provides a survival analysis graph in comparison between normal individuals and tumor patients and is presented in the form of curves. For breast cancer, BRCA subtype was selected to present survival curves of 5 genes in breast cancer.

GEPIA2 (gene expression profiling interactive analysis) was used to analyze the cancer genome atlas (TCGA). GEPIA is web-based is a web-based tool that provides quick and targeted functions based on TCGA and Gtex data. Expression DIY was targeted to analyze and compare the expression of normal individuals and tumor patients with BRCA cancer type. GEPIA 2 was used for lncRNAs subtype analysis. This study allows choosing a subtype and finding its expression analysis or survival analysis. Then for the breast cancer subtype, subtype filter BRCA was applied and box plot was plotted for normal and tumor differential expression of selected lncRNAs. PhyloCSF was used for comparative differentiation to analyze the coding potential of lncRNA by selecting phyloCSF tracks. PhyloCSF was used for the alignment of multispecies genomes to recognize coding regions in the genome. Similarly, selected genes (lncRNAs) were aligned with 100 vertebrate genome to recognize the protein-coding potential of genes.

lncATLAS is a bioinformatics tool that was used to find lncRNAs subcellular localization because lncRNAs functionality is dependent on their location. For this purpose, it uses various RNA sequencing datasets. Relative concentration index (RCI) was used to find the location of 6768 lncRNAs which were represented in different compartments of 15 cell lines. lncATLAS was approachable through an informative web server, where lncRNA of interest was retrieved through names. Localization was given across cell types and organelles. BcGenExMiner is a recently developed web-based application to evaluate prognostic information of breast cancer genes using a prognostic module known as a correlation module. This module involves three kinds of gene expression correlation analysis. In the first type of analysis, 10 targeted lncRNA correlation coefficient can be computed. In the second type, targeted lncRNA can be compared with 2 sets of genes for correlation coefficient. In the third type, targeted lncRNA can be compared with genes in close vicinity for correlation coefficient. The correlation analysis was performed in molecular subtypes of TNBC (HER2+, luminal A, luminal B and normal). In a gene correlation targeted analysis, 3 to 16 different genes were selected and analyzed in 4 molecular subtypes of BC. Results were displayed in the form of a heat map where the dark

red coefficient is represented as (-1) and dark blue is represented as (+1). The correlation of normal and basal subtypes was compared. The selected LncRNA was correlated with cis and trans-protein-coding genes.

UALCAN is an interactive web portal that was utilized to check the expression of positively correlated cis or trans-protein-coding genes with LncRNA. It allowed users to perform and analyze the relative expression of a protein-coding gene across basal and normal subtypes, as well as in other subtypes like HER2, luminalA and luminal B so to interpret over and under-expressed (up and down-regulated) genes in breast cancer. In silico validation of targeted genes was done and further identification of tumor subgroup specific candidate biomarkers.

### 3. Results

#### 3.1. RNA extraction

Blood and tissue samples i.e. normal tissue and tumor from breast cancer patients were taken and processed for RNA extraction using TRIZOL reagent. After this, agarose gel was used to check the quality of extracted RNA by visualizing band on the gel. After that, formamide was used to remove the secondary structure of RNA by giving initial denaturation at 70 degrees centigrade. Figure 1 shows intact bands of rRNA of the size of 28SrRNA, 18SrRNA and 5.8SrRNA and it is indicating RNA is not denatured and of good quality.

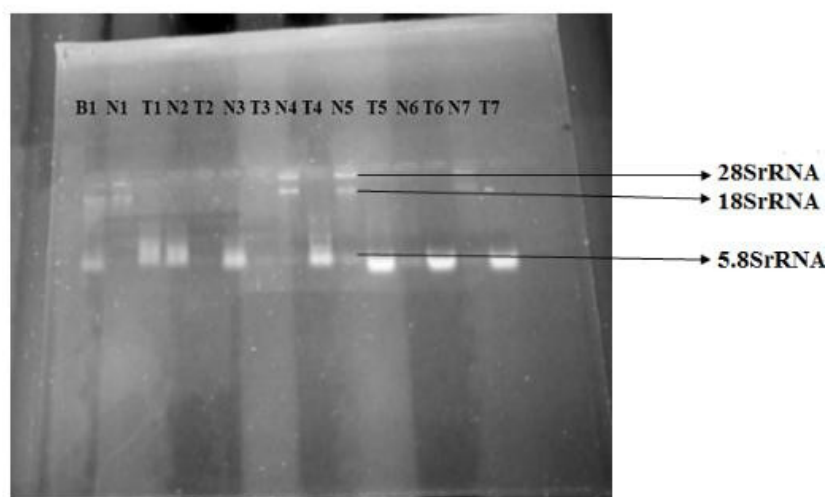


**Figure 1.** Extraction of RNA from tissue and blood samples from breast cancer patients.

LncRNA having differential expression was selected and shortlisted based on tumor and normal samples database from TCGA and GTEx. They were analyzed by comparing their values between tumor and normal samples. Six potential candidate lncRNA genes were selected based on their fold difference between the two datasets.

**Table 1.** List of selected lncRNA that differentially expressed in breast cancer

Rank	Transcript ID	Name	$F_{pkm}$ value subset 1 breast cancer/ TNB C	$F_{pkm}$ value subset 2 Breast cancer/ normal TNB C
1	ENSG00000269926	DDIT4-AS1	13.10	2.49
2	ENSG00000235919	ASHIL-AS1	2.83	1.39
3	ENSG00000215866	LINC01356		
4	ENSG00000224167	LINC01357		
5	ENSG00000272146	ARF4-AS1		

## 3.2. DDIT4-AS1

### 3.2.1. Subtype analysis of DDIT4-AS1 using GEPIA-2

DDIT4-AS1 is located at chromosome 10q22.1 having 2 exons. DDIT4-AS1 is anti-sense, non-coding RNA with 1 transcript only. Expression analysis among four subtypes of BC was performed using GEPIA2. Results showed that DDIT4-AS1 is significantly upregulated in all four subtypes of breast cancer and can play a role in the progression of all these types.

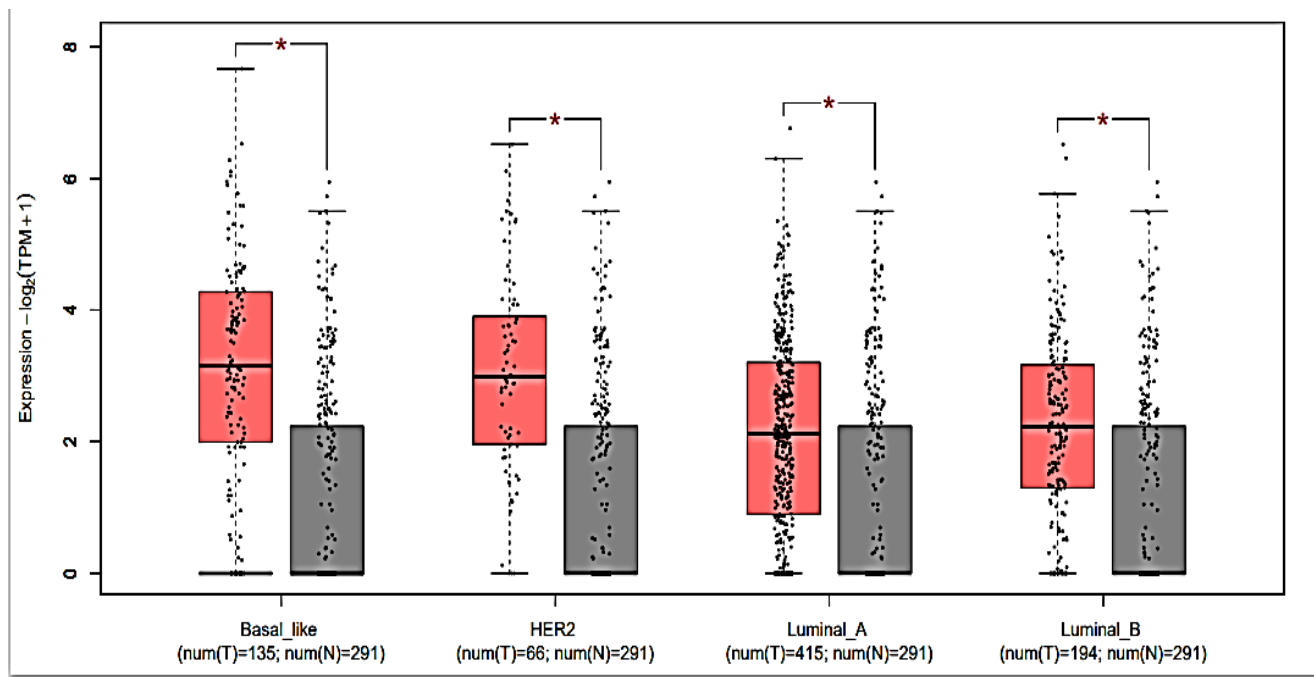


**Figure 2.** Subtype analysis of DDIT4-AS1 based on TCGA data. The box plot in red represents tumor while in grey represents normal. DDIT4-AS1 expression is upregulated in all four subtypes of BC.

### 3.2.2. Survival analysis of DDIT4-AS1

The impact of DDIT4-AS1 on basal breast cancer patient survival probability was evaluated using GEPIA2 and showed less difference between the survival probability of the low and high expression group. However, the high expression group showed less survival probability after 250 months showing it is not oncogenic.

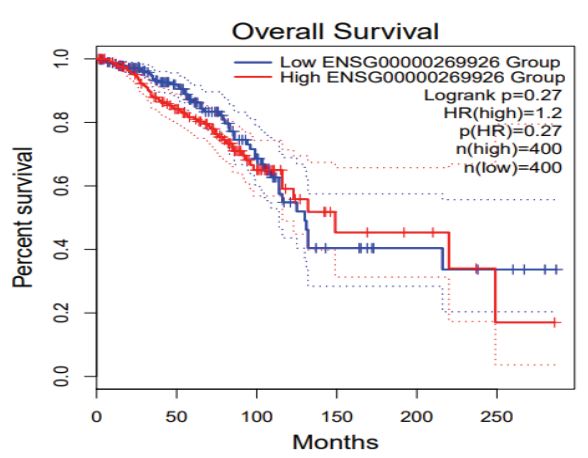


**Figure 3.** Survival analysis of DDIT4-AS1 using GEPIA-2. The above graph showed less difference between the survival probability of low and high expression groups in the basal subtype of breast cancer. The survival probability is shown on the y-axis whereas the time duration in months is shown on the x-axis. HR represents the hazard ratio.

### 3.4. ASHIL-AS1

#### 3.4.1. Subtype analysis ASHIL-AS1

ASHIL-AS1 is located at chromosome 1q22 having 2 exons. This gene encodes for a non-coding RNA with 2 different transcript isoforms. Tissue specific expression analysis using GTex showed high expression in normal breast-mammary tissue.

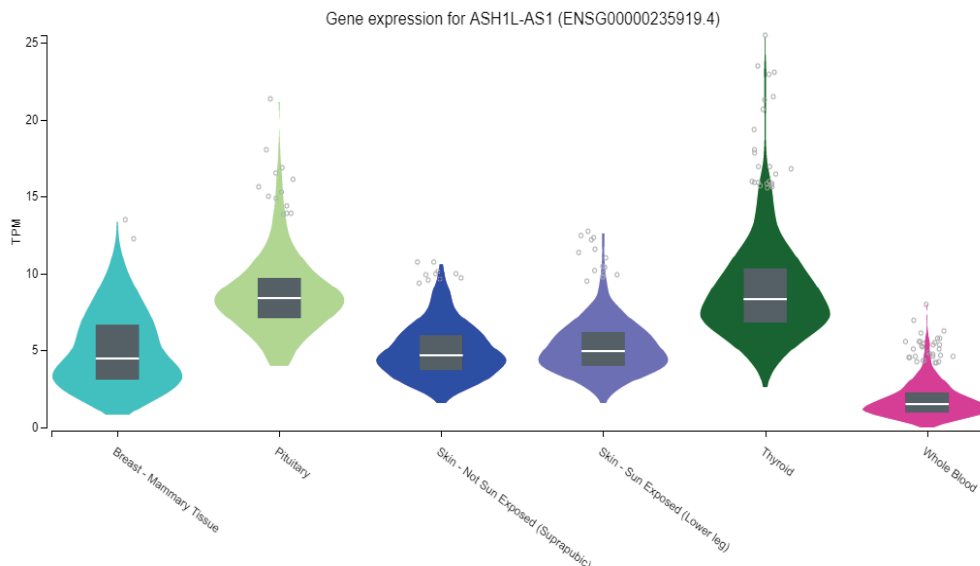
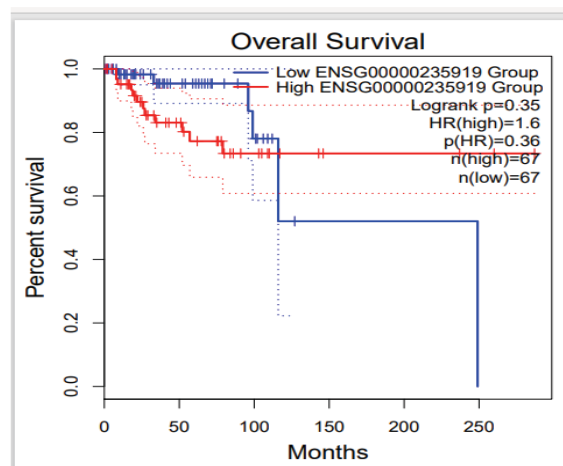


**Figure 4.** Tissue-specific expression analysis of ASHIL-AS1 Expression analysis showed around 13TPM expression of ASHIL-AS1 in normal breast mammary tissue. Expression values are in transcript per million (TPM). Light Blue color represents breast mammary tissue, mustard represents pituitary, dark blue represents non-exposed skin, light purple represents exposed skin, dark green represents thyroid and pink represents whole blood.

#### Figure 5. Survival analysis of ASHIL-AS1 using GEPIA-2.

The above graph showed a decrease in the survival possibility of the low survival group and indicated a constant level of survival for the high group at 0.8 so it is not oncogenic. The survival probability is shown on the y-axis whereas the time duration in months is shown on the x-axis. HR represents the hazard ratio.



#### 3.4.2. Survival analysis of ASHIL-AS1

The impact of ASHIL-AS1 on basal breast cancer patient survival probability was evaluated using GEPIA2 and showed a decrease in the survival percentage of the low group whereas the high group became constant at 0.8 indicating not oncogenic nature.

### 3.5. LINC01356

#### 3.5.1. Tissue-based expression analysis of LINC01356

LINC01356 is located at chromosome 1p13.2 having 7 exons. This gene is long intergenic non protein

coding RNA with 5 different transcript isoforms. Tissue specific expression analysis using GTex showed low expression in normal breast mammary tissue.

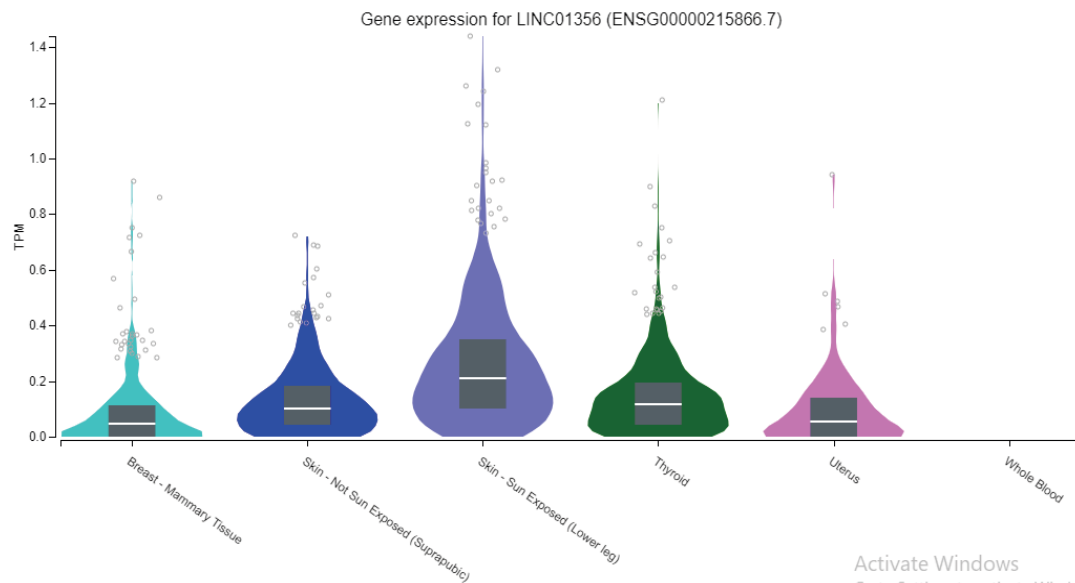


**Figure 6.** Tissue specific expression analysis of LINC01356 Expression analysis showed insignificant expression of around 0.8 TPM expression of LINC01356 in normal breast mammary tissue. Expression values are in transcript per million (TPM). Light blue shows breast mammary tissue, dark blue shows unexposed skin, light purple shows exposed skin, dark green shows the thyroid, magenta shows the uterus and pink shows whole blood.

### 3.5.2. Subtype analysis of LINC01356

Expression analysis was performed among four subtypes of BC using GEPIA2. It was calculated by mean value of  $\log_2(\text{TPM}+1)$  in each subtype of breast cancer. Results showed that LINC01356 is upregulated in basal-like breast cancer as compared to the other three subtypes. However, the upregulation of linc01356 is not significant.

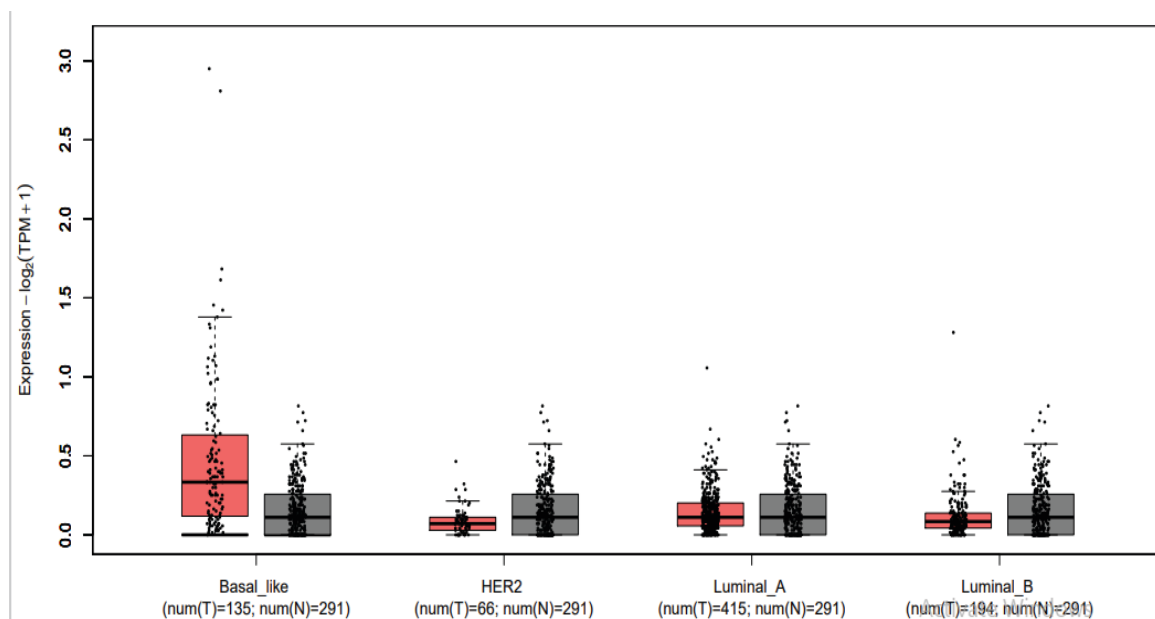


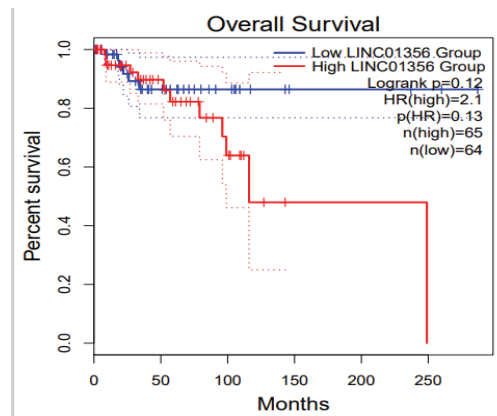
**Figure 7.** Subtype analysis of LINC01356 based on TCGA data. The box plot in red represents the tumor while in grey represents normal. LINC01356 expression is upregulated in the basal subtype of BC as compared to the other three subtypes.



### 3.5.3. Survival analysis of LINC01356

LINC01356 is upregulated in the basal subtype survival graph as we evaluated it through GEPIA2. There are two groups i.e. red represents the high expression group whereas blue represents the low expression group. HR represents the hazard ratio which is an indication of the association between different treatments (radiotherapy and chemotherapy) and survival time. The graph shows a decrease in survival rate for 250 months for high survival groups.

**Figure 8.** Graph showing overall survival analysis of LINC01356. The higher expression group showed low survival probability as it decreases to 0 during 250 months so it is oncogenic. The percent survival is shown on the y-axis and the time duration in months is shown on the x-axis.



### 3.5.4. Gene structure LINC01356

LINC01356 is a long intergenic non-coding RNA having a size of 1819 bp. It has 5 transcript isoforms. Table 2 shows multiple transcripts of LINC01356 along with their transcript length.

**Table 2.** List of transcripts of LINC01356

Transcript ID	Name	Bp	Protein	Bio type
ENST00000401018.5	LINC01356-201	1819	No protein	lncRNA
ENST00000661136.1	LINC01356-204	1430	No protein	lncRNA
ENST00000667852.1	LINC01356-205	1222	No protein	lncRNA
ENST00000433505.5	LINC01356-202	767	No protein	lncRNA
ENST00000449572.2	LINC01356-203	702	No protein	lncRNA

### 3.5.5. Protein coding potential using PhyloCSF

The coding potential of LINC01356 was further evaluated by using PhyloCSF tool uses a calculate the phylogenetic conservation score multi-species nucleotide sequence alignment, which represents a probable protein-coding region. LINC01356 shows all the peaks towards negative axis indicating that it does not code for any protein or shorter peptide.

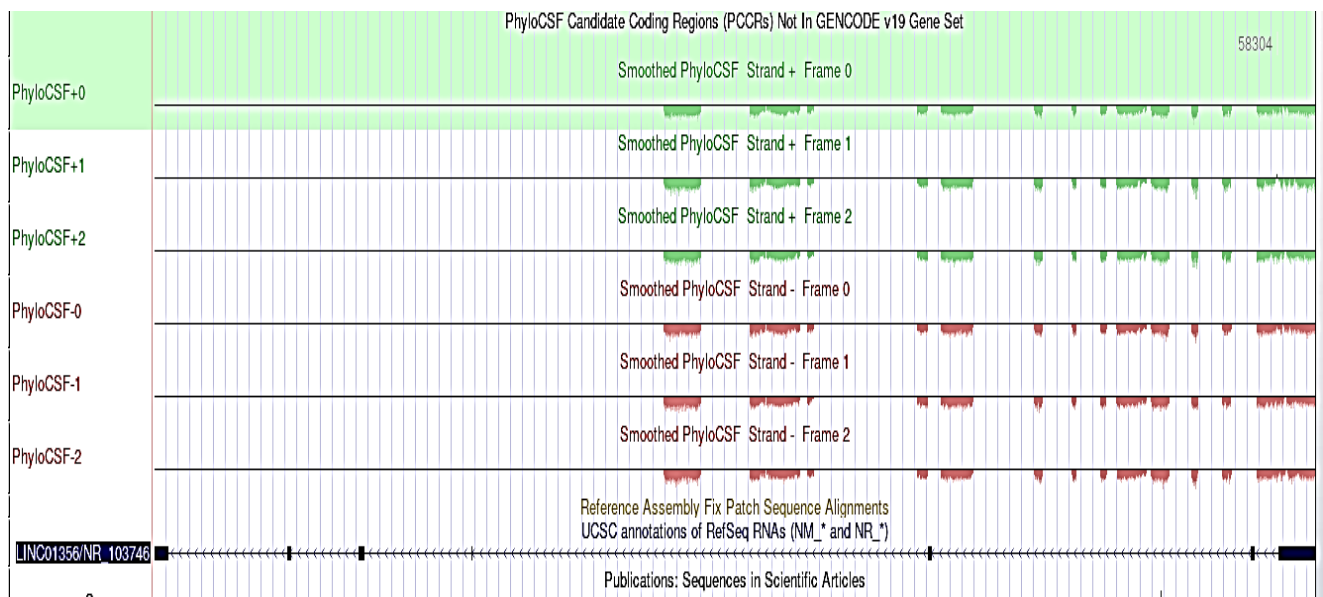


**Figure 9.** Protein coding potential of LINC01356. The coding potential was evaluated and PhyloCSF. The coding potential was evaluated in three frames indicated as 0, 1 and 2. All the peaks lie in the negative axis indicating that LINC01356 has no coding potential.

### 3.5.6. Conservation of sequence and structure

Few alignments of 100 vertebrates showed little conservation of LINC01356 in rhesus and elephant.

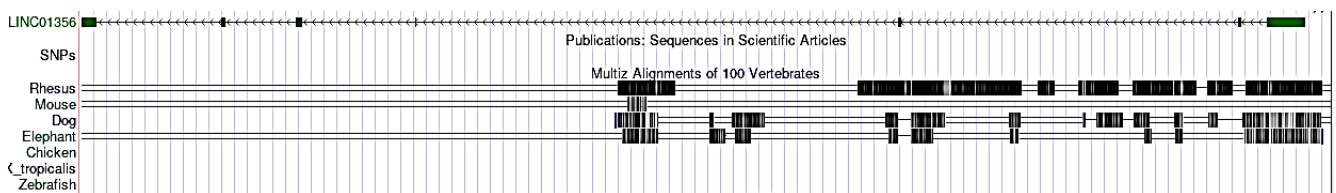


**Figure 10.** Multiz alignment of 100 vertebrates showing little bit conservation of LINC01356 in rhesus and elephant.

### 3.5.7. Nucleo-cytoplasmic localization of LINC01356

The nucleo-cytoplasmic localization of LINC01356 was determined by using lnc-ATLAS. MALATI was used as a reference nuclear gene whereas DANCER was used as a reference cytoplasmic gene. LINC01356 showed cytoplasmic localization in different cell lines i.e. H1, HESC and HUVEC and indicating their role in regulating gene expression via RNA-RNA or RNA-protein interaction.

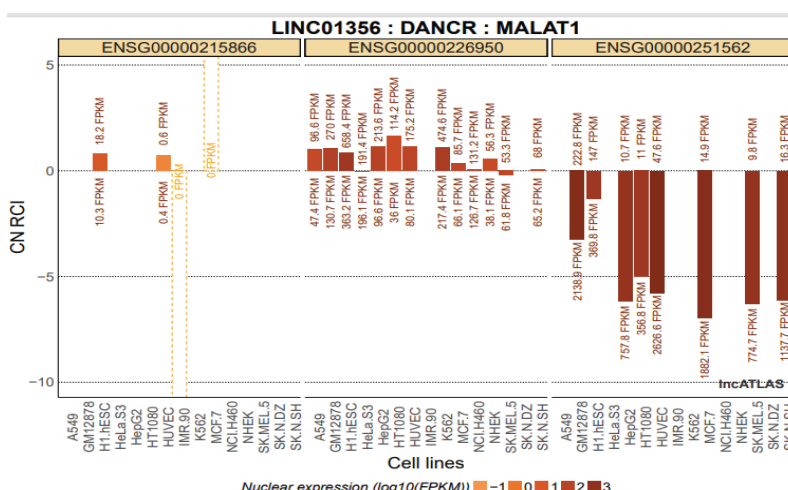


**Figure 11.** Nucleo-cytoplasmic localization of LINC01356. LINC01356 showed few cytoplasmic localizations in multiple cell lines. MALATI was used as a reference nuclear gene for the nucleus and DANCER was used as a reference gene for the cytoplasm. RCI represents the relative concentration index based on the comparison of gene concentration per unit RNA mass between two cellular compartments.

3.5.8. Macromolecular interactions involving LINC01356

LINC01356 can interact with neighboring genes or genes on other chromosomes in a cis or trans manner. Two protein-coding genes (TAF A3 and SLC16A1) which are in close vicinity were selected for correlation expression with LINC01356 (non-coding gene). BcGenExMinor4.5 tool was used to evaluate the correlation expression of coding and non-coding genes between four breast cancer subtypes.

**Figure 12.** Correlation of Cis interactors TAF A3 and SLC16A1 with LINC01356 predicted by BcGenExMinor4.5 in the normal subtype. TAF A3 showed a strong correlation as compared to SLC16A1 in a normal subtype of breast cancer. Blue color represents a negative correlation whereas red represents a strong positive correlation.

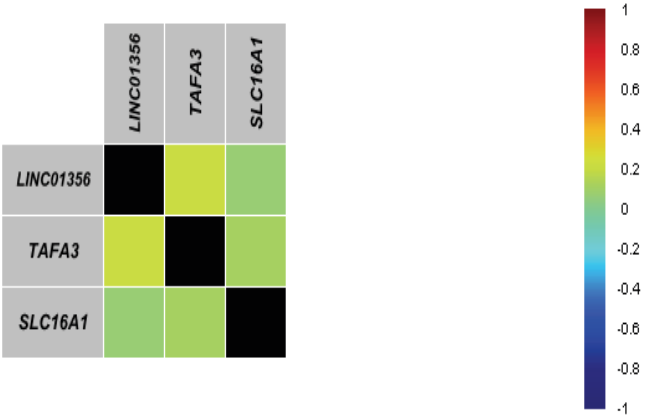
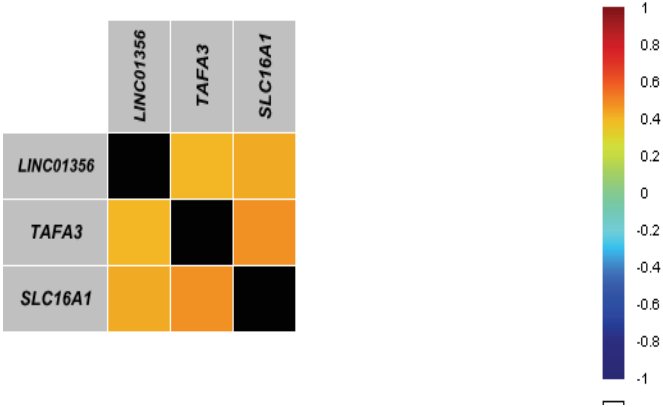
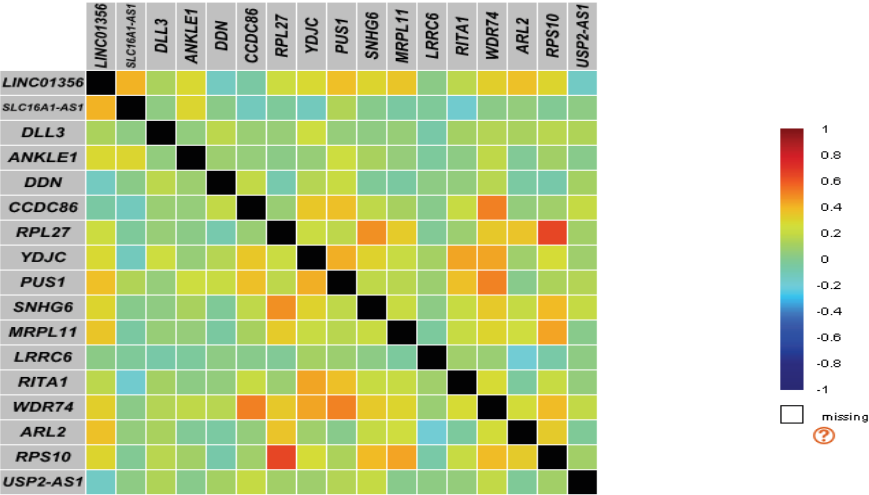


**Figure 13.** Correlation of Cis interactors TAF A3 and SLC16A1 with LINC01356 predicted by BcGenExMinor4.5 in basal (TNBC) subtype. Both TAF A3 and SLC16A1 showed a strong correlation with LINC01356.



Linc01356 has cytoplasmic localization. Therefore, different trans-acting genes were explored using BcGenExMinor4.5. The following heat map exhibits different trans-interacting genes with positive expression correlation with LINC01356.

**Figure 14.** Heat map showing the correlation of LINC01356 with different genes in normal breast cancer tissue. SLC16A1-AS1 showed a positive correlation with LINC01356 based on TCGA RNA seq data as predicted by bcExGenMinor4.5. Blue color represents a negative correlation whereas red represents a strong positive correlation.



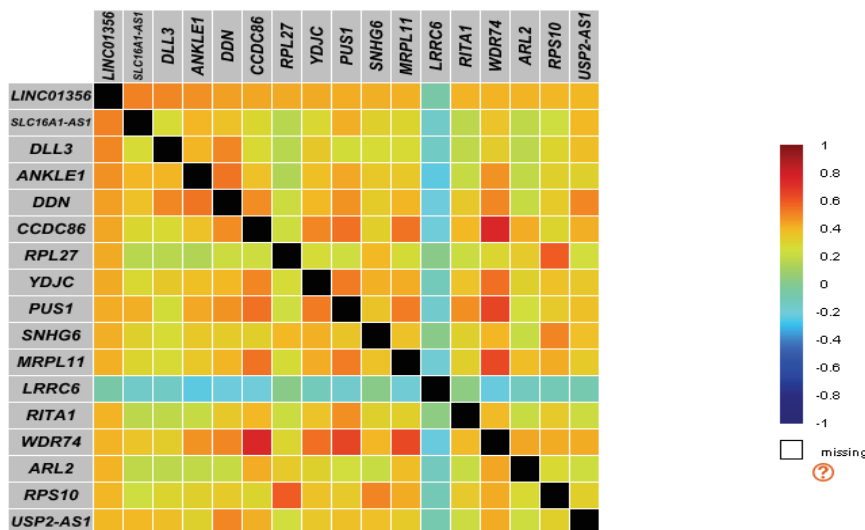


**Figure 15.** Heat map showing the correlation of LINC01356 with different genes in the basal subtype. SLC16A1-AS1, DLL3, ANKLE1, and DDN showed a more positive correlation with LINC01356 as compared to other genes based on TCGA RNA seq data as predicted by bcExGenMiner4.5. Blue color represents a negative correlation whereas red represents a strong positive correlation.

### 3.6. LINC01357

#### 3.6.1. Tissue-based expression analysis of LINC01357

LINC01357 is located at chromosome 1p13.2 having 3 exons. This gene is long intergenic non-protein coding RNA with 3 different transcript isoforms. Tissue-specific expression analysis using GTex showed insignificant expression in normal breast mammary tissue.

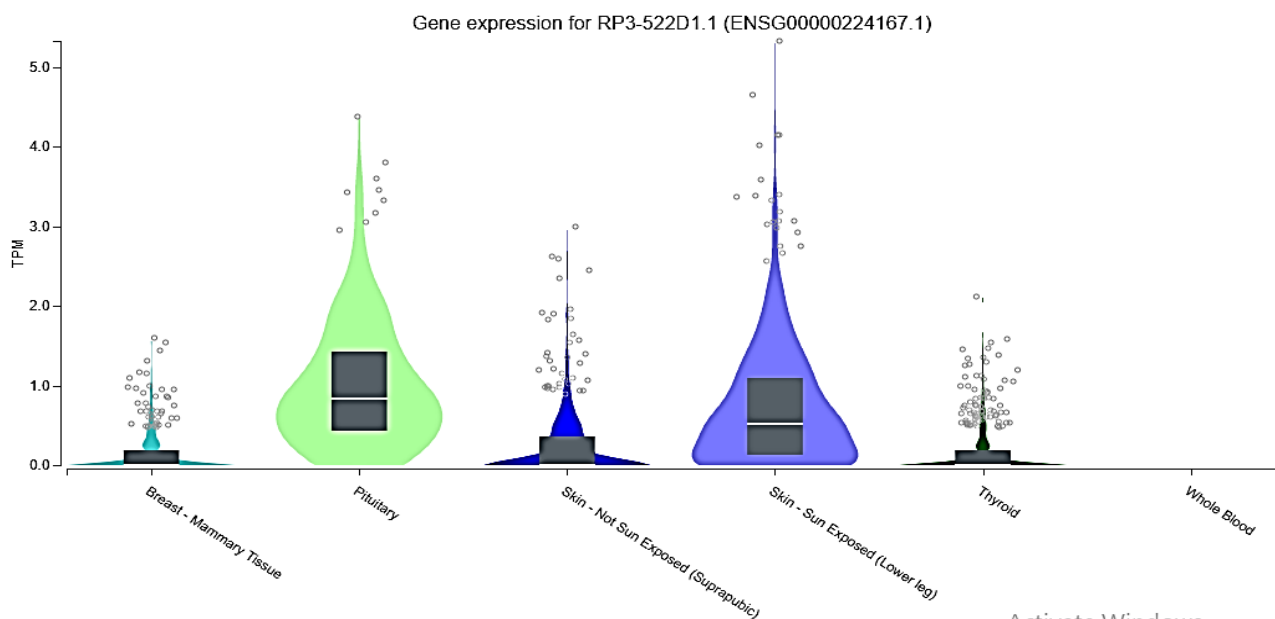


**Figure 16.** Tissue-specific expression analysis of LINC01357 Expression analysis showed insignificant expression around 1TPM expression of LINC01357 in normal breast mammary tissue. Expression values are in transcript per million (TPM). Light blue shows breast mammary tissue, mustard shows the pituitary gland, DARK blue shows unexposed skin, sky blue shows exposed skin, dark green represents the thyroid and pink represents whole blood.

#### 3.6.2. Subtype analysis of LINC01357

Expression analysis was performed among four subtypes of BC using GEPIA2. It was calculated by mean value of log2 (TPM+1) in each subtype of breast cancer. Results showed that LINC01357 is upregulated in basal-like breast cancer as compared to the other three subtypes.

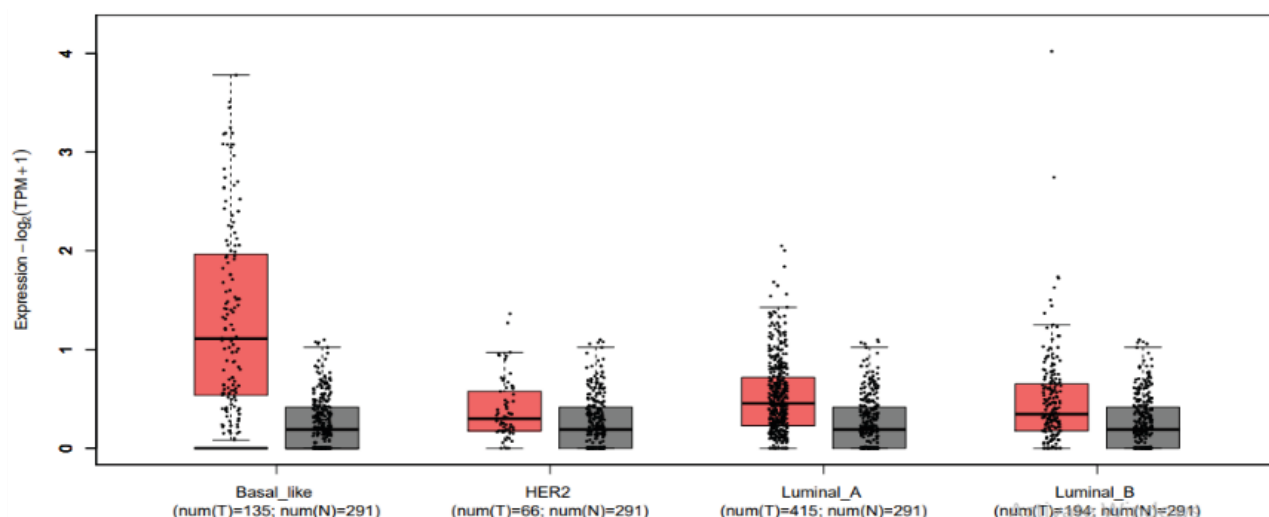


**Figure 17.** Subtype analysis of LINC01357 based on TCGA data. The box plot in red represents the tumor while in grey represents normal. LINC01357 expression is upregulated in a basal subtype of BC than the other three subtypes.

### 3.6.3. Survival analysis of LINC01357

LINC01357 is highly upregulated in the basal subtype survival graph as we evaluated it through GEPIA2. There are two groups i.e. red represents the high expression group whereas blue represents the low expression group. HR represents the hazard ratio which is an indication of the association between different treatments (radiotherapy and chemotherapy) and survival time.

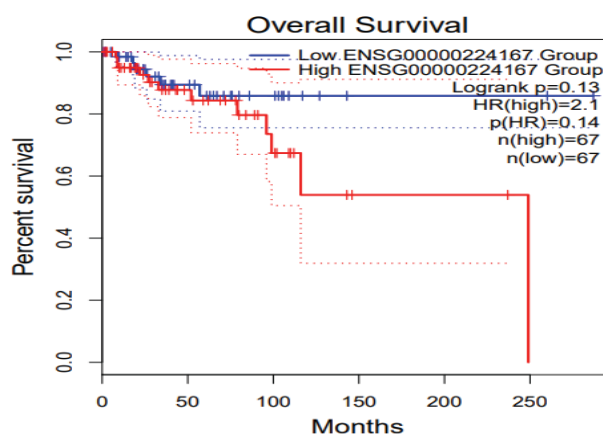


**Figure 18.** Graph showing overall survival analysis of LINC01357. The higher expression group showed low survival probability. Blue color represents low expression; red represents high expression and n represents the number of patients. The percent survival is shown on the y-axis and the time duration in months is shown on the x-axis.

### 3.6.4. Gene structure

LINC01357 is a long intergenic non-coding RNA having a size of 1819 bp. It has 3 transcript isoforms. Table 3 shows multiple transcripts of LINC01357 along with their transcript length.

**Table 3.** List of transcripts of LINC01357

Transcript ID	Name	Bp	Protein	Bio type
ENST00000658577.1	LINC01357-203	749	No protein	lncRNA
ENST00000456651.1	LINC01357-202	587	No protein	lncRNA
ENST00000422022.1	LINC01357-201	490	No protein	lncRNA



### 3.6.5. Protein coding potential using PhyloCSF

The coding potential of LINC01357 was further evaluated by using the PhyloCSF tool. PhyloCSF uses a calculate the phylogenetic conservation score multi-species nucleotide sequence alignment, which represents a probable protein-coding region LINC01357 shows all the peaks towards the negative axis and does not code for any protein.

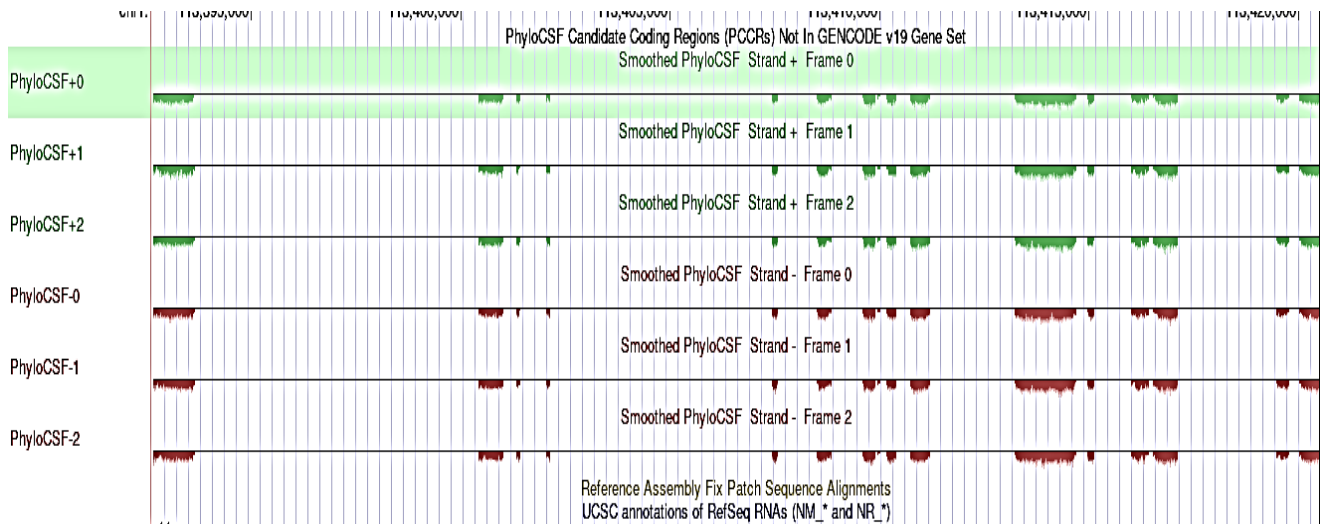


**Figure 19.** Protein coding potential of LINC01357. The coding potential was evaluated and PhyloCSF. The coding potential was evaluated in three frames indicated as 0, 1 and 2. All the peaks lie in the negative axis indicating that LINC01357 does not code for a protein.

### 3.6.6. Conservation of sequence and structure

Few alignments of 100 vertebrates showed conservation of LINC01357 in rhesus. However, less conservation is observed in elephants and mice.

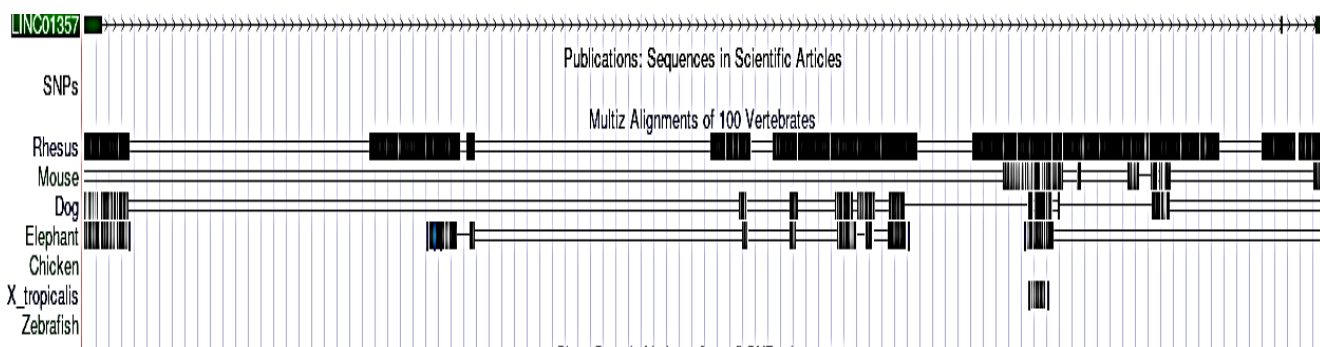
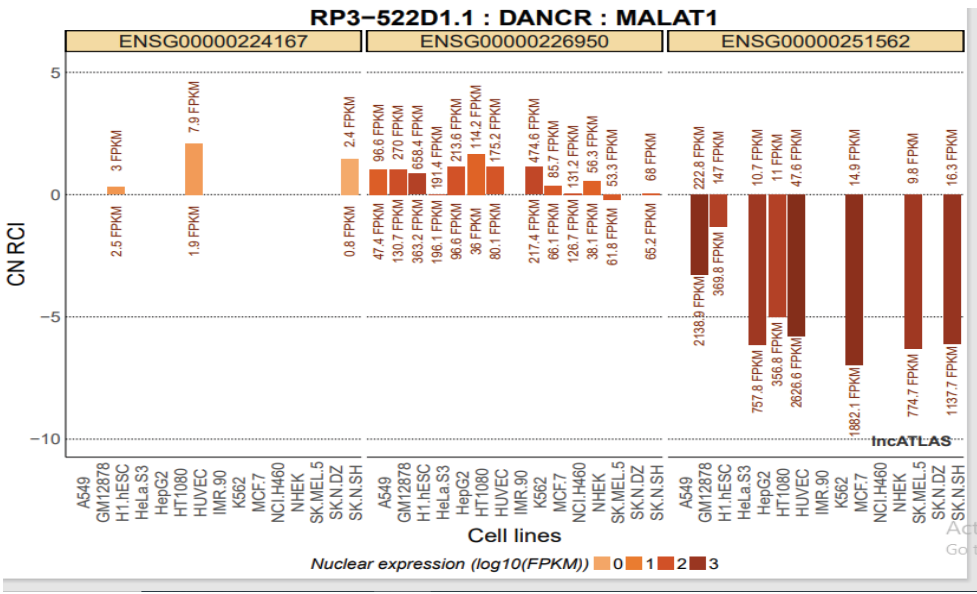


**Figure 20.** Multiz alignment of 100 vertebrates showing little bit of conservation of LINC01357.

### 3.6.7. Nucleo-cytoplasmic localization of LINC01357

The nucleo-cytoplasmic localization of LINC01357 was determined by using lnc-ATLAS. MALAT1 was used as a reference nuclear gene whereas DANCR was used as a reference cytoplasmic gene. LINC01357 showed few cytoplasmic localization in different cell lines indicating its role in regulating gene expression via RNA-RNA or RNA-protein interaction.

**Figure 21.** Nucleo-cytoplasmic localization of LINC01357 LINC01357 showed few cytoplasmic localizations in multiple cell lines. MALAT1 was used as a reference gene for the nucleus and DANCR was used as the reference gene for the cytoplasm. RCI represents the relative concentration index based on the comparison of gene concentration per unit RNA mass between two cellular compartments.



### 3.6.8. Macromolecular interactions involving LINC01357

LINC01357 can interact with neighboring genes or genes on other chromosomes in a cis or trans manner. Two protein-coding genes (TAF3 and SLC16A1) which are in close vicinity were selected for correlation expression with LINC01357 (non-coding gene). BcGenExMinor 4.5 tool was used to evaluate the correlation expression of coding and non-coding genes between four breast cancer subtypes.

**Figure 22.** Correlation of Cis interactors TAF3 and SLC16A1 with LINC01357 predicted by BcGenExMiner 4.5 in normal subtype. TAF3 showed a negative correlation whereas SLC16A1 is negatively correlated in normal subtype of breast cancer. Blue color represents a negative correlation whereas red represents a strong positive correlation.

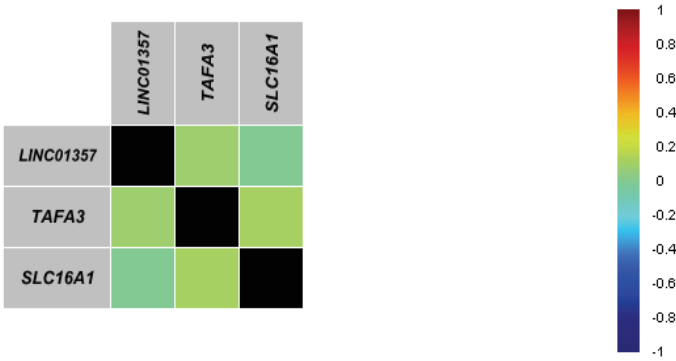
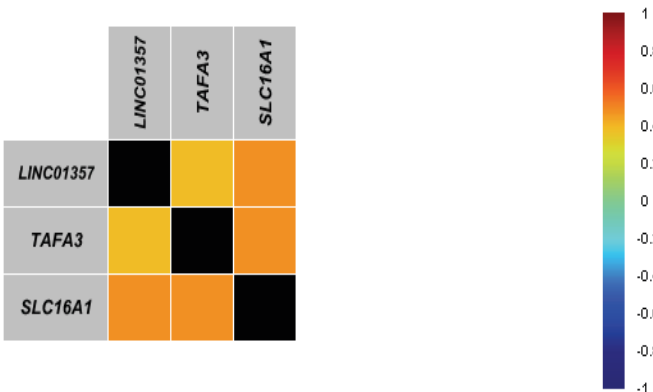


**Figure 23.** Correlation of Cis interactors TAF3 and SLC16A1 with LINC01357 predicted by BcGenExMiner4.5 in basal (TNBC) subtype. SLC16A1 and TAF3 showed strong correlation with LINC01357.



### 3.6.9. UALCAN database analysis

SLC16A1 is a protein coding gene which interact with LINC01357. It is highly up regulated in TNBC subtype as compared to other subtypes which is calculated through UALCAN database.

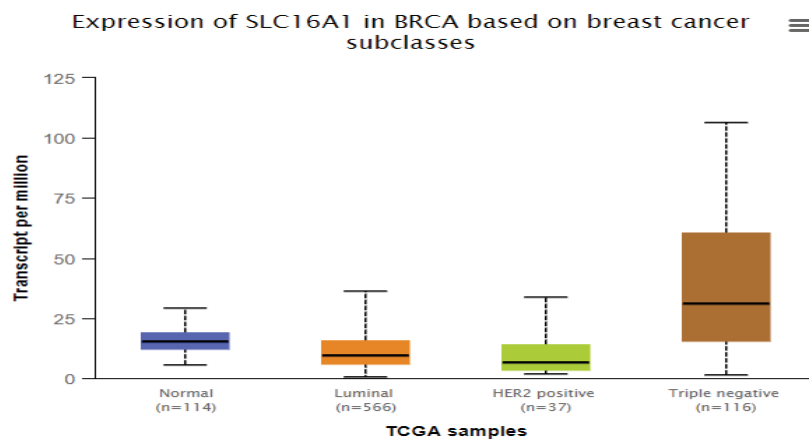


**Figure 24.** Box whisker plot showing SLC16A1 expression in breast cancer subtypes. SLC16A1 is significantly upregulated in TNBC while showing nominal expression in other subtypes as illustrated by the box plot.

**Table 4.** Statistical Significance of SLC16A expression in BRCA

Comparison	Statistical significance
Normal-vs-Luminal	3.863800E-02
Normal-vs-HER2 Positive	9.416100E-02
Normal-vs-TNBC	7.597200E-03
Luminal-vs-HER2 Positive	3.771600E-01
Luminal-vs-TNBC	2.843500E-02
HER2 Positive-vs-TNBC	2.218000E-01

### 3.7. ARF4-AS1

#### 3.7.1. Tissue-based expression analysis of ARF4-AS1

ARF4-AS1 is located at chromosome 3p14.3 having 3 exons. This gene is long intergenic non-protein coding RNA with 4 different transcript isoforms. Tissue-specific expression analysis using GTEx showed significant expression in normal breast mammary tissue.

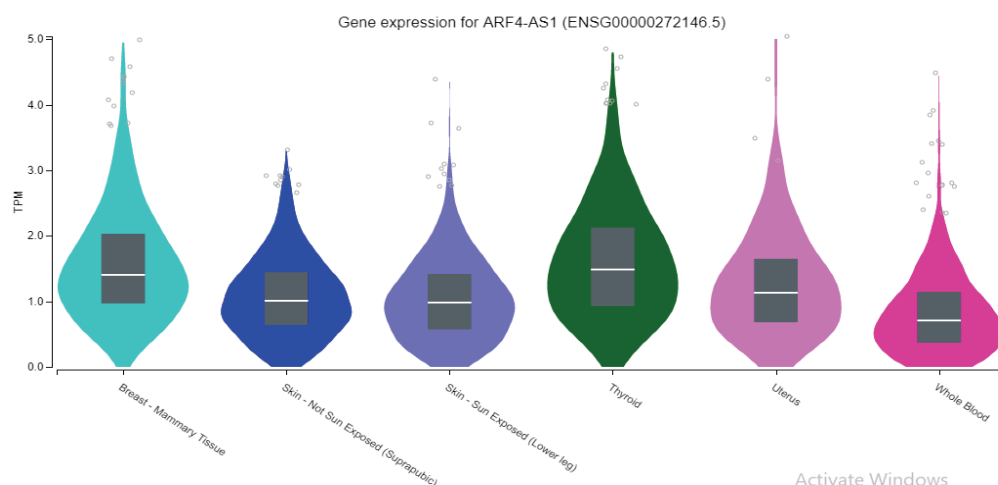
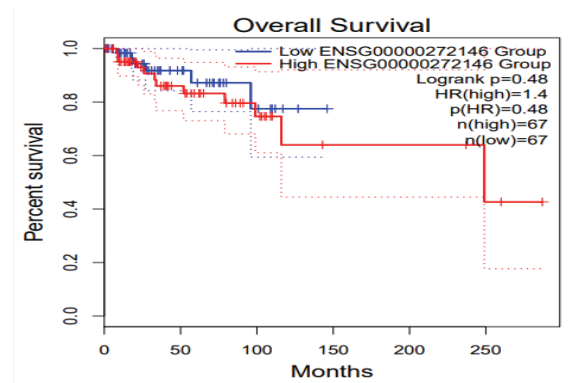


**Figure 25.** Tissue-specific expression analysis of ARF4-AS1 Expression analysis showed insignificant expression around 5TPM expression of ARF4-AS1 in normal breast mammary tissue. Expression values are in transcript per million (TPM). Light blue represents breast mammary tissue, dark blue represents unexposed skin, sky blue represents exposed skin, dark green represents the thyroid, light purple represents the uterus and pink represents whole blood.

### 3.7.2. Survival analysis of ARF4-AS1

ARF4-AS1 is highly upregulated in the basal subtype survival graph as the study evaluated it through GEPIA2. There are two groups i.e. red represents the high expression group whereas blue represents the low expression group. HR represents the hazard ratio which is an indication of the association between different treatments (radiotherapy and chemotherapy) and survival time. Figure 26 represents a decrease in the survival rate of the high expression group so it is oncogenic.

**Figure 26.** Graph showing overall survival analysis of ARF4-AS1. The higher expression group showed low survival probability. Blue color represents low expression; red represents high expression and n represents a number of patients. The percent survival is shown on the y-axis and the time duration in months is shown on the x-axis.



### 3.7.3. Gene structure

ARF4-AS1 is a long intergenic non-coding RNA having a size of 327bp. It has 4 transcript isoforms. Table 5 shows multiple transcripts of ARF4-AS1 along with their transcript length.

**Table 5.** List of transcripts of ARF4-AS1

Transcript ID	Name	Bp	Protein	Bio type
ENST00000606192.5	ARF4-AS1-201	327	No protein	lncRNA
ENST00000658756.1	ARF4-AS1-204	588	No protein	lncRNA
ENST00000607782.1	ARF4-AS1-203	552	No protein	lncRNA
ENST00000607297.1	ARF4-AS1-202	437	No protein	lncRNA

### 3.7.4. Protein coding potential using PhyloCSF

The coding potential of ARF4-AS1 was further evaluated by using PhyloCSF tool. PhyloCSF uses a calculate the phylogenetic conservation score multi-species nucleotide sequence alignment, which represents a probable protein-coding region. All peaks are towards negative axis showing it does not code for protein or small peptides.

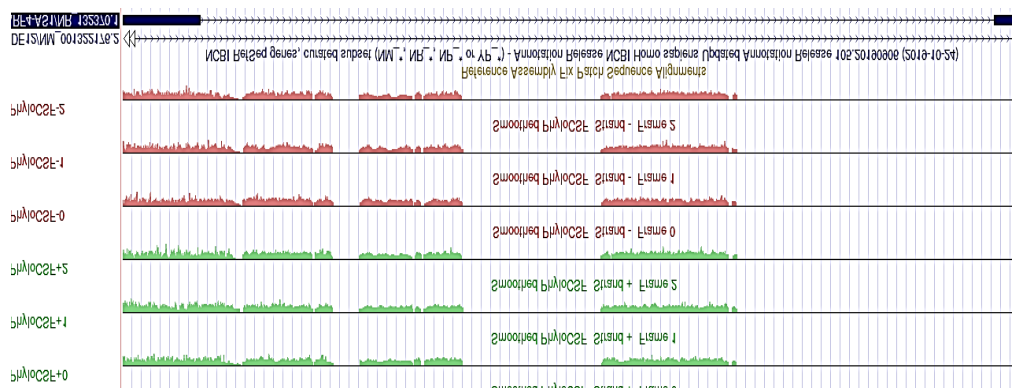


**Figure 27.** Protein coding potential of ARF4-AS1. The coding potential was evaluated and PhyloCSF. The coding potential was evaluated in three frames indicated as 0, 1 and 2.

3.7.5. Conservation of sequence and structure

Few alignments of 100 vertebrates showed little conservation of ARF4-AS1 in rhesus, mouse and dog.

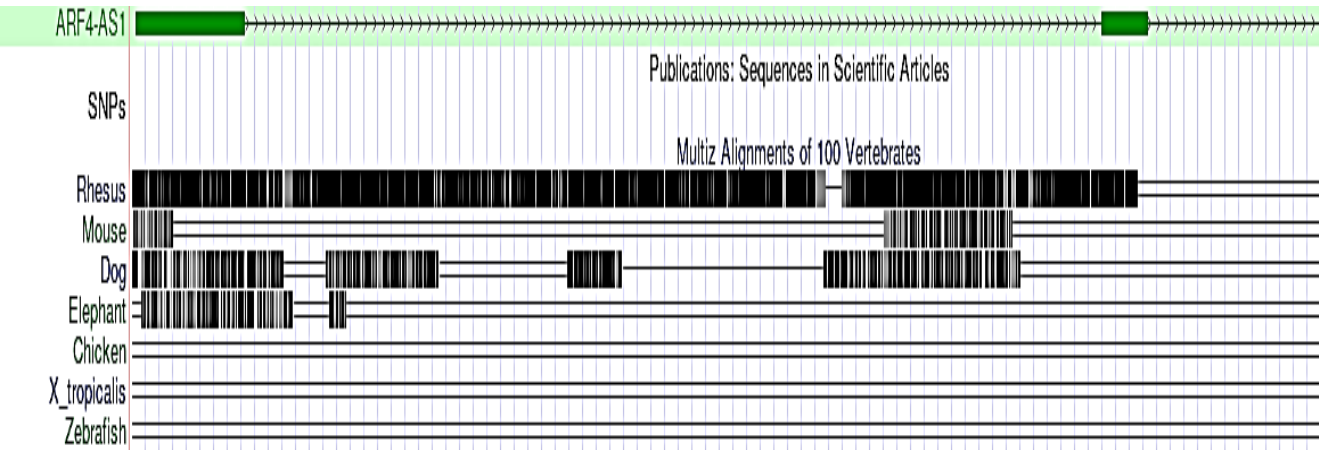


Figure 28. Multiz alignment of 100 vertebrates showing little bit of conservation of LINC01357.

3.7.6. Nucleo-cytoplasmic localization of ARF4-AS1

The nucleo-cytoplasmic localization of ARF4-AS1 was determined by using Inc-ATLAS. MALATI was used as a reference nuclear gene whereas DANCER was used as a reference cytoplasmic gene. LINC01357 showed various cytoplasmic localization in different cell lines i.e., HT1080. A549 indicates its role in regulating gene expression via RNA-RNA or RNA-protein interaction whereas a single line shows its nuclear localization.

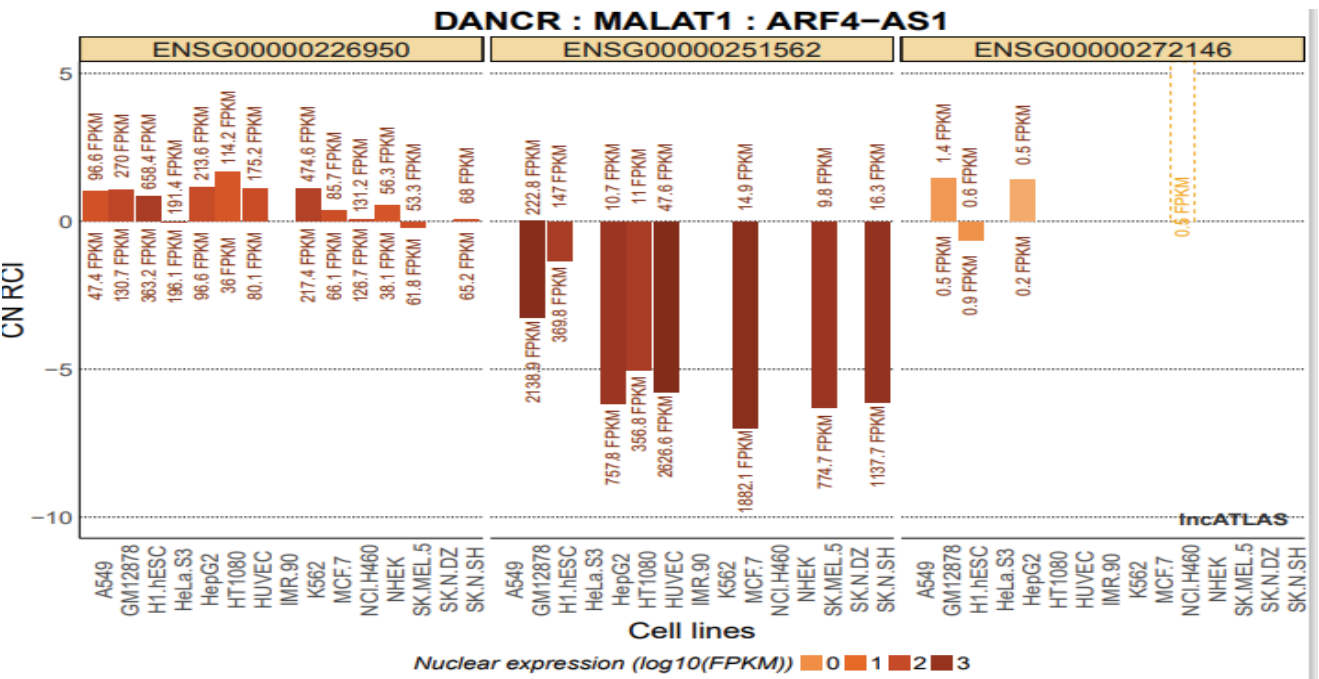


Figure 29. Nucleo-cytoplasmic localization of ARF4-AS1 ARF4-AS1 showed few cytoplasmic localizations in multiple cell lines. MALATI was used as the reference gene for the nucleus and DANCER was used as the reference gene for the cytoplasm. RCI represents the relative concentration index based on the comparison of gene concentration per unit RNA mass between two cellular compartments.

3.7.7. Macromolecular interactions involving ARF4-AS1

ARF4-AS1 can interact with neighboring genes or genes on other chromosomes in a cis or trans manner.



Two protein coding genes (ASB14 AND SPATA 12) which are in close vicinity were selected for correlation expression with ARF4-AS1 (non-coding gene). BcGenExMinor4.5 tool was used to evaluate the correlation expression of coding and non-coding genes between four breast cancer subtypes.

**Figure 30.** Correlation of cis interactors ASB14 and SPATA12 with ARF4-AS1 predicted by BcGenExMinor4.5 in normal subtype. ASB14 showed a strong correlation as compared to SPATA12. Blue color represents a negative correlation whereas red represents a strong positive correlation.

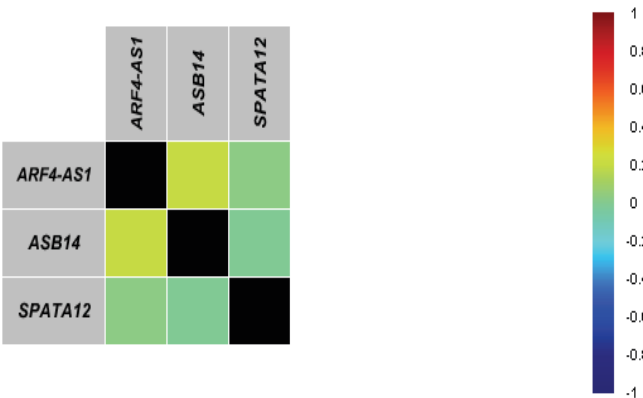
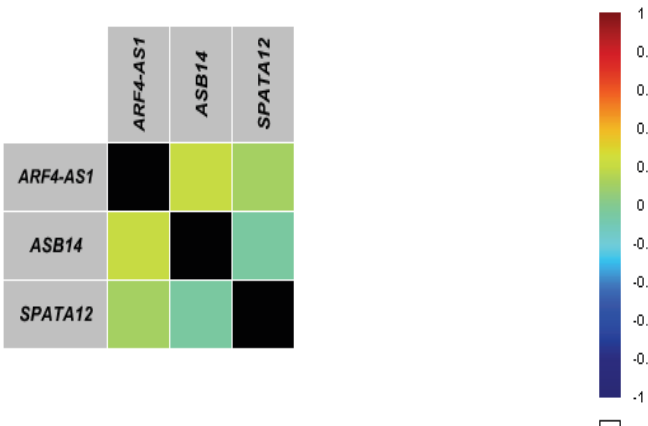


**Figure 31.** Correlation of Cis interactors ASB14 and SPATA12 with ARF4-AS1 predicted by BcGenExMinor4.5 in basal (TNBC) subtype. ASB14 showed more stronger correlation than SPATA12.



### 3.7.8. UALCAN database analysis

SPATA12 is a protein coding gene that interacts with ARF4-AS1. It is highly upregulated in the TNBC subtype as compared to other subtypes. It is calculated through the UALACAN database.

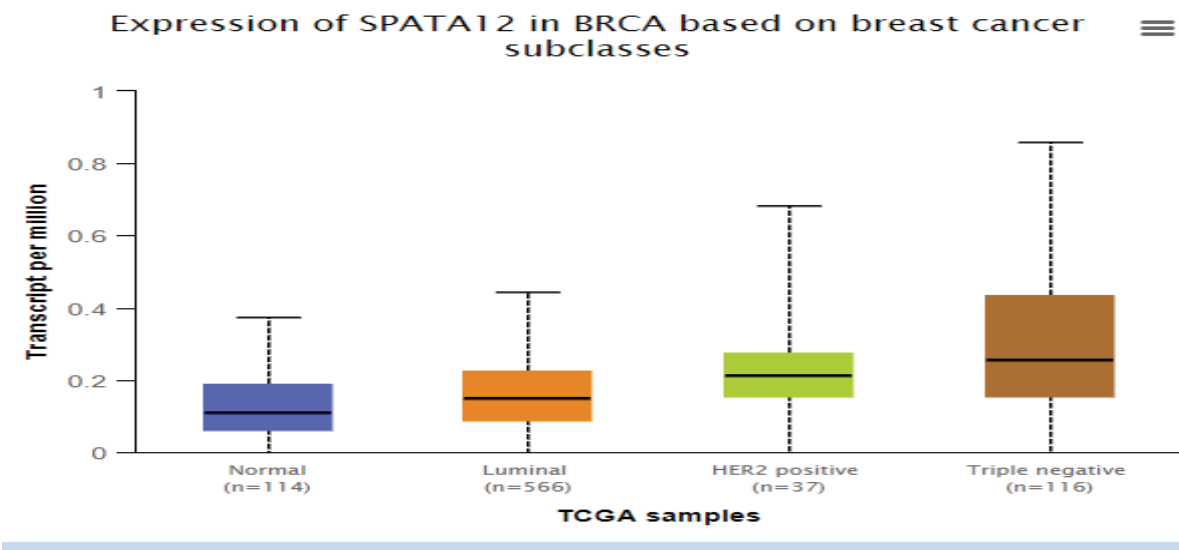


**Figure 32.** Box whisker plot showing SAPATA12 expression in breast cancer subtypes. SPATA12 is significantly upregulated in TNBC while showing nominal expression in other subtypes as illustrated by the box plot.

**Table 6.** Statistical significance of SPATA12 expression in BRCA

Comparison	Statistical significance
Normal-vs-Luminal	1.849390E-04
Normal-vs-HER2 Positive	5.232200E-04
Normal-vs-TNBC	3.89670518075036E-11
Luminal-vs-HER2 Positive	8.264600E-03
Luminal-vs-TNBC	4.59779999628651E-08
HER2 Positive-vs-TNBC	5.185400E-01

### 3.8. FAM83B

#### 3.8.1. Subtype analysis of FAM83B

FAM83B is located at chromosome 6p12.1 having 5 exons. Expression analysis was performed among four subtypes of BC using GEPIA2. It was calculated by mean value of  $\log_2(\text{TPM}+1)$  in each subtype of breast cancer. Results showed that FAM83B is upregulated in basal like breast cancer as compared to the other three subtypes.

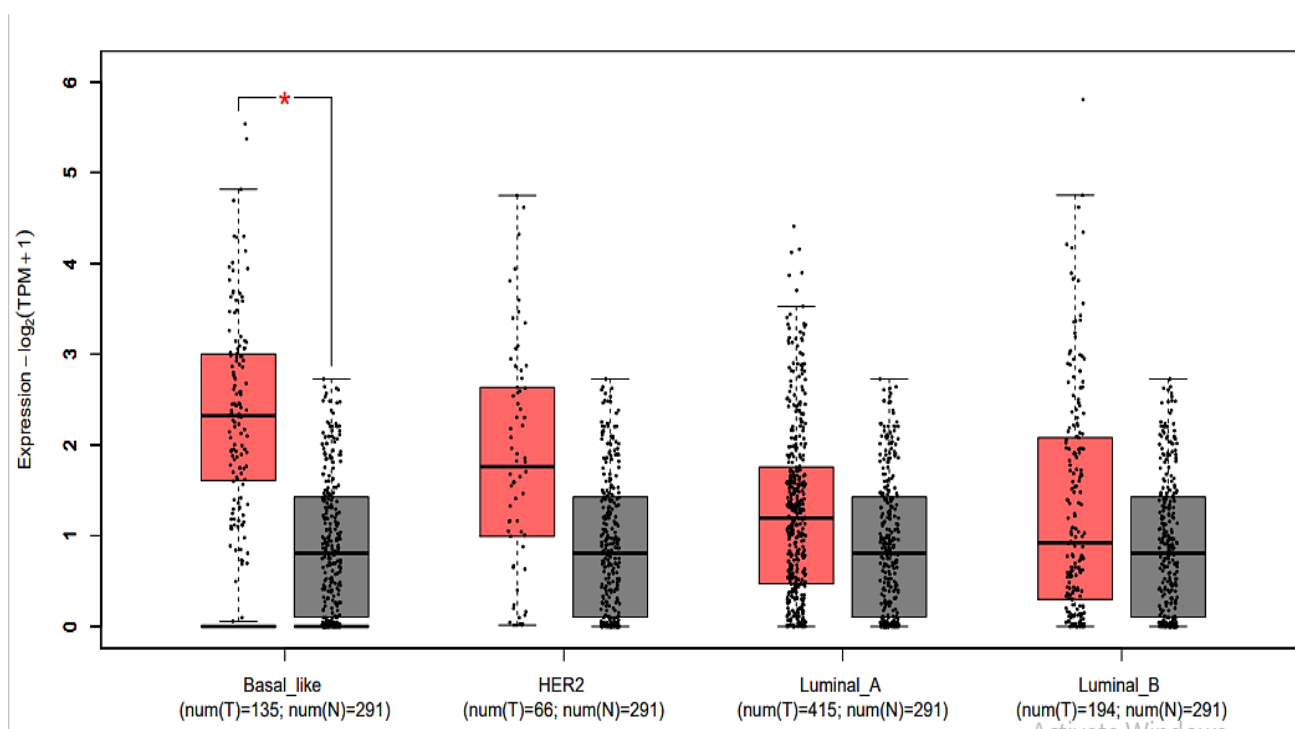
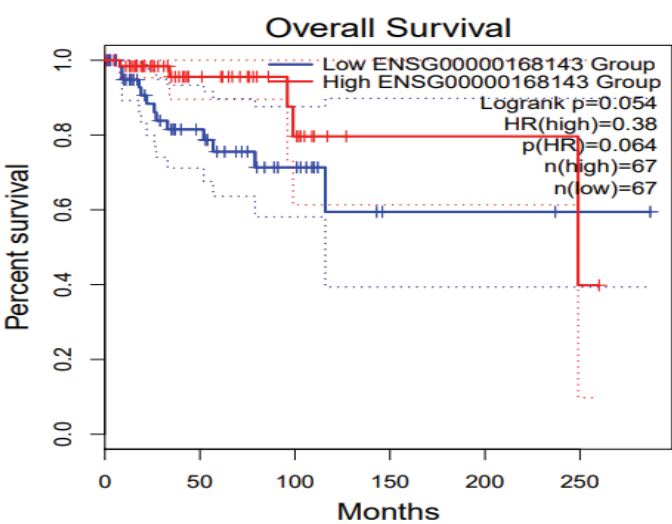


**Figure 33.** Subtype analysis of FAM83B based on TCGA data. The box plot in red represents the tumor while in grey represents normal. FAM83B expression is upregulated in the basal subtype of BC than the other three subtypes.

#### 3.8.2. Survival analysis of FAM83B

FAM83B is highly upregulated in the basal subtype survival graph as we evaluated it through GEPIA2. There are two groups i.e. red represents the high expression group whereas blue represents the low expression group. HR represents the hazard ratio which is an indication of the association between different treatments (radiotherapy and chemotherapy) and survival time. Figure 34 represents there is difference between the two groups. The survival rate of breast cancer is decreasing over 250 months as presented.

**Figure 34.** Graph showing overall survival analysis of FAM83B. The higher expression group showed low survival probability. Blue color represents low expression; red represents high expression and n represents the number of patients. The percent survival is shown on the y-axis and the time duration in months is shown on the x-axis.



### 3.8.3. Gene structure

FAM83B is a long intergenic non-coding RNA having the size of 6244bp. It has 1 transcript isoform. Table 7 shows the transcript of FAM83B along with its transcript length.

**Table 7.** List of transcripts of FAM83B

Transcript ID	Name	Bp	Protein	Bio type
ENST00000306858.8	FAM83B-201	6244	No protein	lncRNA

### 3.8.4. Protein coding potential using PhyloCSF

The coding potential of FAM83B was further evaluated by using PhyloCSF tool. PhyloCSF uses a calculate the phylogenetic conservation score multi-species nucleotide sequence alignment, which represents a probable protein-coding region. All peaks are towards negative axis showing that it does not code for any proteins or small peptide.

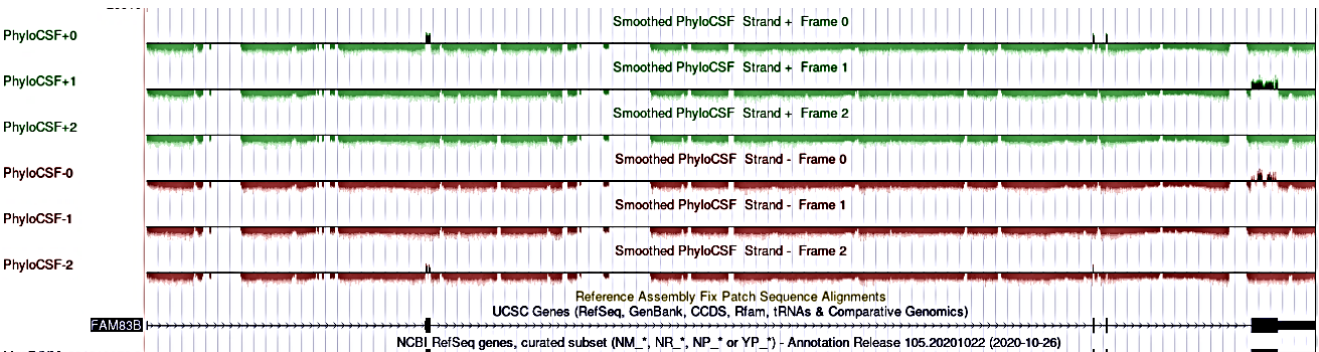


**Figure 35.** Protein coding potential of FAM83B. The coding potential was evaluated and PhyloCSF. The coding potential was evaluated in three frames indicated as 0, 1 and 2.

### 3.8.5. Conservation of sequence and structure

Few alignments of 100 vertebrates showed high conservation of FAM83B in rhesus and few alignments in mouse, dog and elephant.

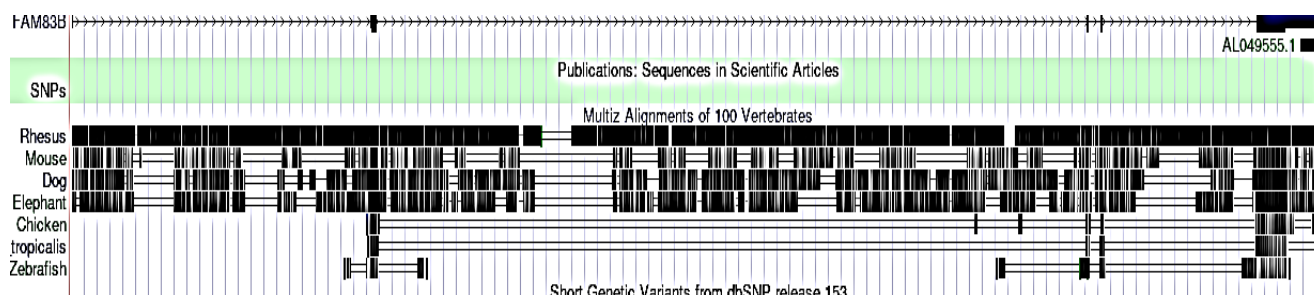


**Figure 36.** Multiz alignment of 100 vertebrates showing little bit conservation of FAM83B.

### 3.8.6. Nucleo-cytoplasmic localization of FAM83B

The nucleo-cytoplasmic localization of FAM83B was determined by using lnc-ATLAS. MALAT1 was used as a reference nuclear gene whereas DANCR was used as a reference cytoplasmic gene. FAM83B showed few cytoplasmic localizations in different cell lines i.e. H1 Hesc and Hela. S3 indicates its role in regulating gene expression via RNA-RNA or RNA-protein interaction whereas a single line shows its nuclear localization.

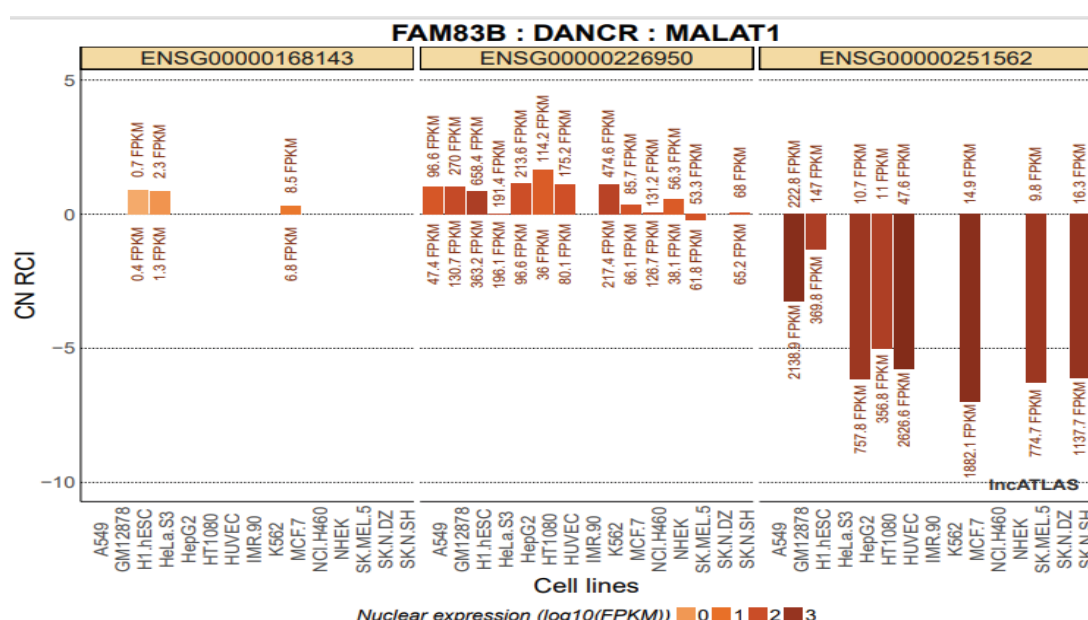


**Figure 37.** Nucleo-cytoplasmic localization of FAM83B. FAM83B showed few cytoplasmic localization in multiple cell lines. MALAT1 was used as a reference gene for the nucleus and DANCR was used as a reference gene for the cytoplasm. RCI represents the relative concentration index based on the comparison of gene concentration per unit RNA mass between two cellular compartments.

### 3.8.7. Macromolecular interactions involving FAM83B

FAM83B can interact with neighboring genes or genes on other chromosomes in a cis or trans manner. Two protein coding genes (HCRTR2 and GFRAL) which are in close vicinity were selected for correlation expression with FAM83B (non-coding gene). BcGenExMinor4.5 tool was used to evaluate the correlation expression of coding and non-coding genes between four breast cancer subtypes.

**Figure 38.** Correlation of Cis interactors HCRTR2 and GFRAL with FAM83B predicted by BcGenExMiner4.5 in the normal subtype. HCRTR2 showed a positive correlation whereas GFRAL showed a negative correlation with FAM83B.

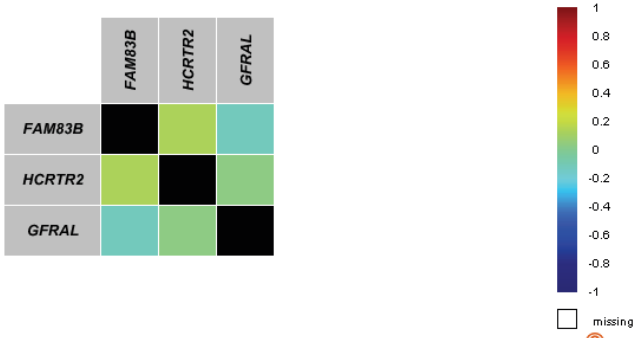
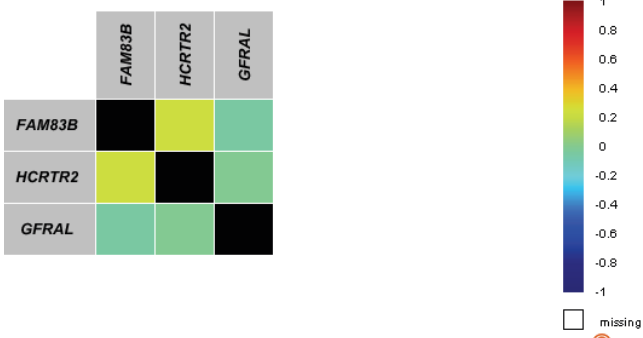


**Figure 39.** Correlation of Cis interactors HCRTR2 and GFRAL with FAM83B predicted by BcGenExMiner4.5 in basal (TNBC) subtype. HCRTR2 showed a strong correlation whereas GFRAL showed a negative correlation.



### 3.8.8. Trans interaction

Trans interaction is the interaction of genes on same chromosomes or on different chromosomes. Different trans-interacting genes were correlated with FAM83B.

**Figure 40.** Heat map showing the correlation of FAM83B with different genes in normal breast cancer tissue. PERP, DSC2, and DSG2 showed strong positive correlation whereas XPO5, SERPINB5, GRHL1 and ATL2 also positively correlated with FAM83B based on TCGA RNA seq data as predicted by bcExGenMiner4.5. Blue color represents a negative correlation whereas red represents a strong positive correlation.

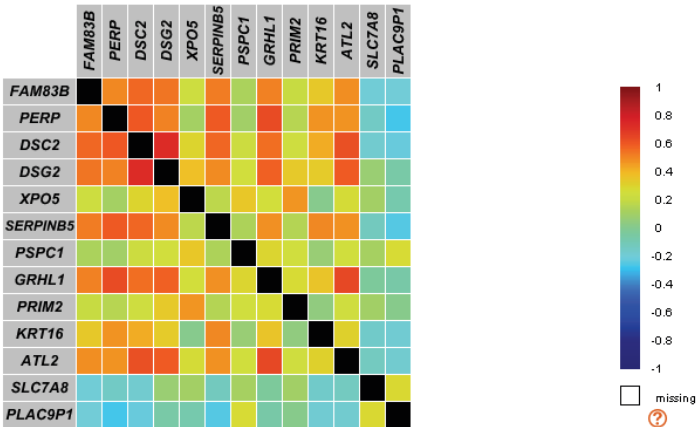
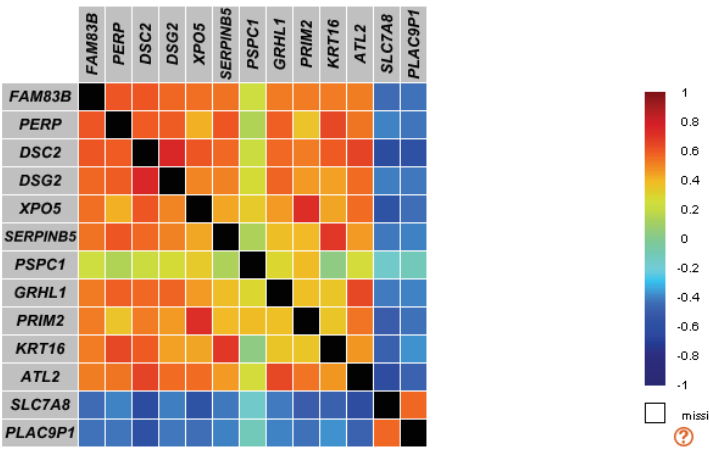


**Figure 41.** Heat map showing the correlation of FAM83B with different genes in the basal subtype. PERP, DSC2, and DSG2 showed a more positive correlation with FAM83B as compared to other genes based on TCGA RNA seq data as predicted by bcExGenMiner4.5. Blue color represents a negative correlation whereas red represents a strong positive correlation.





### 3.8.9. UALCAN database analysis

BMP5 is a protein-coding gene that interacts with FAM83B. It is upregulated in the TNBC subtype as compared to other subtypes. It is calculated through the UALCAN database.

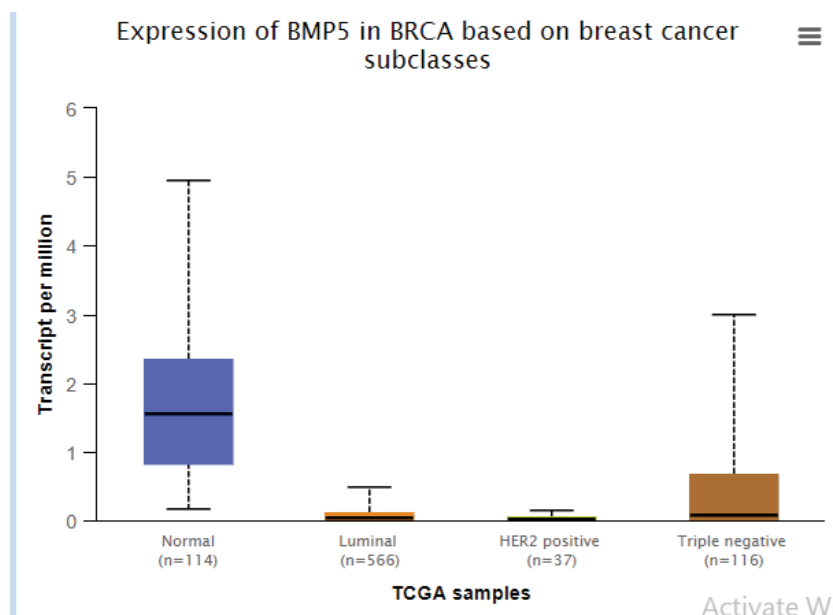


**Figure 42.** Box whisker plot showing expression in breast cancer subtypes. BMP5 is upregulated in TNBC while showing nominal expression in other subtypes as illustrated by the box plot.

**Table 8.** Statistical significance of BMP5 expression in BRCA

Comparison	Statistical significance
Normal-vs-Luminal	2.93720048283319E-10
Normal-vs-HER2 Positive	1.80211401357155E-12
Normal-vs-TNBC	2.239800E-02
Luminal-vs-HER2 Positive	8.882000E-02
Luminal-vs-TNBC	4.309800E-02
HER2 Positive-vs-TNBC	1.896320E-03

## 4. Discussion

Breast cancer is a health dilemma around the globe as it has a high mortality rate. About one million breast cancer cases were reported in the world so it comprises about 18% of all cancer among women. It is predicted that by 2021 incidence increase to 85 per 100,00 women. Breast cancer has two mechanisms that lead the patient towards death i.e. distant metastasis and invasion<sup>[18]</sup>. Long non-coding RNA plays a major role in these mechanisms by epithelial-mesenchymal transition, migration, invasion, and metastasis, and leads towards the progression of BC Related lncRNAs of promoting BC development<sup>[19]</sup>.

This study shortlisted four genes on the basis of their expression analysis on online software. The first two are rejected because of their survival probability. Those genes that are selected for study are LINC01356, LINC01357, ARF4-AS1, and FAM83B. First, lncRNA LINC01356 was evaluated to find its role in the progression of breast cancer. Multiple online software are utilized to conclude the results. Subtype analysis showed high expression in the TNBC subtype of breast cancer. The survival probability was evaluated which showed a decrease in survival probability. By PhyloCSF, its protein-coding potential was evaluated which

showed it is a negative strand so do not code for any protein. Further, it was analyzed for correlation expression. LINC01356 lies in the cytoplasm. In cis interaction, TAF3 and SLC16A showed a positive correlation in the basal subtype of TNBC. In trans interaction, SLC16A-AS1, DLL3, ANKLE1, and DDN were positively correlated in the basal subtype of TNBC. Previous studies on LINC01356 showed that it was upregulated in bladder cancer and promoted bone metastasis and can be utilized as an important diagnostic biomarker and also serve as a therapeutic target for bladder cancer and to control its metastasis for bone. Another study was also coherent with our study in the way that LINC01356 is significantly upregulated for tumor progression by significantly correlating with main immune checkpoints and they serve as major risk factors for bladder cancer.

Second, lncRNA LINC01357 was evaluated for breast cancer development. Results showed it was significantly upregulated in subtype analysis in the TNBC subtype of breast cancer. The survival probability curve showed that LINC01357 was an oncogene as it decreased the survival ratio of the patient over 250 months. LINC01357 has cytoplasmic localization. Two protein coding genes TAF3 and SLC16A1 were correlated in a cis manner with LINC01357. SLC16A1 is a protein called MCT1 is transporter of monocarboxylic acid that transports short-chain fatty acids, lactate and pyruvate. It modifies the metabolic programming of cells to promote the development and progression of tumors <sup>[20]</sup>. It also serves as a target for MYC oncoproteins as SLC16A1 elevated level promotes malignancies targeting MYC or MYC involvement. So, it is also a potential target for therapeutic purposes. Another study also showed the oncogenic role of SLC16A1 as it is upregulated in many human malignancies <sup>[21,22]</sup>. This study demonstrated the effect of stress on cancer cell survival. It showed that suppression of SLC16A1 by specific siRNA blockage or any other inhibitor leads to suppression of glycolysis and lactate homeostasis of breast tumors. Another effect was observed known as the Warburg effect which showed that by suppressing SLC16A1 cells were metabolically shifted from anaerobic glycolysis towards oxidative phosphorylation so they serve as the major factor for tumor suppression.

Thirdly, lncRNA ARF4-AS1 was evaluated for breast cancer progression. Results showed significant expression in tissue specific expression and further survival analysis showed high expression in the basal subtype of TNBC so it is also oncogenic. It is highly conserved in rhesus. ASB14 was a protein coding gene that was correlated in cis manner ARF4-AS1. SPATA12 is a novel spermatogenesis-associated gene and plays a role in the inhibition of spermatogenesis and tumor genesis through the regulation of various genes of the cell cycle <sup>[23,24]</sup>.

Fourth, lncRNA FAM83B was evaluated for its role in breast cancer development. Results concluded that it was highly upregulated in subtype analysis of TNBC subtype using GEPIA 2. It has a low survival possibility as shown by the survival probability curve found highly conserved in rhesus and has cytoplasmic localization. Two protein-coding genes HCRTR2 and GFRAL were correlated in a cis manner in which HCRTR2 showed a positive correlation in the basal subtype of TNBC <sup>[25]</sup>, which was the protein coding gene for FAM83B. BMP5 (bone morphogenetic protein 5), a member of the TGF- $\beta$  family was known to have a role in cancer progression and metastasis and previous studies showed it as an oncogene involved in various cancers i.e. lung, bladder, breast, ovarian and colon <sup>[26]</sup>.

## 5. Conclusion

In the current study, lncRNAs were investigated for progression in breast cancer through different online bioinformatics tools and exploring their different features i.e. structure, multiple transcript isoforms, subtype analysis, survival probability and correlation expression with cis and trans interacting protein and RNA coding genes. This study analyzed four lncRNAs (LINC01356, LINC01357, ARF4-AS1, and FAM83B). LINC01356

showed a positive correlation with these protein coding genes i.e. TAF3 and SLC16A1. LINC01357 showed a positive correlation with cis acting genes TAF3 and SLC16A1 in a basal subtype of TNBC. ARF4-AS1 showed a strong correlation with ASB14 and SPATA12 which are protein-coding genes. FAM83B showed a good correlation with BMP5. Therefore, all these findings paved the way to consider lncRNAs as therapeutic targets for the development of breast cancer.

## Authors contribution

Usama Ahmed – Literature review, Sampling, Experiment design, Experimental work, Result analyses

Muhammad Abubakar – Literature review, Methodology, Resources

Salma Saeed Khan – Experiment design, Methodology,

Baqar ur Rehman – Primer design, Methodology, Resources

## Disclosure statement

The author declares that they have no conflict of interest.

## References

- [1] Zubair M, Wang S, Ali N, 2021, Advanced Approaches to Breast Cancer Classification and Diagnosis. *Frontiers in Pharmacology*, 11: 632079.
- [2] Zavala VA, Bracci PM, Carethers JM, et al., 2021, Cancer Health Disparities in Racial/Ethnic Minorities in the United States. *British Journal of Cancer*, 124(2): 315–332.
- [3] Martini R, Newman L, Davis M, 2022, Breast Cancer Disparities in Outcomes; Unmasking Biological Determinants Associated with Racial and Genetic Diversity. *Clinical & Experimental Metastasis*, 39(1): 7–14.
- [4] Roheel A, Khan A, Anwar F, et al., 2023, Global Epidemiology of Breast Cancer Based on Risk Factors: A Systematic Review. *Frontiers in Oncology*, 13: 1240098.
- [5] Kazemi A, Barati-Boldaji R, Soltani S, et al., 2021, Intake of Various Food Groups and Risk of Breast Cancer: A Systematic Review and Dose-Response Meta-Analysis of Prospective Studies. *Advances in Nutrition*, 12(3): 809–849.
- [6] Mattick JS, Amaral PP, Carninci P, et al., 2023, Long Non-Coding RNAs: Definitions, Functions, Challenges and Recommendations. *Nature Reviews Molecular Cell Biology*, 24(6): 430–447.
- [7] Mangiavacchi A, Morelli G, Orlando V, 2023, Behind the Scenes: How RNA Orchestrates the Epigenetic Regulation of Gene Expression. *Frontiers in Cell and Developmental Biology*, 11: 1123975.
- [8] Kazimierczyk M, Wrzesinski J, 2021, Long Non-Coding RNA Epigenetics. *International Journal of Molecular Sciences*, 22(11): 6166.
- [9] Yu W, et al., 2021, Identification of Immune-Related lncRNA Prognostic Signature and Molecular Subtypes for Glioblastoma. *Frontiers in Immunology*, 12: 706936.
- [10] Constanty F, Shkumatava A, 2021, lncRNAs in Development and Differentiation: From Sequence Motifs to Functional Characterization. *Development*, 148(1): dev182741.
- [11] Deogharia M, Gurha P, 2022, The “Guiding” Principles of Noncoding RNA Function. *Wiley Interdisciplinary Reviews: RNA*, 13(4): e1704.
- [12] Kan RL, Chen J, Sallam T, 2022, Crosstalk Between Epitranscriptomic and Epigenetic Mechanisms in Gene Regulation. *Trends in Genetics*, 38(2): 182–193.

- [13] Lee JE, Kim M-Y, 2022, Cancer Epigenetics: Past, Present and Future. *Seminars in Cancer Biology*, 83: 4–14.
- [14] De Martino M, Esposito F, Pallante P, 2021, Long Non-Coding RNAs Regulating Multiple Proliferative Pathways in Cancer Cells. *Translational Cancer Research*, 10(6): 3140.
- [15] Gandhi P, Wang Y, Li G, Wang S, 2024, The Role of Long Noncoding RNAs in Ocular Angiogenesis and Vascular Oculopathy. *Cell & Bioscience*, 14(1): 39.
- [16] Wang M-Q, Zhu W-J, Gao P, 2021, New Insights into Long Non-Coding RNAs in Breast Cancer: Biological Functions and Therapeutic Prospects. *Experimental and Molecular Pathology*, 120: 104640.
- [17] Wang W, Min L, Qiu X, et al., 2021, Biological Function of Long Non-Coding RNA (LncRNA) Xist. *Frontiers in Cell and Developmental Biology*, 9: 645647.
- [18] Burstein HJ, 2022, Unmet Challenges in Systemic Therapy for Early-Stage Breast Cancer. *The Breast*, 62: S67–S69.
- [19] Yi Y, et al., 2021, Tumor-Derived Exosomal Non-Coding RNAs: The Emerging Mechanisms and Potential Clinical Applications in Breast Cancer. *Frontiers in Oncology*, 11: 738945.
- [20] Nguyen YT, Ha HT, Nguyen TH, et al., 2022, The Role of SLC Transporters for Brain Health and Disease. *Cellular and Molecular Life Sciences*, 79: 1–21.
- [21] Gaballah A, Bartosch B, 2022, An Update on the Metabolic Landscape of Oncogenic Viruses. *Cancers*, 14(23): 5742.
- [22] Chan KI, Zhang S, Li G, et al., 2024, MYC Oncogene: A Druggable Target for Treating Cancers with Natural Products. *Aging Disease*, 15(2): 640–697.
- [23] Cheung S, Ng L, Xie P, et al., 2024, Genetic Profiling of Azoospermic Men to Identify the Etiology and Predict Reproductive Potential. *Journal of Assisted Reproduction and Genetics*, 41(4): 1111–1124.
- [24] Xie D, Dai L, Yang X, et al., 2023, A Survival Model Based on the ASB Genes and Used to Predict the Prognosis of Kidney Renal Clear Cell Carcinoma. *Genetics Research*, 2023: e22.
- [25] Krebs LC, Santos MMM, Siqueira MC, et al., 2024, Candidate Genes for Height Measurements in Campolina Horses. *Animal Production Science*, 64(1): 23071.
- [26] Shao Y, Zhao C, Pan J, et al., 2021, BMP5 Silencing Inhibits Chondrocyte Senescence and Apoptosis as Well as Osteoarthritis Progression in Mice. *Aging (Albany NY)*, 13(7): 9646–9664.

**Publisher's note**

Bio-Byword Scientific Publishing remains neutral with regard to jurisdictional claims in published maps and institutional affiliations.

# Clinical Effects of Laparoscopic Radical Colon Cancer Treatment with Complete Mesocolic Resection for Colon Cancer

Liang Xue, Zhe Shi, Shugang Sun, Guodong Zhao\*

Affiliated Hospital of Hebei Engineering University, Handan 056000, Hebei Province, China

\*Corresponding author: Guodong Zhao, zgdzl@163.com

**Copyright:** © 2024 Author(s). This is an open-access article distributed under the terms of the Creative Commons Attribution License (CC BY 4.0), permitting distribution and reproduction in any medium, provided the original work is cited.

**Abstract:** Objective: This paper aims to evaluate the effect of laparoscopic complete mesocolic resection on the efficacy and survival of patients with colon cancer. Methods: 80 colon cancer patients were included in this study, 40 of whom were treated with traditional radical colon cancer surgery as the control group, and the other 40 were treated with laparoscopic complete mesocolic resection radical colon cancer surgery as the observation group. The study period lasted from April 2022 to April 2023, and the surgical indexes, postoperative recovery, quality of life, and the occurrence of complications of the two groups were monitored throughout the whole process and compared and analyzed. Results: The therapeutic effect of the observation group was better than that of the control group ( $P < 0.05$ ). The operation time, bleeding volume and postoperative hospitalization time of the observation group were significantly lower than those of the control group, and the number of lymph node dissection was significantly higher than that of the control group, with highly significant differences (all  $P < 0.001$ ). The postoperative recovery of the observation group (time of first anal defecation, time of first solid food intake, and time of wound healing) was significantly better than that of the control group (all  $P < 0.001$ ). The quality of life of the observation group was significantly improved with a highly significant correlation ( $P < 0.001$ ), and the complication rate was significantly lower than that of the control group ( $P < 0.05$ ). Conclusion: Laparoscopic radical colon cancer surgery with complete mesocolic resection for colon cancer shows better clinical effects and advantages in the treatment of colon cancer, which is worth further promotion and application in clinical practice.

**Keywords:** Colon cancer; Traditional radical surgery for colon cancer; Laparoscopic complete mesocolic resection for colon cancer

**Online publication:** October 2, 2024

## 1. Introduction

Colon cancer is a common malignant tumor of the digestive tract, and its incidence has been gradually increasing in recent years. This cancer has a certain degree of invisibility, and there are often no obvious symptoms in the early stage, which is easy to neglect and delayed treatment<sup>[1]</sup>. With the improvement of people's living standards and the change in dietary structure, the incidence trend of colon cancer is on the rise,



which poses certain threats to people's health. Therefore, it is crucial to strengthen awareness, early screening, and standardized treatment of colon cancer, which can effectively improve the cure rate and survival quality of patients <sup>[2]</sup>. Although traditional direct-vision open radical surgery for colon cancer can ensure complete removal of the lesion, the trauma during surgery is large, postoperative complications are more common, and patient recovery is slow, all of which may affect the overall outcome of the surgery and the quality of life of patients <sup>[3]</sup>. Therefore, colon cancer patients must find safer and more effective treatment modalities. With the continuous development and promotion of minimally invasive technology, laparoscopic surgery plays an increasingly important role in the treatment of colon cancer. Laparoscopic surgery utilizes advanced microscope equipment to assist in the operation, which avoids the abdominal incision necessary for traditional direct-vision open surgery and significantly reduces trauma and damage to the surrounding organs during the operation. At the same time, due to the more delicate surgical interventions, the chances of postoperative complications are also relatively low, favoring faster and better recovery for patients <sup>[4,5]</sup>. The application of this minimally invasive technique brings a new treatment option for colon cancer patients and improves the surgical effect while reducing the risks and discomfort associated with surgery, providing a more reliable guarantee for patients' health recovery. The purpose of this paper is to discuss the clinical effect of laparoscopic radical colon cancer treatment with complete mesocolic resection for colon cancer.

## **2. Data and methods**

### **2.1. General information**

80 patients diagnosed with colon cancer were included in this study and were randomly divided into a control group and an observation group. Inclusion criteria: (1) diagnosed by colonoscopy and confirmed by pathological examination; (2) patients with different degrees of colon cancer symptoms; (3) patients with carcinoma in situ and not yet metastasized, and need to sign the informed consent. Exclusion criteria: (1) patients with a history of pelvic surgery, (2) coagulation disorders, (3) inability to tolerate the treatment regimen of this study, (4) organ failure, combined with other malignant tumors, (5) patients with audio-visual disorders that prevent normal communication.

### **2.2. Methods**

The control group undergoes traditional radical surgery for colon cancer, which is usually carried out under general anesthesia, and the main steps include:

- (1) Open abdominal exploration: the doctor will first carry out abdominal exploration to understand the size, location, invasion range and whether there is any metastasis of the tumor.
- (2) Free the intestinal canal: according to the location of the tumor, free the intestinal canal and corresponding blood vessels and lymph nodes that need to be resected.
- (3) Resection of the intestinal canal: resect the intestinal segment where the tumor is located and a certain range of normal tissues around it.
- (4) Lymph node clearance: clear the lymph nodes around the tumor to remove possible tiny metastases.
- (5) Intestinal reconstruction: anastomose the two ends of the resected intestine to restore the continuity of the intestine.
- (6) Placement of drainage: after the operation, the surgeon will place a drainage tube in the abdominal cavity to drain the fluid from the operation area.

The observation group was treated with laparoscopic radical colon cancer surgery with complete mesocolic resection of the colon. During the colon cancer surgery, firstly, patients will be given general anesthesia to

ensure comfort and safety during the surgery. The surgeon then creates a small pneumoperitoneum, which is a small hole in the abdominal wall that is filled with carbon dioxide gas to provide room for the operation. A laparoscope and surgical instruments are placed through these holes to allow precise exploration of the tumor's location, size, and relationship to the surrounding tissue, as well as to check for metastases. With a clear understanding of the tumor, the surgeon will delicately free the colonic mesentery, carefully separating it from the surrounding tissue and performing lymph node dissection if necessary. The segment of the bowel containing the tumor, as well as the associated lymph nodes and mesentery, is precisely resected, removing the lesion for the patient. This is followed by an intestinal reconstruction phase where the remaining healthy bowel segments are anastomosed to restore bowel continuity. Tumors and surrounding tissues removed during surgery will be removed and sent for pathology to evaluate the surgical outcome and subsequent treatment plan. Small holes in the abdominal wall will be carefully sutured to mark the end of the surgical procedure.

### **2.3. Observation indicators**

#### **2.3.1. Therapeutic effect**

Apparent effect: patients' colon cancer lesions are completely resected after surgery, postoperative symptoms are significantly improved, there is no residual lesion around the lesion, postoperative recovery is fast, and postoperative complication rate is low.

Effective: after surgery, the patient's colon cancer lesions are controlled, the larger part of the lesions is removed, the postoperative symptoms are improved, the postoperative recovery is better, and there is no sign of recurrence or metastasis within a certain period of time.

Ineffective: patients' colon cancer lesions are not effectively controlled after surgery, the disease recurs or continues to develop after surgery, more postoperative complications, slow postoperative recovery, signs of recurrence or metastasis.

#### **2.3.2. Surgical indicators**

Surgical time: Measure the total time from the beginning of the incision to the completion of the suture.

Bleeding amount: Record the amount of blood loss during surgery to assess the fineness of surgery and the impact on the patient.

Number of lymph nodes cleared: Count the number of lymph nodes removed during surgery as an indicator to assess the thoroughness of surgery.

Postoperative hospitalization time: Record the average hospitalization days from the end of surgery to discharge, reflecting the patient's recovery and the use of hospital resources.

#### **2.3.3. Postoperative recovery**

Time of the first anal gas evacuation: The time of the first postoperative gas evacuation, reflects the speed of the recovery of intestinal function.

Time of first solid eating: The time from the start of solid eating after surgery, indicating the recovery of digestive tract function.

Wound healing time: Record the time of complete healing of postoperative incision, and assess the quality of postoperative recovery.

#### **2.3.4. Quality of life assessment**

A self-developed quality-of-life assessment form of the hospital was used, covering the following four dimensions, with a total score of 100 for each item.

Physiological function score: To assess the patients' physiological function recovery after surgery.

Psychological state assessment: To understand the patient's psychological adaptation state and emotional changes such as depression and anxiety after surgery.

Social function recovery: To evaluate the recovery of patients' ability to return to work or daily social activities after surgery.

Pain management: Record the postoperative pain feelings and their impact on the quality of life, and evaluate the effectiveness of analgesic measures.

### 2.3.5. Occurrence of complications

Record the specific types of postoperative complications in patients, such as wound infection, urinary tract infection, intestinal obstruction, etc. Count the frequency of each complication in the patient group.

## 2.4. Statistical methods

Data were statistically analyzed using SPSS 26.0, count data were expressed as [n (%)], and measurement data were demonstrated as mean  $\pm$  standard deviation (SD), with t-test or chi-square test.  $p < 0.05$  indicated that the difference was statistically significant.

## 3. Results

### 3.1. Comparison of general information

The general data (including gender, average age, and average body mass) of the two groups of patients were not statistically significant (all  $P > 0.05$ ). See Table 1.

**Table 1.** Comparison of general information of patients in the two groups

Groups	Sex		Mean age (mean $\pm$ SD, years)	Mean body mass (mean $\pm$ SD, kg)
	Male	Female		
Control group ( $n = 40$ )	22	18	60.51 $\pm$ 5.40	65.43 $\pm$ 6.63
Observation group ( $n = 40$ )	20	20	62.59 $\pm$ 5.37	66.76 $\pm$ 6.84
$\chi^2/t$ -value	0.201		1.727	0.883
$P$ -value	0.654		0.088	0.380

### 3.2. Comparison of the treatment effect of the two groups of patients

The total effective rate of the treatment effect of the observation group was significantly higher than that of the control group, which was 90.00% and 65.00%, respectively. After the  $\chi^2$  test, the calculated  $\chi^2$  value was 7.169, corresponding to a  $P$  value of 0.007, which was lower than the traditional significance threshold of 0.05, and the difference was statistically significant. See Table 2.

**Table 2.** Comparison of treatment effects between the two groups of patients [ $n$  (%)]

Groups	Apparent effect	Effective	Ineffective	Overall effective rate
Control group ( $n = 40$ )	16 (40.00%)	10 (25.00%)	14 (35.00%)	26 (65.00%)
Observation group ( $n = 40$ )	21 (52.50%)	15 (37.50%)	4 (10.00%)	36 (90.00%)
$\chi^2$ -value	-	-	-	7.169
$P$ -value	-	-	-	0.007

### 3.3. Comparison of surgical indexes between the two groups of patients

The surgical indexes of patients in the observation group (including operation time, bleeding volume, and postoperative hospitalization time) were significantly lower than those of patients in the control group, and the number of lymph nodes cleared in patients in the observation group was much higher than that in the control group, and the differences all showed highly significant correlation (all  $P < 0.001$ ). See Table 3.

**Table 3.** Comparison of surgical indexes between the two groups of patients (mean  $\pm$  SD)

Groups	Operative time (min)	Bleeding (mL)	Number of lymph nodes cleared (pcs)	Postoperative hospitalization (days)
Control group ( $n = 40$ )	176.68 $\pm$ 20.38	140.37 $\pm$ 15.16	18.24 $\pm$ 2.34	15.07 $\pm$ 3.17
Observation group ( $n = 40$ )	135.24 $\pm$ 15.67	82.97 $\pm$ 13.49	24.17 $\pm$ 3.87	10.25 $\pm$ 2.15
<i>t</i> -value	10.195	17.889	8.293	7.959
<i>P</i> -value	< 0.001	< 0.001	< 0.001	< 0.001

### 3.4. Comparison of postoperative recovery of patients in the two groups

The postoperative recovery of patients in the observation group (including the time of the first anal exhaustion, the time of the first solid food intake and the time of wound healing) was significantly lower than that of the control group, and the differences all showed highly significant correlations (all  $P < 0.001$ ). See Table 4.

**Table 4.** Comparison of postoperative recovery of patients in the two groups (mean  $\pm$  SD)

Groups	Time to first anal defecation (days)	Time to first solid meal (days)	Time to wound healing (weeks)
Control group ( $n = 40$ )	3.58 $\pm$ 0.43	4.34 $\pm$ 0.56	4.74 $\pm$ 0.84
Observation group ( $n = 40$ )	2.21 $\pm$ 0.31	2.97 $\pm$ 0.49	2.71 $\pm$ 0.67
<i>t</i> -value	16.346	11.644	11.949
<i>P</i> -value	< 0.001	< 0.001	< 0.001

### 3.5. Comparison of quality of life assessment of patients in two groups

Before surgery, the difference in the quality of life (including physiological function score, psychological state assessment, social function recovery and pain management) between the two groups was not statistically significant (all  $P > 0.05$ ). After surgery, compared with the control group, the quality of life comparison of the observation group all increased, and the differences all showed highly significant correlation (all  $P < 0.001$ ). See Table 5.

**Table 5.** Comparison of quality of life assessment between the two groups (mean  $\pm$  SD)

Groups	Physiological function scoring		Psychological assessment		Recovery of social functioning		Pain management	
	Before Surgery	After Surgery	Before Surgery	After Surgery	Before Surgery	After Surgery	Before Surgery	After Surgery
Control group ( $n = 40$ )	48.51 $\pm$ 5.48	56.62 $\pm$ 5.01	50.25 $\pm$ 4.74	73.04 $\pm$ 6.19	43.38 $\pm$ 4.59	68.17 $\pm$ 5.42	50.87 $\pm$ 4.27	61.28 $\pm$ 5.18
Observation group ( $n = 40$ )	48.69 $\pm$ 5.31	65.81 $\pm$ 5.32	50.20 $\pm$ 4.86	80.84 $\pm$ 6.74	43.51 $\pm$ 4.33	75.43 $\pm$ 6.20	50.67 $\pm$ 4.34	70.38 $\pm$ 5.32
<i>t</i> -value	0.149	7.954	0.047	5.391	0.130	5.576	0.208	7.751
<i>P</i> -value	0.882	< 0.001	0.963	< 0.001	0.897	< 0.001	0.836	< 0.001

### 3.6. Comparison of the complication rate of patients in the two groups

The complication rate of the observation group was lower than that of the control group ( $P < 0.05$ ). See Table 6.

**Table 6.** Comparison of the complication rate of patients in the two groups [ $n$  (%)]

Groups	Incisional infections	Urinary tract infection	Bowel obstruction	Total adverse reactions
Control group ( $n = 40$ )	3 (7.50%)	3 (7.50%)	2 (5.00%)	8 (20.00%)
Observation group ( $n = 40$ )	1 (2.50%)	0 (0.00%)	0 (0.00%)	1 (2.50%)
$\chi^2$ -value	-	-	-	4.507
$P$ -value	-	-	-	0.034

## 4. Conclusion

Colon cancer is an insidious disease with atypical early symptoms, so many patients are often diagnosed only when the disease has progressed to the middle or late stage, resulting in patients missing the best time for treatment, and the survival rate of patients with advanced colon cancer is less than 30%<sup>[6,7]</sup>. Therefore, early diagnosis and treatment are crucial for improving the survival rate of patients. Through early detection and early intervention, the survival time of patients can be effectively prolonged and the therapeutic effect can be improved to gain more chances of survival for patients. Surgery is one of the most direct and effective methods for treating colon cancer, and radical colon cancer surgery aims to prevent further spreading and metastasis of cancer cells to other parts of the body by removing the affected intestinal segment and related tissues<sup>[8]</sup>. In the past, conventional open radical colon cancer surgery was usually performed, in which a large abdominal incision is required and prolonged exposure of the abdominal organs to air significantly increases the risk of infection, leading to a higher incidence of postoperative complications<sup>[9]</sup>. Laparoscopic complete mesenteric resection is an innovative method for the treatment of colon cancer, by completing a series of surgical operations in the abdominal cavity, without the need for substantial opening of the abdomen, this surgical method has the advantages of small incisions, low bleeding, and fast operation, and at the same time can effectively remove the deep mesentery and lymph nodes, ensuring the thoroughness of lymph node removal, thus effectively preventing the risk of postoperative recurrence<sup>[10]</sup>. This study suggests that after treatment with laparoscopic complete mesenteric resection for radical colorectal cancer, the surgical effect is significantly better than that of the traditional method, surgical time, bleeding, and postoperative hospitalization time are reduced, and the number of lymph nodes cleared is increased. Postoperative recovery (time to first anal defecation, time to first solid meal, and time to wound healing) was significantly shorter, quality of life was significantly improved, and the complication rate was significantly reduced. The results of this study show that this method has obvious advantages in the treatment of colon cancer.

In conclusion, laparoscopic complete mesocolic resection is a superior method for the treatment of colon cancer, showing good clinical efficacy and obvious advantages. The procedure can effectively eradicate colon cancer by complete resection of colonic mesentery through laparoscopic technique. The operation is safe, with less intraoperative bleeding, mild postoperative pain, small incision, fast recovery, and low postoperative infection rate. Patients have rapid postoperative recovery and significantly improved quality of life. Therefore, it is worthy of further promotion and application in clinical practice to provide safer and more effective treatment options for colon cancer patients.



## Disclosure statement

The authors declare no conflict of interest.

## References

- [1] Zhu X, Shen Z, Ruan H, et al., 2021, Feasibility and Recent Results of Laparoscopic Complete Mesocolic Resection Guided by Superior Mesenteric Artery for the Treatment of Right Hemicolonic Cancer. *Zhejiang Medicine*, 43(20): 2226–2228 + 2278.
- [2] Tan D, Zhang F, Ye J, et al., 2020, Preliminary Application of Single-Hole Plus One-Hole Laparoscopic Transabdominal Synchronization Combined with Robotic Transanal Total Mesorectal Excision in Low Rectal Cancer Surgery. *Chinese Journal of Gastrointestinal Surgery*, 23(6): 605–609.
- [3] Yu A, Li Y, Zhang H, et al., 2023, Development and Validation of a Preoperative Nomogram for Predicting the Surgical Difficulty of Laparoscopic Colectomy for Right Colon Cancer: A Retrospective Analysis. *International Journal of Surgery*, 109(4): 870–878.
- [4] Ye Y, Zhang Q, Hu K, et al., 2021, Efficacy Analysis of da Vinci Robotic Surgical System-Assisted and Laparoscopic-Assisted Total Mesocolic Resection for the Treatment of Right Hemicolonic Cancer. *Chinese Journal of Gastrointestinal Surgery*, 20(5): 535–542.
- [5] Luo W, Song Y, Sun S, et al., 2021, Comparison of Long-Term Efficacy of Laparoscopic Complete Mesocolic Resection and D3 Radical Surgery for Stage III Right Hemicolonic Cancer. *Progress of Modern General Surgery in China*, 24(7): 522–526.
- [6] Du X, Liu J, Zhou W, et al., 2021, Clinical Effect of Laparoscopic Total Mesocolic Resection Combined with Root Ligation of Mesenteric Vessels in the Treatment of Right Hemicolonic Cancer. *Journal of Clinical and Experimental Medicine*, 20(23): 2544–2548.
- [7] Li M, Li K, Shen J, et al., 2020, Clavien-Dindo Grading of Complications After Laparoscopic Complete Mesocolic Resection for Right Hemicolonic Cancer and Analysis of Influencing Factors. *Chinese Journal of Gastrointestinal Surgery*, 2020(1): 51–55.
- [8] Yang Y, Chen S, Zhang G, et al., 2020, Effect of Laparoscopic Total Mesocolic Resection on Nutritional Status and Safety of Patients with Right Hemicolonic Cancer. *Hebei Medicine*, 42(22): 3379–3382 + 3387.
- [9] Zhao H, Pan J, Yan R, et al., 2020, Comparison of the Effect of Intermediate Caudolateral Combined Approach and Cephalad Intermediate Approach in Laparoscopic Complete Mesocolic Resection in Patients with Incomplete Intestinal Obstruction Complicated by Right Hemicolonic Cancer. *China Comprehensive Clinical*, 2020(2): 121–124.
- [10] Wang F, Zhang H, Chu H, et al., 2020, Clinical Effect and Prognosis Analysis of Right Hemicolonic Cancer in the Elderly Treated by Laparoscopic Total Mesocolic Resection. *Chinese Journal of Basic and Clinical Surgery*, 27(1): 69–74.

### Publisher's note

Bio-Byword Scientific Publishing remains neutral with regard to jurisdictional claims in published maps and institutional affiliations.

# Expression of Serum DCLK1 in Gastric Cancer Patients and Its Relationship with CEA, CA19-9, and CA72-4

Baoming Guo<sup>1</sup>, Zheng Jiao<sup>1</sup>, Jianzhou Li<sup>1</sup>, Jing Pan<sup>1</sup>, Huiqi Liu<sup>\*2</sup>

<sup>1</sup>Xining Second People's Hospital, Qinghai 810001, Xining Province, China

<sup>2</sup>Clinical Medical School of Qinghai University, Qinghai 810001, Xining Province, China

*\*Corresponding author:* Huiqi Liu, neillhq@126.com

**Copyright:** © 2024 Author(s). This is an open-access article distributed under the terms of the Creative Commons Attribution License (CC BY 4.0), permitting distribution and reproduction in any medium, provided the original work is cited.

**Abstract: Objective:** To investigate the expression of Doublecortin-like kinase-1 (DCLK1) in the serum of gastric cancer patients and its relationship with carcinoembryonic antigen (CEA), carbohydrate antigen 19-9 (CA19-9), and carbohydrate antigen 72-4 (CA72-4). **Methods:** Fifty patients diagnosed with gastric cancer at the hospital from January to December 2021 were selected as the gastric cancer group, and 50 patients diagnosed with chronic atrophic gastritis during the same period were selected as the control group. The serum concentrations of DCLK1, CEA, CA19-9, and CA72-4 were measured in both groups. Cut-off values and AUC (Area Under the Curve) were determined based on the ROC curve, and the expression of DCLK1 and its relationship with CEA, CA19-9, and CA72-4 were analyzed. **Results:** The average concentrations of DCLK1, CEA, CA19-9, and CA72-4 in the serum of gastric cancer patients were significantly higher than those in the control group ( $P < 0.05$ ). CA72-4 had the highest sensitivity (62%), CEA had the highest specificity (98%), and DCLK1 had the largest AUC (0.709). The combined diagnosis of gastric cancer using DCLK1, CEA, and CA19-9 resulted in the largest AUC (0.826), with a sensitivity of 82% and a specificity of 76%. **Conclusion:** The expression of DCLK1, CEA, CA19-9, and CA72-4 in the serum of gastric cancer patients is significantly higher than that in the control group. The combined detection of DCLK1, CEA, and CA19-9 offers better sensitivity and specificity for the diagnosis of gastric cancer.

**Keywords:** DCLK1; CEA; CA19-9; CA72-4; Gastric Cancer; Expression

**Online publication:** October 2, 2024

## 1. Introduction

The International Agency for Research on Cancer (IARC) conducted a study on the global cancer burden across 185 countries. The data from 2020 show that new cases of gastric cancer and deaths amounted to approximately 1.089 million and 769,000, respectively, accounting for the fifth (5.6%) and fourth (7.7%) positions in cancer incidence and mortality rates <sup>[1]</sup>. Despite the current comprehensive treatment strategies, including surgical resection, chemotherapy, radiotherapy, and gene therapy, the overall survival rate for gastric cancer remains low. The primary method for diagnosing gastric cancer is pathological diagnosis through endoscopic biopsy,

however, most cases are detected at an advanced stage. Tumor markers serve as an auxiliary tool for tumor diagnosis, efficacy evaluation, and recurrence monitoring, offering certain guidance in clinical diagnosis and treatment. CA19-9, CA72-4, and CEA are commonly used serum markers in the diagnosis of gastric cancer, but these markers lack organ specificity, and their sensitivity and specificity are not ideal when tested individually. Studies have reported that Doublecortin-like kinase-1 (DCLK1) is a molecular marker of gastrointestinal tumor stem cells and is highly expressed in gastric cancer tissues<sup>[2]</sup>, but the expression of this protein in the serum of gastric cancer patients remains unclear. This study aims to investigate the expression of DCLK1 in the serum of gastric cancer patients and analyze its relationship with CA19-9, CA72-4, and CEA.

## **2. Materials and methods**

### **2.1. General data**

Fifty newly diagnosed gastric cancer patients admitted to our department from January to December 2021 were selected, including 23 males and 27 females, with an average age of  $56.37 \pm 6.45$  years. All patients were confirmed by endoscopic pathology. Additionally, 50 patients with chronic atrophic gastritis (CAG) admitted during the same period were selected as the control group, including 26 males and 24 females, with an average age of  $54.17 \pm 7.29$  years. All patients were excluded from other malignancies. Statistical analysis showed no significant differences in general data such as gender and age between the gastric cancer group and the control group ( $P > 0.05$ ).

### **2.2. Detection methods and result determination**

All patients had 5 mL of venous blood drawn into a non-anticoagulant blood collection tube in the morning after fasting. The blood was left to stand at 4 °C until coagulation, then centrifuged at 3000 r/min for 10 minutes, after which the serum was carefully collected, aliquoted, and stored frozen at -20 °C for later use. The Roche Cobas e6801 analysis system and corresponding CEA, CA19-9, and CA72-4 quantitative detection kits were used to measure the levels of these markers in the serum of patients in the gastric cancer and control groups. The DCLK1 content in the serum of both groups was measured using a Wuhan USCN enzyme-linked immunosorbent assay (ELISA) kit. All operations were conducted strictly according to the instructions. The cut-off values for DCLK1, CEA, CA19-9, and CA72-4 were determined using the receiver operating characteristic (ROC) curve to interpret the results. For the combined detection of DCLK1, CEA, CA19-9, and CA72-4, a positive result for any one marker was considered a positive result for the combined detection.

### **2.3. Statistical analysis**

Data processing and statistical analysis were performed using SPSS 26.0 software. The mean and standard deviation (SD) were used to describe normally distributed measurement data and the independent samples t-test was used to compare means between groups. M (P25, P75) was used to describe skewed distribution data, and the rank-sum test was used to compare medians between groups. Prediction analysis was conducted based on the ROC curve, with a significance level of  $\alpha = 0.05$ .

## **3. Results**

### **3.1. Expression of DCLK1, CEA, CA19-9, and CA72-4 in serum of gastric cancer and control groups**

SPSS 26.0 was used to analyze the data from the two groups. The serum concentration of DCLK1 followed a

normal distribution in both groups, while the other data exhibited a skewed distribution. Therefore, the DCLK1 data are presented as mean  $\pm$  standard deviation (SD), and the CEA, CA19-9, and CA72-4 data are presented as median and percentiles (Table 1). A significance test of the differences in the results between the two groups showed that the expression levels of DCLK1, CEA, CA19-9, and CA72-4 in the serum of gastric cancer patients were significantly higher than those in the CAG group ( $P < 0.05$ ) (Table 1).

**Table 1. Serum concentrations of DCLK1, CEA, CA19-9, and CA72-4 in the two groups [mean  $\pm$  SD/M(P25, P75)]**

Group	DCLK1 (ng/mL)	CEA (ng/mL)	CA19-9 (ng/mL)	CA72-4 (U/mL)
Control	11.50 $\pm$ 5.79	1.765 (1.13, 3.14)	10.10 (6.43, 15.65)	2 (1.5, 3)
Gastric Cancer	16.47 $\pm$ 6.03	3.62 (1.45, 11.76)	13.76 (8.33, 32.41)	3 (2, 6.3)
z/t-value	-4.198	-3.468	-2.585	-2.763
p-value	< 0.001	0.001	0.01	0.006

### 3.2. AUC and cut-off values for independent diagnosis of gastric cancer by DCLK1, CEA, CA19-9, and CA72-4

SPSS 26.0 was used to analyze the data from the two groups, calculate the ROC curve, and derive the area under the curve (AUC) and cut-off values. The results showed that the AUCs of DCLK1, CEA, CA19-9, and CA72-4 were all greater than 0.5, with the AUCs for DCLK1 and CEA both exceeding 0.7, specifically 0.709 and 0.701, respectively (Table 2).

**Table 2. AUC and cut-off values for DCLK1, CEA, CA19-9, and CA72-4**

Marker	AUC	Cut-off value
DCLK1	0.709	15.6
CEA	0.701	5.075
CA19-9	0.65	24.38
CA72-4	0.659	2.85

### 3.3. Sensitivity and specificity of independent diagnosis of gastric cancer by DCLK1, CEA, CA19-9, and CA72-4

Based on the cut-off values determined by the ROC curve, the sensitivity and specificity of DCLK1, CEA, CA19-9, and CA72-4 for independent diagnosis of gastric cancer were calculated. CA72-4 had the highest sensitivity (62%), while CA19-9 had the lowest sensitivity (38%). CEA had the highest specificity (98%), while CA72-4 had the lowest specificity (74%). The accuracy results for gastric cancer diagnosis showed that CEA had the highest accuracy (73%), while DCLK1 and CA19-9 had the lowest accuracy, both at 66% (Table 3).

**Table 3. Sensitivity, specificity, and accuracy of DCLK1, CEA, CA19-9, and CA72-4 for gastric cancer detection (%)**

Marker	Control group	Gastric cancer group	Sensitivity	Specificity	Accuracy
DCLK1					
+	10	26	52%	80%	66%
-	40	24			

**Table 3 (Continued)**

Marker	Control group	Gastric cancer group	Sensitivity	Specificity	Accuracy
CEA					
+	1	24	48%	98%	73%
-	49	26			
CA19-9					
+	3	19	38%	94%	66%
-	47	31			
CA72-4					
+	13	31	62%	74%	68%
-	37	19			

### 3.4. Combined detection of DCLK1, CEA, CA19-9, and CA72-4 in the diagnosis of gastric cancer

Various combinations of DCLK1, CEA, CA19-9, and CA72-4 were used to detect gastric cancer, with a positive diagnosis defined as any one of the markers reaching or exceeding the diagnostic standard. The sensitivity, specificity, and AUC of each combination were calculated (Table 4). The results showed that the combination of all four markers had the highest sensitivity (90%), but the lowest specificity (60%). The accuracy of each combination was above 70%, with the highest accuracy for the CEA+CA19-9 combination (80%) and the lowest accuracy for the DCLK1+CA19-9 combination (71%). The AUC of each combination was above 0.7 and greater than the AUC of any single marker, with the combination of DCLK1+CEA+CA19-9 having the largest AUC (0.826), followed closely by the combination of all four markers (0.825), which was only 0.001 less than the three-marker combination (Table 4, Figure 1).

**Table 4. Sensitivity, specificity, accuracy, and AUC of DCLK1, CEA, CA19-9, and CA72-4 for gastric cancer detection**

Marker combination	Sensitivity	Specificity	Accuracy	AUC
DCLK1+CEA	74%	72%	76%	0.794
DCLK1+CA72-4	82%	64%	73%	0.744
DCLK1+CA19-9	64%	78%	71%	0.754
CEA+CA72-4	72%	72%	72%	0.718
CEA+CA19-9	68%	92%	80%	0.786
CA72-4+CA19-9	76%	70%	73%	0.702
DCLK1+CEA+CA72-4	84%	62%	73%	0.795
DCLK1+CEA+CA19-9	82%	76%	79%	0.826
DCLK1+CA72-4+CA19-9	86%	62%	74%	0.784
CEA+CA72-4+CA19-9	82%	68%	75%	0.786
DCLK1+CEA+CA72-4+CA19-9	90%	60%	75%	0.825



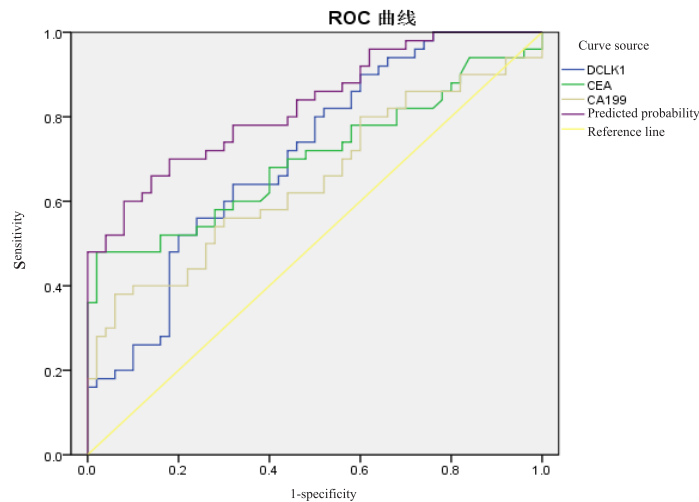


Figure 1. ROC curves for combined detection of three gastric cancer markers.

## 4. Discussion

During the development of malignant tumors, substances that are not expressed or are expressed at significantly higher levels in normal tissues can be produced or secreted. These substances can be released into the serum or other body fluids, reflecting the presence and status of tumors to some extent. Because of their association with malignant tumors, they are referred to as tumor markers <sup>[3]</sup>. An ideal tumor marker should have the following characteristics: (1) high sensitivity; (2) strong specificity; (3) organ specificity; (4) relevance to tumor occurrence and development; (5) presence in body fluids, making it easy to detect; (6) correlation with therapeutic effects; and (7) ability to assess prognosis <sup>[4]</sup>. Although tumor markers hold great clinical potential, markers with both very high sensitivity and specificity have yet to be applied in clinical practice. Moreover, apart from alpha-fetoprotein and prostate-specific antigen, no other tumor markers with strong organ specificity have been identified. Clinically, a particular marker may appear in multiple types of tumors, and various markers may also be present in a single tumor. Therefore, there is a need to explore new tumor markers actively.

Tumor stem cells are a small subset of tumor cells within tumor tissues that have the potential for self-renewal, and multi-lineage differentiation, and can induce the formation of tumor heterogeneity. These cells are closely associated with biological characteristics such as tumor resistance and recurrence <sup>[5,6]</sup>. Doublecortin-like kinase-1 (DCLK1) is a member of the protein kinase superfamily and the doublecortin (DCX) family. It is primarily expressed in fetal and adult brain tissues under normal conditions <sup>[7]</sup>. Still, it is also expressed in the heart, liver, spleen, thymus, prostate, testes, ovaries, small intestine, and colon <sup>[8]</sup>. Recent studies suggest that DCLK1 is a tumor stem cell marker, closely related to the development of tumors such as pancreatic cancer, colon cancer, and breast cancer <sup>[9–11]</sup>. It is also increasingly expressed in tumors and can be detected in the blood, making it a potential new marker for gastrointestinal tumors <sup>[12,13]</sup>. In this study, the average concentration of DCLK1 in the serum of gastric cancer patients was significantly higher than that in patients with chronic atrophic gastritis ( $P < 0.001$ ). Its sensitivity for diagnosing gastric cancer was 52%, with a specificity of 80%, indicating relatively high specificity but low sensitivity. This result suggests that the tumor stem cell marker DCLK1 can be detected in serum and is related to tumor occurrence and development to some extent, but it cannot be considered an ideal tumor marker for gastric cancer when tested alone and must be combined with other markers. Studies have shown that DCLK1 is also expressed at higher levels in the serum of patients with

liver cancer and esophageal cancer than in normal subjects <sup>[12,13]</sup> and combined with the results of this study, it indicates that this gene is overexpressed in the serum of tumor patients but lacks organ specificity.

Carcinoembryonic antigen (CEA) is a glycoprotein expressed in embryonic cells, consisting of 641 amino acid residues with embryonic antigenic determinant clusters. CEA can be secreted by the digestive tract of a two-month-old embryo and disappears after birth, resulting in very low serum levels in normal individuals. However, when digestive tract tumors occur, tumor cells can re-express CEA, increasing its serum levels in patients. CA19-9 and CA72-4 are glycoprotein tumor markers. Normally, cell membranes are rich in glycoproteins, but when cells undergo malignant transformation, the surface glycoproteins change, forming specific antigens different from normal cell antigens, which can reflect cellular changes to some extent. CA19-9 and CA72-4 are mostly distributed in epithelial tissues of the pancreas, stomach, and intestines, and are common markers for gastrointestinal tumors. Several studies have shown that the expression of CEA, CA19-9, and CA72-4 in the serum of gastric cancer patients is higher than in non-gastric cancer patients, but their sensitivity and specificity are not high when tested individually, and there are no significant differences in the expression of these three markers in the serum of gastric cancer patients <sup>[14-16]</sup>. In this study, the sensitivity of individual marker tests ranged from 38% to 62%, and specificity ranged from 74% to 98%. The sensitivity of combined marker tests ranged from 64% to 82%, and specificity ranged from 64% to 92%. The sensitivity of three-marker combined tests ranged from 82% to 86%, and specificity ranged from 62% to 76%. The sensitivity of four-marker combined tests was 90%, with a specificity of 60%. These results indicate that as the number of combined markers increases, sensitivity gradually increases, but specificity decreases. A meta-analysis showed that the sensitivity and specificity of combined detection of CEA, CA19-9, and CA72-4 for gastric cancer are superior to those of individual markers <sup>[17]</sup>, consistent with the results of this study.

In tumor screening, higher sensitivity is needed to avoid missed diagnoses, while in tumor diagnosis, higher specificity is required to avoid misdiagnosis. Combined marker detection can improve both sensitivity and specificity, but it also increases the financial burden on patients. Therefore, it is necessary to determine the appropriate sensitivity and specificity to determine the number of markers to test. The area under the ROC curve (AUC) is an indicator of diagnostic accuracy, with larger values indicating higher prediction accuracy. It is generally believed that when AUC exceeds 0.8, the diagnosis has practical application value <sup>[18]</sup>. In this study, the combined detection of DCLK1, CEA, and CA19-9 had the largest AUC (0.826), with a sensitivity of 82%, specificity of 76%, and accuracy of 79%. These results suggest that DCLK1 has potential as a serological marker for gastric cancer, and among the three markers CEA, CA199, and CA724, its combination with CEA and CA199 offers the best detection results.

## Funding

Xining Science and Technology Bureau People's Livelihood Science and Technology Special Program (Project No.: 2019-M-15)

## Disclosure statement

The authors declare no conflict of interest.

## References

- [1] Sung H, Ferlay J, Siegel RL, et al., 2021, Global Cancer Statistics 2020: GLOBOCAN Estimates of Incidence and

Mortality Worldwide for 36 Cancers in 185 Countries. *CA: A Cancer Journal for Clinicians*, 71(3): 209–249.

- [2] Cao Z, Weygant N, Chandrakesan P, et al., 2020, Tuft and Cancer Stem Cell Marker DCLK1: A New Target to Enhance Anti-Tumor Immunity in the Tumor Microenvironment. *Cancers (Basel)*, 12(12): 3801.
- [3] Sarhadi VK, Armengol G, 2022, Molecular Biomarkers in Cancer. *Biomolecules*, 12(8): 1021.
- [4] Zong J, Fan Z, Zhang Y, 2020, Serum Tumor Markers for Early Diagnosis of Primary Hepatocellular Carcinoma. *Journal of Hepatocellular Carcinoma*, 7: 413–422.
- [5] Zhang DY, Monteiro MJ, Liu JP, et al., 2021, Mechanisms of Cancer Stem Cell Senescence: Current Understanding and Future Perspectives. *Clinical and Experimental Pharmacology and Physiology*, 48(9): 1185–1202.
- [6] Paul R, Dorsey JF, Fan Y, 2022, Cell Plasticity, Senescence, and Quiescence in Cancer Stem Cells: Biological and Therapeutic Implications. *Pharmacology & Therapeutics*, 231: 107985.
- [7] Ye L, Liu B, Huang J, et al., 2024, DCLK1 and Its Oncogenic Functions: A Promising Therapeutic Target for Cancers. *Life Science*, 336: 122294.
- [8] Nakanishi Y, Seno H, Fukuoka A, et al., 2013, Dcl1 Distinguishes Between Tumor and Normal Stem Cells in the Intestine. *Nature Genetics*, 45(1): 98–103.
- [9] Chhetri D, Vengadassalopathy S, Venkadassalopathy S, et al., 2022, Pleiotropic Effects of DCLK1 in Cancer and Cancer Stem Cells. *Frontiers in Molecular Biosciences*, 9: 965730.
- [10] Wang Y, Yi J, Liu X, 2022, Roles of Dcl1 in the Pathogenesis, Diagnosis, Prognosis and Treatment of Pancreatic Cancer: A Review. *Expert Review of Gastroenterology & Hepatology*, 16(1): 13–19.
- [11] Kalantari E, Razmi M, Tajik F, et al., 2022, Oncogenic Functions and Clinical Significances of DCLK1 Isoforms in Colorectal Cancer: A Systematic Review and Meta-Analysis. *Cancer Cell International*, 22(1): 217.
- [12] Sureban SM, Madhoun MF, May R, et al., 2015, Plasma DCLK1 is a Marker of Hepatocellular Carcinoma (HCC): Targeting DCLK1 Prevents HCC Tumor Xenograft Growth via a MicroRNA-Dependent Mechanism. *Oncotarget*, 6(35): 37200–37215.
- [13] Whorton J, Sureban SM, May R, et al., 2015, DCLK1 is Detectable in Plasma of Patients with Barrett’s Esophagus and Esophageal Adenocarcinoma. *Digestive Diseases and Sciences*, 60(2): 509–513.
- [14] Shibata C, Nakano T, Yasumoto A, et al., 2022, Comparison of CEA and CA19-9 as a Predictive Factor for Recurrence After Curative Gastrectomy in Gastric Cancer. *BMC Surgery*, 22(1): 213.
- [15] Xu Y, Zhang P, Zhang K, et al., 2021, The Application of CA72-4 in the Diagnosis, Prognosis, and Treatment of Gastric Cancer. *Biochimica et Biophysica Acta*, 1876(2): 188634.
- [16] Wang R, Zuo CL, Zhang R, et al., 2023, Carcinoembryonic Antigen, Carbohydrate Antigen 199 and Carbohydrate Antigen 724 in Gastric Cancer and Their Relationship with Clinical Prognosis. *World Journal of Gastrointestinal Oncology*, 15(8): 1475–1485.
- [17] Wang H, Jin W, Wan C, et al., 2022, Diagnostic Value of Combined Detection of CA72-4, CA19-9, and Carcinoembryonic Antigen Comparing to CA72-4 Alone in Gastric Cancer: A Systematic Review and Meta-Analysis. *Translational Cancer Research*, 11(4): 848–856.
- [18] Nahm FS, 2022, Receiver Operating Characteristic Curve: Overview and Practical Use for Clinicians. *Korean Journal of Anesthesiology*, 75(1): 25–36.

#### **Publisher’s note**

Bio-Byword Scientific Publishing remains neutral with regard to jurisdictional claims in published maps and institutional affiliations.

# Clinical Efficacy of Autologous Bone Marrow Mesenchymal Stem Cell Transplantation for the Treatment of Patients with Refractory Cirrhotic Ascites

Lianqing Li, Haibo Chen\*, Hongfei Zhao, Jiping Zhu, Shaofeng Li

Qitaihe People's Hospital, Qitaihe 154600, Heilongjiang Province, China

\*Corresponding author: Haibo Chen, zlkxllq@126.com

**Copyright:** © 2024 Author (s). This is an open-access article distributed under the terms of the Creative Commons Attribution License (CC BY 4.0), permitting distribution and reproduction in any medium, provided the original work is cited.

**Abstract:** Objective: To analyze the efficacy of autologous bone marrow mesenchymal stem cell (BMSC) transplantation for the treatment of cirrhotic ascites (refractory). Methods: 64 patients with cirrhosis ascites (refractory) who were admitted to the hospital between May 2022 and April 2024 were selected and divided equally by random number table, the observation group was treated with BMSC autologous transplantation, and the reference group was treated with conventional medication, and the total effective rate, therapeutic indexes, liver and renal function indexes, and the change of urine volume were compared. Results: The total effective rate of the observation group was higher than that of the reference group ( $P < 0.05$ ). Before treatment, there was no difference between the two groups in terms of therapeutic indexes such as depth of ascites, liver and kidney function indexes and 24-hour urine volume ( $P > 0.05$ ). After treatment, the observation group's ascites depth and other indicators were better than that of the reference group, liver and kidney function indicators were better than that of the reference group, and 24h urine volume was more than that of the reference group ( $P < 0.05$ ). Conclusion: BMSC autotransplantation can improve the clinical efficacy of patients with cirrhosis ascites (refractory), accelerate the absorption of ascites, reduce the values of body mass and abdominal circumference, and protect the liver and kidney functions and increase the amount of urination.

**Keywords:** Autologous bone marrow mesenchymal stem cell transplantation; Refractory cirrhotic ascites; Clinical efficacy

**Online publication:** October 2, 2024

## 1. Introduction

Cirrhosis is the end-stage manifestation of many liver diseases such as alcoholic liver disease, viral hepatitis, etc., and its loss-of-compensation stage leads to the symptoms of ascites<sup>[1]</sup>. Ascites, i.e. the pathological state, the fluid content inside the patient's abdominal cavity is  $> 200$  mL, and its condition is critical and difficult to treat. For patients with cirrhotic ascites (refractory), conventional diuretic therapy is not effective in discharging ascites and surgical treatment is required. Conventional drug therapy is a common therapy for this

disease, which can reduce the symptoms of the disease and relieve the degree of pain of patients <sup>[2,3]</sup>. However, the long-term efficacy of this therapy is average, which may lead to more obvious adverse reactions and poor patient compliance. In comparison, BMSC autotransplantation is highly minimally invasive and can lead to the continuous differentiation of BMSC to bile ducts and hepatocytes, thereby protecting liver function and alleviating the manifestation of ascites <sup>[4]</sup>. Based on this, 64 patients with cirrhotic ascites (refractory) were selected in this study to evaluate the therapeutic advantages of BMSC autotransplantation.

## 2. Information and methods

### 2.1. General information

Sixty-four cases of cirrhotic ascites (refractory) patients admitted for treatment between May 2022 and April 2024 were selected and delineated by random number table, 32 cases in the observation group, 19 cases of male patients and 13 cases of female patients; their ages ranged from 41 to 81 years old, with a mean value of  $(55.27 \pm 5.18)$  years old; and the duration of cirrhosis ranged from 0.5 to 3 years, with a mean value of  $(1.53 \pm 0.49)$  years. In the reference group, there were 32 cases, 20 male patients and 12 female patients; their ages ranged from 40 to 82 years, with a mean value of  $(55.36 \pm 5.15)$  years; the duration of cirrhosis ranged from 0.4 to 3 years, with a mean value of  $(1.56 \pm 0.41)$  years. The general information between the two groups was compared  $P > 0.05$ .

Inclusion criteria: (1) meeting the criteria for cirrhosis listed in the Guidelines for the Diagnosis and Treatment of Ascites and Related Complications of Liver Cirrhosis; (2) accompanied by signs of ascites, whose ascites persisted for more than 3 months; (3) the patient's clinical data were relatively complete and (4) they were informed and consented to the study.

Exclusion criteria: (1) accompanied by hepatic encephalopathy, haemorrhagic ascites and other diseases; (2) combined with myocardial infarction and other cardiovascular and cerebral vascular diseases; (3) abnormal communication ability; (4) accompanied by depression; (5) accompanied by upper gastrointestinal bleeding in the past 3 months.

### 2.2. Methods

The treatment method of the reference group is as follows: conventional medication, anti-infective, hepatoprotective and hepatoprotective basic treatment, and take 20 mg dose of tachycardia and 10 g dose of albumin daily, to be administered intravenously, for 4 weeks consecutively. A 3-step diuretic regimen was also combined, and in the first week, mercaptopropionic acid was chosen at a daily oral dose of 75 mg, i.e., a single dose, and oral ambrisentan at a daily dose of 120 mg, i.e., a single dose. In the second week, ascites absorption was checked, and if it still did not meet the standard, tachyphylaxis was used, with a daily dose of 40–80 mg for intraperitoneal treatment, and dopamine was injected every other day, with a dose of 20–40 mg, both once daily. In the third week of poor efficacy, oral mannitol (20%) can be taken, the daily oral dose of 100–150 mL, once-a-day medication, treatment for 4 weeks.

The treatment method of the observation group is as follows: BMSC autotransplantation treatment: keep the patient in the lying position, and the location of the bone marrow puncture point is at the bilateral posterior superior iliac spine. Disinfection and toweling, local infiltration anesthesia puncture point to the periosteal area. A bone marrow puncture needle (18 gauge) was taken so that it was vertically inserted into the puncture point, which was effectively fixed after entering the medullary cavity, and the bone marrow was withdrawn. The volume of bone marrow blood aspirated at the puncture point was 60 mL bilaterally and anticoagulation was done by adding sodium heparin at a dose of 7500 U. In vitro isolation operation and purification of bone



marrow stem cells was carried out by density centrifugation. Flow cytometry was performed to detect the markers of surface antigen-enriched monocytes: CD45-, CD34-, CD29+, CD90+ & CD44+. Mesenchymal hepatocytes, all with a body mass of  $1.0 \times 10^6/\text{kg}$ , were stored at 4 °C and sent to the intervention room. Local treatment was performed under the guidance of a digital subtraction angiography machine, and the right femoral artery was punctured by the Seldinger technique with an indwelling arterial sheath (5F), and an R-H hepatic artery catheter (5F) was placed with the innominate hepatic artery. The characteristics of vascular distribution were assessed using a contrast technique to observe the presence of abnormal vascular mass at the tumor site. The BMSC suspension after the separation operation was taken and injected into the interior of the liver. After treatment, the arterial sheath was slowly withdrawn, pressure was applied and the puncture point was bandaged, and the patient was instructed to lie in a flat position for 24h.

### 2.3. Observation indicators

- (1) Overall effective rate: Significant efficacy: no ascites, only a small amount of diuretics used daily; Preliminary efficacy: the amount of ascites is significantly reduced, a large amount of diuretics is needed daily, intermittently combined with human blood albumin preparation; No efficacy: no change in ascites, a large number of diuretics and human blood albumin preparation are needed daily.
- (2) Therapeutic indexes: Before and after 3 months of treatment, the depth of ascites was evaluated by a Doppler ultrasonic diagnostic instrument; the abdominal circumference was measured by a soft ruler; and the body mass was measured by weight measuring instrument (weight scale).
- (3) Liver function indexes: At the same time, venous blood was collected from patients in fasting state, centrifuged and processed, and then total bilirubin (TBIL), aspartate aminotransferase (AST), and plasma albumin (ALB) levels were measured by automatic biochemistry analyzer.
- (4) Renal function indexes and urine volume: At the same time, fasting venous blood was collected, and the levels of blood creatinine (Scr), urea nitrogen (BUN) and 24h urine volume were measured by the fully automatic biochemical analyzer.

### 2.4. Statistical analysis

The data processing software is SPSS 28.0, the expression of measurement data is mean  $\pm$  standard deviation (SD), compare and test with t value, the expression of count data is (n%), compare and test with  $\chi^2$  value, statistically significant i.e.  $P < 0.05$ .

## 3. Results

### 3.1. Comparison of the total effective rate of the two groups

The total effective rate of the observation group was higher than that of the reference group ( $P < 0.05$ ). See Table 1.

**Table 1.** Comparison of the total effective rate of the two groups (n%)

Subgroups	<i>n</i>	Remarkable results	Initial effect	No effect	Overall effective
Observation group	32	21 (65.63)	10 (31.25)	1 (3.13)	96.88 (31/32)
Reference group	32	17 (53.13)	8 (25.00)	7 (21.88)	78.13 (25/32)
$\chi^2$	-	-	-	-	5.143
<i>P</i>	-	-	-	-	0.023

### 3.2. Comparison of treatment indicators between the two groups

Before treatment, there is no difference in the comparison of the clinical indicators of the two groups ( $P > 0.05$ ). After 3 months of treatment, the clinical indicators of the observation group are lower than those of the reference group ( $P < 0.05$ ). See Table 2.

**Table 2.** Comparison of the treatment indexes of the two groups (mean  $\pm$  SD)

Subgroups	<i>n</i>	Depth of ascites (mm)		Abdominal circumference (cm)		Body mass (kg)	
		Before treatment	After treatment	Before treatment	After treatment	Before treatment	After treatment
Observation group	32	72.28 $\pm$ 6.91	31.53 $\pm$ 4.12	94.36 $\pm$ 8.71	86.24 $\pm$ 4.15	62.53 $\pm$ 6.11	57.40 $\pm$ 3.62
Reference group	32	72.21 $\pm$ 6.83	52.19 $\pm$ 4.17	94.33 $\pm$ 8.66	89.02 $\pm$ 4.20	62.58 $\pm$ 6.13	59.44 $\pm$ 3.15
<i>t</i>	-	0.041	19.937	0.014	2.663	0.033	2.405
<i>P</i>	-	0.968	0.000	0.989	0.010	0.974	0.019

### 3.3. Comparison of liver function indexes between the two groups

Before treatment, there is no difference in the comparison of liver function indexes between the two groups ( $P > 0.05$ ). After 3 months of treatment, the liver function indexes of the observation group were better than those of the reference group ( $P < 0.05$ ). See Table 3.

**Table 3.** Comparison of liver function indexes between the two groups (mean  $\pm$  SD)

Subgroups	<i>n</i>	TBIL ( $\mu$ mol/L)		AST (U/L)		ALB (g/L)	
		Before treatment	After treatment	Before treatment	After treatment	Before treatment	After treatment
Observation group	32	88.25 $\pm$ 6.12	60.73 $\pm$ 5.11	67.63 $\pm$ 5.93	28.75 $\pm$ 2.42	27.51 $\pm$ 4.11	33.62 $\pm$ 3.18
Reference group	32	88.29 $\pm$ 6.20	70.29 $\pm$ 5.27	67.66 $\pm$ 5.91	38.91 $\pm$ 2.58	27.58 $\pm$ 4.16	30.15 $\pm$ 3.14
<i>t</i>	-	0.026	7.367	0.020	16.248	0.068	4.392
<i>P</i>	-	0.979	0.000	0.984	0.000	0.946	0.000

### 3.4. Comparison of renal function indexes and urine volume of the two groups

Before treatment, there was no difference in the comparison of renal function indexes and 24-hour urine volume between the two groups ( $P > 0.05$ ). After 3 months of treatment, the renal function indexes of the observation group were lower than those of the reference group, and the 24h urine volume was more than that of the reference group ( $P < 0.05$ ). See Table 4.

**Table 4.** Comparison of renal function indexes and urine volume between two groups (mean  $\pm$  SD)

Subgroups	<i>n</i>	Renal function indicators ( $\mu$ mol/L)				24h urine volume (mL)	
		Scr		BUN		Before treatment	After treatment
		Before treatment	After treatment	Before treatment	After treatment		
Observation group	32	177.53 $\pm$ 15.35	105.39 $\pm$ 8.31	12.35 $\pm$ 2.08	6.81 $\pm$ 1.57	845.95 $\pm$ 17.36	1386.92 $\pm$ 29.37
Reference group	32	177.01 $\pm$ 16.23	131.65 $\pm$ 8.44	12.39 $\pm$ 2.11	9.23 $\pm$ 1.61	844.53 $\pm$ 17.23	1089.53 $\pm$ 25.41
<i>t</i>	-	0.132	12.542	0.076	6.088	0.328	43.317
<i>P</i>	-	0.896	0.000	0.939	0.000	0.744	0.000

## 4. Discussion

The pathogenesis of liver cirrhosis is complex, as follows: (1) plasma colloid osmotic pressure decreases, and the ALB content in the body decreases, which produces a persistent extravasation reaction of the blood components; (2) the generation of lymphatic fluid increases and the reabsorption capacity decreases, which causes lymphatic fluid to penetrate into the interior of the patient's abdominal cavity<sup>[5]</sup>; and (3) the dysfunction of inactivation of hepatic tissues increases the secretion of a variety of substances, such as aldosterone or antidiuretic hormone that induces water and sodium retention. Based on the above pathogenesis, cirrhotic ascites (refractory) are treated with water and salt restriction, and ALB supplementation with drainage of ascites<sup>[6,7]</sup>.

Pharmacological treatment is a common treatment for this disease, in which tachycardia has a strong effect on the renal tubules, amphotericin can act efficiently on the aldosterone receptor in the body, and mannitol can significantly increase blood volume so that the osmolality of the intra-tubular fluid in the renal tubules can be significantly increased. The combination of the three drugs can have a diuretic effect. At the same time, the combination of dopamine and mercaptopropionic acid can enhance renal blood flow, which in turn enhances the therapeutic effect. However, it is difficult to improve liver and kidney functions with drug treatment, so the long-term efficacy is general<sup>[8,9]</sup>. BMSC autotransplantation selects the patient's autologous cells, and there is no immune rejection after transplantation, which is safe and can reduce treatment complications. BMSC has strong differentiation ability and proliferation function, and can effectively differentiate hepatocytes and hematopoietic cells, etc. Therefore, it has more therapeutic targets. BMSC can secrete cytokines and growth factors in vivo to repair the damaged tissues and can improve the immune function of the patients<sup>[10]</sup>.

The results showed that the indicators of ascites depth and other indicators of the observation group after treatment were better than those of the reference group, the indicators of liver and kidney function were better than those of the reference group, and the 24h urine volume was more than that of the reference group ( $P < 0.05$ ). The reason is that the collection method of BMSC is relatively simple, and bone marrow blood can be extracted by the bone marrow aspiration method, and the treatment is less painful. BMSC can regulate vascular permeability, promote the flow of ascites into the blood circulation through the wall of the blood vessels, and accelerate its absorption<sup>[11]</sup>. BMSC has a strong and continuous stimulating effect on the primitive progenitor cells of the liver, which can increase the number of newborn hepatocytes, cause them to produce a large number of ALBs, and improve the level of plasma osmolality, and promote the discharge of ascites from the body<sup>[12]</sup>, prompting the drainage of ascites out of the body. In addition, BMSC autotransplantation can have a direct effect on the patient's liver tissue, improve the systemic microenvironment, regulate the function of water and sodium metabolism, and improve the ability of liver and kidney tissues to excrete electrolytes and excess water, so that the 24h urine output increased significantly<sup>[12]</sup>.

## 5. Conclusion

In conclusion, BMSC autotransplantation can enhance the therapeutic efficiency of patients with cirrhotic ascites (refractory), improve the level of abdominal circumference and body mass of patients, reduce the number of ascites, and protect the liver and kidney functions of patients, which has a high therapeutic feasibility.

## Disclosure statement

The authors declare no conflict of interest.

## References

- [1] Xie L, Chen H, Hao J, et al., 2023, Clinical Study on the Treatment of Refractory Ascites in Liver Cirrhosis with Spleen Deficiency and Water-Stopping Type by Applying Umbilical Cord with Soft Liver and Water-Relieving Formula Combined with Water-Expelling Formula. *Journal of Liver Diseases of Chinese and Western Medicine*, 33(3): 220–223.
- [2] Zhang H, Wu X, Xu C, 2020, Analysis of the Efficacy of Terlipressin Combined with Prostaglandin in the Treatment of Patients with Cirrhosis Complicated by Refractory Ascites by Assisting Ultrafiltration and Concentration Reflux of Ascites. *Journal of Practical Liver Diseases*, 23(2): 244–247.
- [3] Zhu T, Lan K, 2020, Clinical Treatment Analysis of Patients with Cirrhosis and Refractory Ascites. *Jilin Medicine*, 41(6): 1461–1462.
- [4] Qu X, 2020, Analysis of the Effect of Regular Ascites Discharge and Combining with Anti-Infection in the Treatment of Cirrhosis Combined with Refractory Hepatic Ascites. *Journal of General Oral Medicine (Electronic Edition)*, 7(5): 111, 124.
- [5] Chen H, Wu Y, Liu G, 2023, Clinical Observation on 36 Cases of Patients with Cirrhosis Refractory Ascites with Blood Stasis and Water Stagnation in Patients with Umbilical Cord Penetration and Diuresis Patch Assisted Treatment. *Journal of Traditional Chinese Medicine*, 64(14): 1462–1468.
- [6] Hu X, Zhang L, Wang Y, et al., 2024, The Effect of Fu-Spleen, Li-Water and Drum Elimination Formula Combined with Chinese Medicine Identification and Dietary Administration on Liver Function and Nutritional Index of Ascites in Cirrhotic Liver with Viral Hepatitis B. *Chinese Journal of Traditional Chinese Medicine*, 42(7): 193–196.
- [7] Wang Z, Hou W, Zhang W, et al., 2022, Rifaximin Improves Clinical Symptoms and Short-Term Survival in Patients with Cirrhosis-Refractory Ascites. *Chinese Journal of Liver Diseases*, 30(11): 1170–1174.
- [8] Ge J, Li X, Wang Z, et al., 2022, Analysis of the Similarities and Differences in the Medication Patterns of Traditional Chinese Medicine for the Treatment of Cirrhotic Ascites and Cirrhotic Recalcitrant Ascites Based on Data Mining. *Journal of Integrated Chinese and Western Medicine and Liver Disease*, 32(4): 347–351.
- [9] Zhan H, Du Y, Wang S, 2022, Study on the Effect of Terlipressin Combined with Ascites Concentrating Retraction in the Treatment of Patients with Cirrhosis Complicated by Recalcitrant Ascites. *Journal of Practical Liver Diseases*, 25(3): 395–398.
- [10] Shi S, He D, Lin S, 2021, Effectiveness and Safety of Tolvaptan Tablets in the Treatment of Ascites and Hyponatraemia in Liver Cirrhosis. *Infectious Disease Information*, 34(3): 246–249.
- [11] Ma J, Liu Y, 2021, Clinical Study on the Treatment of Intractable Ascites in Liver Cirrhosis by Nourishing Yin and Inducing Diuresis Formula Together with Excretion of Ascites and Infusion of Albumin. *Shaanxi Traditional Chinese Medicine*, 42(1): 87–89.
- [12] Wang G, Zhu Q, Tang J, et al., 2021, Clinical Study on the Treatment of Intractable Ascites in Hepatitis B Cirrhosis by Diuresis and Dropsy Elimination Formula Combined with External Treatment of Traditional Chinese Medicine. *Journal of Integrated Chinese and Western Medicine and Liver Disease*, 31(7): 609–612.

### Publisher's note

Bio-Byword Scientific Publishing remains neutral with regard to jurisdictional claims in published maps and institutional affiliations.

# Research Progress on Negative Emotions Influencing the Incidence of Breast Cancer

Wei Liu<sup>1</sup>, Ruibo Shi<sup>2</sup>, Yurong Zhou<sup>2</sup>, Rong Guo<sup>2</sup>, Jianjun Wei<sup>2</sup>, Xinming Fan<sup>2</sup>, Zhizhong Ren<sup>2</sup>, Rongtian Zhang<sup>2\*</sup>

<sup>1</sup>Department of Psychiatry, Bayannaoer City Hospital, Bayannaoer 015000, Inner Mongolia Province, China

<sup>2</sup>Department of General Surgery, Linhe District People's Hospital, Bayannaoer 015000, Bayannaoer, Inner Mongolia Province, China

\*Corresponding author: Rongtian Zhang, 15047298887@163.com

**Copyright:** © 2024 Author(s). This is an open-access article distributed under the terms of the Creative Commons Attribution License (CC BY 4.0), permitting distribution and reproduction in any medium, provided the original work is cited.

**Abstract:** At present, breast cancer is the largest malignant tumor endangering women's health, and has become one of the most common cancer types in the world. In recent years, the relationship between psychosocial factors and the incidence of breast cancer has attracted extensive attention. Traditional Chinese medicine research of the motherland suggests that emotional disorder is an important factor leading to breast cancer, and emotional theory and negative emotional accumulation have something in common in some aspects. This article reviews the impact of negative emotions on the risk of breast cancer and the current research progress and explores the possibility of reducing the progress of breast cancer and improving the quality of life of breast cancer patients through negative emotion intervention.

**Keywords:** Negative emotions; Emotional disorders; Breast cancer; Pathogenesis mechanism

**Online publication:** October 2, 2024

## 1. Introduction

Breast cancer (BC) is one of the most common malignant tumors among women in several countries around the world. The Global Cancer Report 2020 pointed out that the incidence of breast cancer ranked first among female cancers worldwide <sup>[1]</sup>, and in China, the incidence of breast cancer is among the major malignant tumors among women, and the situation of prevention and control is grim <sup>[2]</sup>. Accompanied by the gradual deepening of medical research, the clinical understanding of the causes of breast cancer has become increasingly clear, and a large number of research data that the psychological state and negative emotions can lead the body to produce a stress response, and can induce a variety of abnormal behaviors, long-term anxiety and depression, panic, anger, and other adverse emotional states can lead to myocardial infarction, malignant arrhythmia and other cardiac diseases such as the incidence of a significantly higher risk, but also induces psychological diseases such as depression, and the onset of some chemo-mammary tumors is also closely related to emotional problems <sup>[3]</sup>. Traditional Chinese medicine (TCM) has a more in-depth study on emotions and diseases, and it is believed



that the long-term accumulation of negative emotions will lead to abnormalities in psychological and somatic physiology and induce various diseases. This paper takes negative emotions, the pathogenicity of emotions in traditional Chinese medicine and breast cancer as the starting point, and discusses the research progress related to the influence of negative emotions on the risk of breast cancer by combining the association between emotional disorders and negative emotions in traditional Chinese medicine.

## **2. Negative emotions**

Emotions can be divided into positive and negative emotions, and Watson D et al. (1988) believe that negative emotions, as opposed to positive emotions, belong to unpleasant subjective emotional experiences induced by various factors such as the environment, and common negative emotions mainly include depression, anxiety, sadness, anger, and panic, etc. <sup>[4]</sup>. In recent years, negative emotions have gradually become the most popular emotions among scholars at home and abroad, and they have become the most common negative emotions. In recent years, negative emotions have gradually become a research hotspot for scholars at home and abroad, and a large number of studies have found that negative emotions have a great impact on the physical and mental health of individuals <sup>[5]</sup>.

## **3. Breast cancer**

### **3.1. Research status of breast cancer in modern medicine**

It is pointed out in the Global Cancer Report 2020 that the incidence rate of breast cancer and the death rate of the disease are significantly higher than that of other female malignant tumors <sup>[6]</sup> and the incidence rate of breast cancer in the adult female population in China also has a relatively high level <sup>[7]</sup>. Through the research and analysis of breast cancer, it can be seen that this disease belongs to the malignant tumor formed in the ductal epithelial tissue of the breast under the action of many types of carcinogenic factors, and in the early stage of the development of the disease, the patients only show that the breasts can be touched with painless lumps, and along with the continuous aggravation of the disease, the tumor can be metastasized to lymph nodes, which can lead to the local pain and the skin condition abnormality, and make the patient's quality of life decline. The causes of breast cancer are complicated, among which environmental factors and family heredity are important triggers. In addition, a poor lifestyle can also affect the health of the breast, leading to an increased risk of breast cancer <sup>[6,7]</sup>. According to the latest clinical research data, many hormone levels in breast cancer patients are abnormal, and it is believed that hormone disorders can promote the development of breast cancer. Since the pathogenesis of breast cancer is not clear in modern medicine, it is difficult to carry out primary prevention, and it is generally believed that physical examination can detect breast cancer at an early stage and reduce the mortality rate. Breast cancer adopts different treatment plans according to different stages of the disease, including surgery, chemotherapy, radiotherapy, endocrine tumor, targeted therapy and so on. In conclusion, as the most serious cancer threatening women's lives, the prevention and treatment of breast cancer is in a severe form, and it is of great practical significance to clarify the pathogenesis of adenocarcinoma and formulate the prevention and treatment plan accurately.

### **3.2. Research on breast cancer in traditional Chinese medicine**

Traditional Chinese medicine theory has very in-depth and systematic research on breast cancer, and most of the Chinese medical texts classify breast cancer as breast stone carbuncle, breast rock and other categories <sup>[8]</sup>, among which the name of breast rock was first recorded in the traditional Chinese medical text "Woman's

Complete Recipes.” According to Chinese medicine research on breast cancer, the development of breast cancer is a process of continuous accumulation of various factors, which leads to the formation of lumps in the local tissues of the breast, which are painless at the early stage of development and can lead to skin sores with the progression of the disease. According to some Chinese medicine research, the core factors of breast cancer are emotional upset, liver and stomach Qi against the egg, stagnation of Qi and blood stasis, and depression will turn into fire, which will eventually lead to the formation of local tumors.

### **3.3. Modern medical research on the correlation between negative emotions and breast cancer**

Domestic research has found that any disease will seriously affect the health of the patient’s body and even threaten the patient’s life, and all kinds of treatments will make the patient’s body and mind suffer from different degrees of influence and lead to the emergence of anxiety, depression and other negative emotions easily <sup>[9,10]</sup>. Research has found that these negative emotions can lead to the destruction of the patient’s body functions, affecting the therapeutic effect of the disease <sup>[11,12]</sup>. Accompanied by the development of medical technology, the means of breast cancer treatment are becoming increasingly abundant, and most hospitals provide comprehensive treatment through radiotherapy, endocrine regulation and surgical treatment, biological therapy and other programs <sup>[13]</sup>, which cause serious trauma to both the physiology and psychology of patients, resulting in the emergence of patients with negative emotions such as low self-esteem, depression, anxiety and other negative emotions <sup>[14]</sup>. Overseas studies have found that the incidence of anxiety, depression and other negative emotions in cancer patients is significantly higher than that in the normal population <sup>[15]</sup>.

A study in the UK found that the prevalence of anxiety disorders, depression or both in breast cancer patients during the first year was about twice as high as that of the general female population, and then women in the recovery state showed similar levels of depression and anxiety to those of the general female population, but the levels of depression and anxiety increased dramatically after the disease recurred <sup>[16]</sup>.

Regarding negative emotions, most researchers have confirmed that it is due to the disease or traumatic stress after the occurrence of negative emotions, but whether the emotions lead to the occurrence of the disease has become a research hotspot over the years, especially the application of the concept of humane medical concepts, humanistic care services and other concepts, the role of the psychological state, the psychological stress response in the incidence of breast cancer has received widespread attention, and the data of the relevant research data believe that Adverse emotional state can lead to severe psychological stress response and can induce abnormal behavior, which increases the risk of breast cancer and cardiovascular diseases <sup>[17]</sup>. Many scholars have also simulated negative emotional stress or accumulation of negative emotions through animal experiments <sup>[18–22]</sup>, and found a variety of pathological manifestations in experimental animals, such as increased norepinephrine and dopamine, inhibition of T-lymphocyte proliferation, up-regulation of Ki67 and VEGF expression, promotion of proliferation and angiogenesis of tumor cells, activation of the HPA axis, elevation of plasma ACTH, and serum CORT. The content of plasma ACTH and serum CORT is also increased. The causes of psychological stress in the human body are complex, considering the correlation with the emotional state, the environment, the physiological state, etc., it can be considered that psychological stress is a complex system <sup>[23]</sup>, that can cause physiological and pathological changes in the organism through the sympathetic nervous system (SNS), the HPA axis and the immune system, affecting the stable state of the internal environment <sup>[24,25]</sup>. The combined effects of the HPA axis and SNS in the neuroendocrine system can lead to different degrees of abnormal immune function, and can affect the endocrine system, causing the internal environment to be in a state of disorder, and can harm a number of physiological functions <sup>[26,27]</sup> and some relevant studies have found that catecholamines, through the role of the nervous system, may have a certain degree of tumor proliferation promotion <sup>[28–30]</sup>. Liu X et al. (2021)

have combined previous studies to describe the effects of emotional stress on the development of breast cancer from the perspective of the molecular biology of the endocrine system and immune system.

#### **4. Research on the correlation between negative emotions and breast cancer in Chinese medicine**

Ancient books of Chinese medicine have recorded the etiology and mechanism of breast cancer for a long time, and the research theory of Chinese medicine has clearly proved that the onset of breast cancer has a correlation with the disorder of liver Qi, and the main reason for the formation of the disorder of liver Qi is the lack of emotional and emotional well-being, and worries and troubles. In Chinese medical texts such as “Surgical Medical Mirror,” the relationship between emotion and breast cancer formation is clearly recorded, and it is believed that emotion can lead to the operation of qi and blood, resulting in liver depression and stagnation of Qi, and affect the balance of Yin and Yang of the organism, which will gradually aggravate the breast cancer. To sum up, the recognition of the etiology and pathogenesis of breast cancer in ancient Chinese medical texts is especially high for liver Qi stagnation and Chong Ren disorders, which shows that the influence of emotional factors on the onset of breast cancer is enormous. The modern research on negative emotions on the development of tumors is very similar to the pathogenesis of emotions and feelings in traditional Chinese medicine.

In conclusion, whether it is traditional Chinese medicine’s “emotion-causing disease” or the modern “bio-psycho-social” medical model of negative emotions on related diseases, all of them suggest the important influence of negative emotions on the onset of breast cancer, and it is important to study the pathogenesis of breast cancer and the effect of negative emotions on the onset of breast cancer. In-depth research on the pathogenesis of breast cancer and the search for therapeutic targets based on emotion regulation will open up new avenues in the prevention, treatment and improvement of prognosis of breast cancer.

#### **Funding**

Linhe District People’s Hospital, Bayannur City, “A Comprehensive Clinical Study on the Correlation between the Onset of Breast Tumors and Negative Emotions” (Project No.: K202148)

#### **Disclosure statement**

The authors declare no conflict of interest.

#### **References**

- [1] World Health Organization (WHO), 2020, World Cancer Report 2020.
- [2] Zheng R, Sun K, Zhang S, et al., 2019, Analysis of Malignant Tumour Prevalence in China in 2015. *Chinese Journal of Tumours*, 41(1): 19–28.
- [3] Strange KS, Kerr LR, Andrews HN, et al., 2000, Psychosocial Stressors and Mammary Tumor Growth: An Animal Model. *Neurotoxicology and Teratology*, 22(1): 89.
- [4] Watson D, Clark LA, Tellegen A, 1988, Development and Validation of Brief Measures of Positive and Negative Affect: The PANAS Scales. *Journal of Personality and Social Psychology*, (6): 1063–1070.
- [5] Zhang J, Zhang D, 2019, College Students’ Psychological Quality Level Is Externally and Implicitly Related to

Positive and Negative Emotions. *Psychological and Behavioural Research*, (1): 91–96.

- [6] Breast Cancer Professional Committee of the Chinese Anti-Cancer Association, 2021, Chinese Anti-Cancer Association Breast Cancer Diagnosis and Treatment Guidelines and Norms (2021 Edition). *Chinese Journal of Cancer*, 31(10): 954–1040.
- [7] Breast Group of the Women's Health Branch of the Chinese Preventive Medical Association, 2017, Lifestyle Guidelines for Breast Cancer Patients in China. *Chinese Surgical Miscellany*, 55(2): 81–85.
- [8] Liu S, Sun YP, 2011, Traceability Examination of Chinese Medicine Literature on Breast Cancer. *Proceedings of the 2011 Annual Conference of Chinese Medicine Surgery of the Chinese Society of Traditional Chinese Medicine*, 118–121.
- [9] Hjerl K, Andersen EW, Keiding N, et al., 2003, Depression as a Prognostic Factor for Breast Cancer Mortality. *Psychosomatics*, 44(1): 30.
- [10] Lesiuk T, 2015, The Effect of Mindfulness-Based Music Therapy on Attention and Mood in Women Receiving Adjuvant Chemotherapy for Breast Cancer: A Pilot Study. *Oncology Nursing Forum*, 42(3): 276.
- [11] Humphris GM, Rogers S, McNally D, et al., 2003, Fear of Recurrence and Possible Cases of Anxiety and Depression in Orofacial Cancer Patients. *International Journal of Oral and Maxillofacial Surgery*, 32(5): 486–491.
- [12] Lebel S, Tomei C, Feldstain A, et al., 2013, Does Fear of Cancer Recurrence Predict Cancer Survivors' Health Care Use? *Supportive Care Cancer*, 21(3): 901–906.
- [13] Li L, Kang F, Li Z, et al., 2019, Effects of Anxiety and Depression and Psychological Resilience on Post-Traumatic Growth in Breast Cancer Patients. *Nursing Research*, 33(6): 960–965.
- [14] Yu W, Zhang A, Xia C, et al., 2018, Study on the Mediating Effect of Psychological Resilience Between Emotional Distress and Post-Traumatic Growth in Breast Cancer Patients. *Modern Preventive Medicine*, 45(10): 105–109.
- [15] Yi JC, Syrjala KL, 2017, Anxiety and Depression in Cancer Survivors. *Medical Clinics of North America*, 101(6): 1099–1113.
- [16] Burgess C, Cornelius V, Love S, et al., 2005, Depression and Anxiety in Women with Early Breast Cancer: Five Year Observational Cohort Study. *BMJ*, 330(7493): 702.
- [17] Gu L, Wang Q, Zhao Y, et al., 2000, Effects of Provocative Stimuli on Monoamine Hormone and T-Lymphocyte Function in Rat Hypothalamus. *Chinese Traditional Medicine Information Magazine*, 7(8): 44.
- [18] Meng L, 2018, Mechanism of Psychological Stress on Liver Tumours Based on the Theory of Anger Injuring the Liver. *Pharmaceutical Biotechnology*, 25(2): 142.
- [19] Sun P, Wei S, Wei X, et al., 2016, Anger Emotional Stress Influences VEGF/VEGFR2 and Its Induced PI3K/AKT/mTOR Signaling Pathway. *Neural Plasticity*, 2016: 4129015.
- [20] Wang Y, Yang J, Qiu L, 2014, Immunomodulatory Effects of Jin Gui Ren Qi Wan on Mice with Fear of Kidney Injury. *Jiangxi Traditional Chinese Medicine*, 45(11): 29.
- [21] Dong Q, Liu X, 2013, Changes of Blood ACTH, CORT, IL-2 and IL-8 Levels in Fear-Stressed Rats. *Journal of Molecular Diagnosis and Therapy*, 5(3): 173.
- [22] Lazarus RS, 1974, Psychological Stress and Coping in Adaptation and Illness. *The International Journal of Psychiatry in Medicine*, 5(4): 321.
- [23] Antoni MH, Dhabhar FS, 2019, The Impact of Psychosocial Stress and Stress Management on Immune Responses in Patients with Cancer. *Cancer*, 125(9): 1417.
- [24] Cohen S, Janicki-Deverts D, Miller GE, 2007, Psychological Stress and Disease. *JAMA*, 298(14): 1685.
- [25] Krhik J, Aboul-Enein BH, Bernstein J, et al., 2019, Psychological Stress and Cellular Aging in Cancer: A Meta-Analysis. *Oxidative Medicine and Cellular Longevity*, 2019: 1270397.
- [26] Shin KJ, Lee YJ, Yang YR, et al., 2016, Molecular Mechanisms Underlying Psychological Stress and Cancer. *Current*

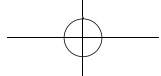
Pharmaceutical Design, 22(16): 2389.

- [27] Chang A, Le CP, Walker AK, et al., 2016,  $\beta$ 2-Adrenoceptors on Tumor Cells Play a Critical Role in Stress-Enhanced Metastasis in a Mouse Model of Breast Cancer. *Brain, Behavior, and Immunity*, 57: 106.
- [28] Le CP, Nowell CJ, Kim-Fuchs C, et al., 2016, Chronic Stress in Mice Remodels Lymph Vasculature to Promote Tumour Cell Dissemination. *Nature Communications*, 7: 10634.
- [29] Childers WK, Hollenbeak CS, Cheriya P, 2015,  $\beta$ -Blockers Reduce Breast Cancer Recurrence and Breast Cancer Death: A Meta-Analysis. *Clinical Breast Cancer*, 15(6): 426.
- [30] Liu X, Liu H, Ma L, et al., 2021, Exploring the Correlation Between the Seven Emotions of Chinese Medicine and the Pathogenesis of Breast Cancer Based on the Perspective of Psychological Stress. *Chinese Journal of Traditional Chinese Medicine*, 46(24): 6377–6386.

**Publisher's note**

Bio-Byword Scientific Publishing remains neutral with regard to jurisdictional claims in published maps and institutional affiliations.





## Integrated Services Platform of International Scientific Cooperation

Innoscience Research (Malaysia), which is global market oriented, was founded in 2016. Innoscience Research focuses on services based on scientific research. By cooperating with universities and scientific institutes all over the world, it performs medical researches to benefit human beings and promotes the interdisciplinary and international exchanges among researchers.

Innoscience Research covers biology, chemistry, physics and many other disciplines. It mainly focuses on the improvement of human health. It aims to promote the cooperation, exploration and exchange among researchers from different countries. By establishing platforms, Innoscience integrates the demands from different fields to realize the combination of clinical research and basic research and to accelerate and deepen the international scientific cooperation.

### Cooperation Mode



Clinical Workers



In-service Doctors



Foreign Researchers



Hospital



University



Scientific institutions

# OUR JOURNALS



The *Journal of Architectural Research and Development* is an international peer-reviewed and open access journal which is devoted to establish a bridge between theory and practice in the fields of architectural and design research, urban planning and built environment research.

Topics covered but not limited to:

- Architectural design
- Architectural technology, including new technologies and energy saving technologies
- Architectural practice
- Urban planning
- Impacts of architecture on environment

*Journal of Clinical and Nursing Research (JCNr)* is an international, peer reviewed and open access journal that seeks to promote the development and exchange of knowledge which is directly relevant to all clinical and nursing research and practice. Articles which explore the meaning, prevention, treatment, outcome and impact of a high standard clinical and nursing practice and discipline are encouraged to be submitted as original article, review, case report, short communication and letters.

Topics covered by not limited to:

- Development of clinical and nursing research, evaluation, evidence-based practice and scientific enquiry
- Patients and family experiences of health care
- Clinical and nursing research to enhance patient safety and reduce harm to patients
- Ethics
- Clinical and Nursing history
- Medicine



*Journal of Electronic Research and Application* is an international, peer-reviewed and open access journal which publishes original articles, reviews, short communications, case studies and letters in the field of electronic research and application.

Topics covered but not limited to:

- Automation
- Circuit Analysis and Application
- Electric and Electronic Measurement Systems
- Electrical Engineering
- Electronic Materials
- Electronics and Communications Engineering
- Power Systems and Power Electronics
- Signal Processing
- Telecommunications Engineering
- Wireless and Mobile Communication

